[redacted] REPORT 317/59

Copy No. 34

H.M.S. C of E

NOV 15 1961

A LIMITED TECHNICAL EVALUATION OF THE AVRO ARROW INTERCEPTOR SYSTEM (U)

by

R.S. Mitchell F.W. Slingerland & C.J. Wilson

DEFENCE RESEARCH BOARD

CANADIAN ARMAMENT RESEARCH AND DEVELOPMENT ESTABLISHMENT

Valcartier, Quebec

January, 1961

CARDE Report 317/59

UNCLASSIFIED

A LIMITED TECHNICAL EVALUATION OF THE AVRO ARROW INTERCEPTOR SYSTEM (U)

by

R.S. Mitchell
F.W. Slingerland
C.J. Wilson

"Systems Wing"

CANADIAN ARMAMENT RESEARCH AND DEVELOPMENT ESTABLISHMENT

Valcartier, Quebec

January, 1961

SUMMARY

A description is given of the concept of an interceptor system and the methods of its evaluation. The limits of this particular study are confined mainly to the AI phase. The concept of placement charts is then outlined. Results are discussed which have been derived from the study of placement probability. These results pertain to the effects of the various parameters of the system, such as AI range, ground environment vectoring accuracy, aircraft performance, armament, etc. Both co-altitude and three-dimensional attacks against straight flying and evading targets were studied. Specific attention has been given to the effects of ECM in regard to both the expected performance of the system under ECM conditions and the methods and means of operating in the face of ECM.

FOREWORD

This report describes the investigations and results of a study of the CF-105 Arrow interceptor system which was carried out from April 1, 1956 to April 1, 1958. The work was executed by CARDE for the Director of Systems Evaluations of the RCAF, under terms of reference laid down by that directorate (PCC No. D46-97-36-21). The Director of Weapons Research was the headquarters liaison within DRB.

This report has been published 'after the event' in the sense that not only it appeared some time after the study was completed but also after the Avro Arrow interceptor program was cancelled. However, it is felt that the study justified a summary report which attempts to set forth in an organized manner the assumptions, the course, and the results of the two-year investigation. Although the specific system of interest is not to be in existence, many of the general results should be applicable to other supersonic interceptor systems and the work on ECM, three-dimensional attacks, and target evasion should contain information that is novel to the art. It is felt that in these three aspects at least, this study has something new to offer to the subject of supersonic aircraft interception.

As pointed out in the text, this study was a limited technical evaluation and was mainly concerned with one phase of the interceptor attack, the AI phase. The conclusions herein must be placed in the proper perspective, in that other aspects of the system such as ground environment, logistics, maintenance, strategy, etc., have not been studied and their contributions to the overall evaluation of the system would modify the results. Furthermore, specific evaluations given should be regarded as smoothed results based on multi-parameter data. Where specific cases are of interest or a more detailed examination is required, the reader is referred to Progress Reports listed in the references. It should also be noted that the combat situation was restricted to the following conditions:

a) One fighter against one bomber.

b) High-altitude threat (above 35,000 ft.).

c) Conventional guided weapon armament.

The Defence Research Telecommunications Establishment, the Director of Air Intelligence and the National Aeronautical Establishment assisted in certain specialized aspects of the study. Contractual support was obtained from Computing Devices of Canada, De Havilland Aircraft, and Canadian Westinghouse Co. During the last year of the study, a close contact was maintained with RCA at Waltham and Camden, and much valuable information was exchanged.

CONTENTS

CHAPTER I – INTERCEPTION BY MANNED AIRCRAFT

INTRODUCTION

This chapter deals with the general subject of an interceptor system: what it is, what it tries to do, and the difficulties imposed by the tactics of the threat. The immediate treatment is general. The discussion is narrowed to the Arrow weapon system in Chapter III.

The prime function of an interceptor system composed of manned aircraft is to destroy the enemy bomber threat before that threat can launch an attack on strategic areas. This function is performed almost entirely by means of some projectile launched from the interceptor to destroy the threat. It is the purpose of the ground controls and air-borne electronics to position the weapon launching platform in such a way that the bomber threat may be destroyed by the interceptor's weapons.

The engagement of high-speed targets by supersonic interceptors armed with air-to-air missiles introduces a variety of new problems which cannot be assessed by extrapolation of data arising from experience with conventionally armed subsonic aircraft. An assessment of the situation requires a fundamental study of the whole system.

The present concept of air defence envisions the interceptor system as an integrated whole consisting of ground radars, communication network, navigation equipment, computers, weapon carrier, air-borne electronics and weapon. The system is 'integrated' in the sense that each unit is to be designed with regard to its function in relation to the other components. The inputs to the various sub-systems are the outputs of some other members, and cognizance must be taken of the limits and tolerances that are imposed on these quantities by the performance of their components.

SUBDIVISION OF THE SYSTEM

The overall system as outlined above is too broad for detailed inspection and must be broken down into component parts for closer examination.

COMPONENTS

An analysis of an interceptor system may be considered from two points of view:

a) The components from which the integrated system is built.

b) The time sequence of events during the operational mission.

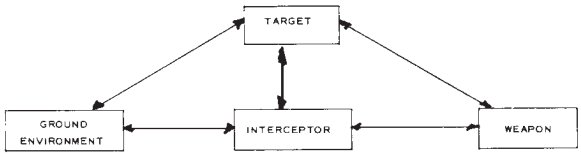

The principal sub-systems are illustrated in *Figure 1*. The interceptor system may be thought of as two interconnected closed loops with numerous sub-loops inside each of the blocks depicted. The complete failure of one section may render the system inoperative; on the other hand, high performance of one part of the system may compensate for poor performance of another. In *Figure 1*, it will be noticed that the arrows point in both directions, which indicates that each entity may influence the others, both in operation and in design requirements. For example, the type of target dictates the kind of ground radars required, while the latter may influence the bomber's ECM requirements and tactics. One might say that the input to the system is the bomber threat and the output, the destruction of that threat. The system may be conveniently considered in terms of automatic control techniques. Unfortunately, the various sub-units are related in most non-linear fashions so that the analysis of such a complex system cannot be made within the framework of classical servo theory.

The Threat

The threat usually envisioned is an enemy aircraft capable of dropping conventional or nuclear bombs or of launching air-to-surface missiles. In the latter case, the geographical position at which the threat must be intercepted is much more restricted.

Various tactics may be employed by the threat to hinder the accomplishment of the interceptor's mission. Today, technically, one of the most effective weapons at the disposal of the air threat is the use of electronic countermeasures. These attempt to render inoperative electronic devices on the ground, in the aircraft and in the weapon. Their use is difficult to predict and also extremely difficult to assess in a study of interception. However, unless the concept of jamming is included in any such study, the overall picture, as far as combat conditions are concerned, will be rather unrealistic.

A second tactic at the disposal of the bomber is evasive action. This concept, although easily understood, makes the calculation of interception potential very complicated, particularly because of the difficulty in assigning probabilities to various tactics which could be used.

The choice of bomber formations and the possibility of extensive use of decoys, both intercontinental and short range, may considerably increase the difficulty of interception, especially under ECM conditions.

Lastly, it may be pointed out that the attacking aircraft is free to approach the threat at whatever altitude is most advantageous within its operational capabilities. Since the interceptor system has an optimum operating altitude and the ground environment has some trouble in coping with low flying aircraft, the interceptors may be forced to operate under unfavourable conditions.

Ground Environment

By ground environment is meant the totality of terrestrial installations that contribute directly to the accomplishment of an interceptor mission. These factors include airfields, ground radars, computers, navigation systems, and communication links. The ground environment is chiefly concerned with the vectoring phase of the attack described in the next section, but it also contributes to the return-to-base phase and to the object that the system is trying to accomplish.

Interceptor

The interceptor, including its associated electronic sub-systems, should be thought of merely as a weapon carrier and launching platform. Its usefulness is practically nil except for the manipulation of the weapon and a few possible fringe benefits, such as direct observation of the threat.

Weapon

Although, in general, the weapon might be any form of projectile, for the main theme of this study it is a guided missile. The choice is limited to the type that would be available in the proposed operational period of the Arrow at the time of writing, that is, so called 'first generation' vehicles.

No consideration is given to advanced versions that might come into existence during the lifetime of the Arrow system, except that a brief look at the possible performance of the interceptor, if such a weapon were available, is given in Chapter VII. Just as the interceptor may be designated as a weapon carrier, similarly, the missile may be thought of as a warhead carrier. In the same way as the physical system may be divided into sub-units, an attack mission may be divided into phases. These phases, illustrated in *Figure 2, Page 9*, are:

a) Early Warning phase

b) Detection phase

c) Scramble phase

d) Vectoring phase

e) Approach or AI phase

f) Weapon phase

g) Engagement phase

h) Re-attack phase

i) Return-to-base phase.

Early Warning, Detection and Scramble Phases

Preliminary to the ground control phase there are a series of events which should culminate in getting the interceptors air-borne. Early warning of an approaching raid may be used to alert the fighters. Whether they are scrambled at early warning, or after a fixed interval, or on GCI detection, depends on the characteristics of the threat, interceptors, and geography. However, procedures in this phase may add materially to the time available for the actual attack.

The Vectoring Phase

During this part of the attack, the interceptor is presumed to be under the control of GCI, which directs the fighter aircraft into a region in space, relative to the bomber, so that AI contact may be made. More specifically, the interceptor must be placed in a proper position relative to the target and with the correct heading, so that the weapon delivery may be completed. Ideally, the orientation of the attack should maximize the kill probability. Indeed, for high-speed targets, positioning accuracy required by the weapon may be a more decisive factor than the particular potential of the weapon per se.

The Approach or AI Phase

Within a certain range from the target, the interceptor is considered to be receiving data from its own Air Intercept (AI) radar. Manoeuvres may be required to correct for GCI placement errors and permit successful launching of the weapon. The success of these manoeuvres will depend on the interceptor's radar and aerodynamic characteristics, the bomber's speed and manoeuvre capabilities, and on ECM considerations.

The Weapon Phase

The missile's characteristics and limitations dictate the range and heading relative to the target required for the weapon to be launched successfully. These restrictions in effect define the objective for the AI phase. The launch conditions of the weapon will influence its flight path which, in turn, will determine the miss-distance that is achieved.

The Engagement Phase

Considerations of fuzing, warhead burst, and target vulnerability determine the weapon's chance of achieving a kill for a given miss-distance vector. Studies of the final engagement are important not only because they determine the overall lethality but also because they reflect back on other phases. If certain approach angles are found to give a higher kill probability, they will dictate a preferred launch position and, therefore, the desired position for AI contact and the required tactics for the ground control phase.

Re-Attack and Return-to-Base Phases

Depending on the relative speed of the bomber and interceptor and the general raid characteristics, re-attack after the first pass at the bomber could be considered. The desirability of such tactics depends mainly on the characteristics of the weapon and its single shot kill probability: if this probability is low, it may be better to fire all missiles at once.

Return-to-base considerations must be examined in any studies wherein the total time duration of a fighter sortie is important. Geographical considerations regarding spacing of airfields and the effect of speed and altitude of the interceptor on fuel consumption will bear on the problem.

OTHER FACTORS

In an overall evaluation of an interception system, many operational properties of the environment in which the system must work should be considered. These may be classified as pertaining to:

a) Geography

b) Manpower

c) Weather

d) Identification.

Geography

Many of the strategic aspects of the ground environment problem are related to geographical questions. These include a definition of the areas to be defended, the amount of penetration which may be allowed and, consequently, the siting of GCI stations and interceptor bases. Considerations of this nature are pertinent to the evaluation of the range, endurance, climb capabilities, and flight programs of the interceptors. Geographical considerations also affect the input assumptions to lethality studies as to what type of kills are of consequence.

Manpower

A consideration which is of extreme importance is the provision of trained manpower for the maintenance of various units of the proposed integrated electronic control system. A careful examination of intelligence, experience, and of the time required for the proper training of electronic technicians is necessary. To keep a proper perspective, cognizance must be taken of the estimated total number of 'black boxes' that will require maintenance in connection with ground environment, families of guided missiles and mobile units. Two factors which enter the problem as assumptions must be recognized as functions of maintenance: accuracies and material reliability, both depending on the care and understanding of the equipment.

Weather

The extent to which atmospheric conditions will affect the operation of the interceptor system is a question that should be studied and clarified. Entities which may be affected by adverse weather are GCI detection, location and height finding accuracies, communication links, time for aircraft to attain combat altitude, AI capabilities, and aircraft recovery after a mission. A statistical evaluation of weather conditions to be encountered should be included in an overall assessment of the system. A factor which may contribute appreciably to the accuracy of the system is the error due to meteorological wind estimates.

Identification

The problem of recognizing enemy from friendly aircraft in a crowded air space can be very difficult. The complexity is increased by the fact that GCI must monitor many tracks and assign targets to specific fighters. These fighters in turn must recognize the enemy bomber when it is detected on the air-borne radar. Saturation of data gathering and communication facilities, mutual interference, and ECM add to the confusion.

CHAPTER II – METHOD OF EVALUATION

EVALUATION OF EFFECTIVENESS

A brief discussion of the considerations involved in the evaluation of an interceptor system is presented in this chapter. The purpose is to demonstrate the complexity of the problem and to place in proper perspective the limited study which is the subject of this report.

SYSTEM ANALYSIS

The methodology by which optimal design of a weapon system is set up, or by which an existing or proposed system is evaluated, is called 'weapon system analysis'. A complete assessment of the worth of an interceptor system considers:

a) performance of equipment

b) base installation and manpower needs

c) deployment and operational use of forces

d) production schedules and cost

in the light of an enemy threat potential.

A more restricted assessment is one in which only technical aspects of component performance and modes of operation are considered without regard to the logistic and economic problems of building up the system. Such a restricted weapon system analysis, which may be called a 'technical evaluation', would show what level of defence can be provided by an existing or a proposed system.

The CARDE assessment of the CF-105 Interceptor System is a restricted study of this sort.

CRITERIA OF EFFECTIVENESS

Attention must be paid to choosing a suitable criterion of success, and the following quantities might serve as standards of evaluation:

a) attrition potential

b) cost

c) interception probability

If operational factors such as the size and deployment of attacking and defending forces can be included in the evaluation, a useful measure of worth is the attrition which can be inflicted on an invading bomber force by the defending interceptors. If economic and logistic aspects of the problem are studied, the cost of providing a given level of defence, whether absolute or partial, becomes the most meaningful criterion. In a purely technical assessment, a more restricted criterion must be used for, here, the effectiveness of the interceptor system may be described in terms of the probability of successful interception of a bomber or of a raid. It is a limited form of this criterion that is used in the present study.

The objective of this evaluation was to state the probability of interception, P_e, of one fighter against one bomber. However, the more restricted probability of placement (P_p) was the goal that was usually achieved. These terms are discussed in more detail in the following paragraphs.

COMPUTATION OF EFFECTIVENESS

Interception and destruction of a bomber threat require success in

a) detection of the threat

b) positioning of the interceptor

c) survival of the interceptor until missile launch

d) missile flight

e) destruction of bomber

f) operation in the face of enemy countermeasures

This concept may be expressed as the probability of successful interception, written symbolically as

$$P_e = P_d \cdot P_p \cdot P_s \cdot P_k \cdot R \cdot P_i$$

where

P_d = probability of detecting the threat

P_p = probability of successful positioning of the interceptor

P_s = probability of survival of the aircraft until missile launch

P_k = lethality or kill probability of the weapon system

R = reliability of the system

P_i = proportion of attacks which remain successful when a clear environment is replaced by the expected ECM environment.

To be complete, an interceptor system effectiveness study must provide numerical values, or ranges of values, for each of these factors.

PORTIONS STUDIED

The CARDE study considered only a limited portion of the interceptor system; limited in respect to both the physical units and the various time phases of the attack. It must be emphasized, therefore, that this report is not in any sense a complete evaluation of the system but definitely a limited technical evaluation. These limitations must constantly be kept in mind when interpreting the results given herein.

The physical units of the system that were studied are the interceptor aircraft, its electronics, and the weapon itself. The various phases of an attack of a bomber by an interceptor were reviewed in Chapter I. The phases of the attack considered in the study are shown in *Figure 2* as heavily outlined boxes, but even these phases were not given equal weight in the study. The one which has received practically the whole attention is the AI phase. A brief review of this phase will show that it is the pivotal part of the whole interceptor sequence.

The AI phase looks forward in time to the launching of a weapon and, in this sense, the weapon launch zone represents a target to which the interceptor must be directed. It also looks back in time to what has been accomplished by the ground environment, for it is the accuracy achieved in the vectoring phase that determines the success with which the interceptor will reach the launch zone. The ground environment accuracy may be considered as an input, and meeting the demands of the weapon system as a final end product of this attack phase. There are several other advantages in concentrating on this phase. The significance of a number of aircraft performance characteristics is highlighted, although such things as time to height are not included. It is felt also that this phase of the attack is the most susceptible to enemy countermeasures, and it is this phase wherein bomber evasion may have the greatest effect. Any stringent requirements imposed by the weapon on the interceptor system will probably be most strongly reflected in this phase of the attack.

The AI phase is conveniently studied by means of placement charts. These charts outline those portions of space from which an interceptor can proceed successfully under its own AI radar information to a weapon launch zone and within which the ground control must place the interceptor for the attack to succeed. The technicalities of producing these placement charts are reviewed in detail in Chapter IV.

It has been mentioned that the target of the AI phase is the weapon launch zone. Before a study of the AI phase could begin, the characteristics of the weapon had to be considered and typical launch zones generated. These launch zones are most conveniently obtained by analogue computer studies. Details of the work involved in obtaining these launch zones and the consequences thereof are reviewed in Chapter VI. It may be noted that the weapon launch zone is itself a placement chart. It represents the zone and orientation in space in which the missile must be placed so that it can proceed on a suitable course to the destruction of the target aircraft.

A final phase of the actual interceptor attack is that of warhead impact. The study of this portion of the attack is mainly concerned with the lethality of the warhead-fuze combination of the weapon. Because of time and effort limitations in this study, these aspects of the interception of a bomber were mainly restricted to geometrical considerations of warhead burst patterns in relation to the bomber target. Only rough estimates of the actual lethality of the missile system were made. It must not be thought, however, that this portion of the attack is divorced from the rest of the system; the actual lethality outcome of the weapon may, in itself, dictate the aspect angles and the conditions within which the missile should be launched.

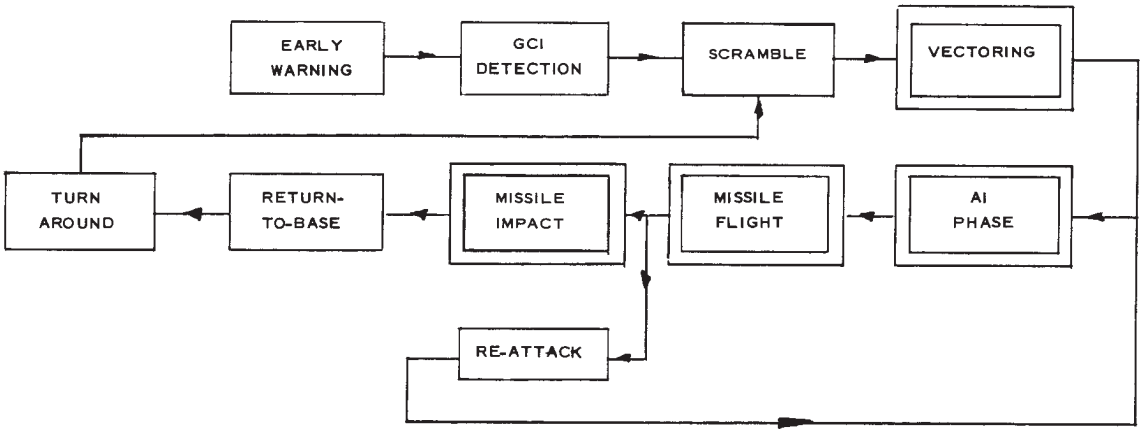

FIGURE 2

ECM CONSIDERATIONS

In the preceding section, the effects of ECM were considered as another probability P_j; however, in the actual treatment of the work, ECM terms can seldom be reduced to an actual probability. The main concern in this study was to see in what respects the system would be degraded by ECM and also to develop tactics which would aid in countering ECM or permit the system to operate in spite of serious degradation in some particular mode.

Electronic countermeasures may be applied to several phases of the attack. However, the effects on the AI phase received the greatest attention. Electronic countermeasures of the ground environment would show up in the method of study as an increase in vectoring errors, that is, an increase in the value of σ (See Chapter III). Determination of the effect of ECM on the weapon itself involves a detailed study of hardware. The actual effects of ECM on the particular weapons under consideration were more thoroughly covered under another project, project 'ASH CAN'. Since most of the results of the present study are expressed in terms of placement probability, they inherently presume that the missile is relatively undegraded by ECM.

The main aspect of electronic countermeasures considered was the possibility of developing passive means of countering this form of warfare. Chapter VIII presents a detailed review of the results of these studies.

OTHER PROBABILITIES

A number of the other probabilities mentioned under "Computation of Effectiveness" were not studied in any detail. Where reference is made to some of these items, they must be considered purely as estimates. This is especially true of the values of reliabilities and probabilities of detection. The probability of survival of the aircraft was not considered at all.

To sum up, the main limitations of the study may again be reiterated. The situation envisaged was one fighter against one target at high altitude, both interceptor and target at supersonic speed in most cases. The majority of the results are given in terms of placement probabilities derived from a study of the AI phase. This study is therefore mainly a technical evaluation of this phase of the attack. Other quantities considered are either taken as input or output parameters or are estimated values. However, this phase of the attack in itself has been studied

in great detail, and it is felt that where recommendations are made, concerning either a particular phase or the effect of this phase on other portions of the attack, these recommendations are well substantiated by a fairly exhaustive review of the various parameters.

This study was essentially parametric. Therefore, as a by-product of this type of investigation, an understanding of the sensitivity of the system to the various parameters is obtained in many cases. Examples of these parameters are:

a) AI range

b) ground environment accuracy

c) missile monoeuvrability

d) aircraft manoeuvrability

e) missile launch characteristics

f) AI look angle requirements.

In all cases where trends or general results are reported, they must be thought of as average values or as smoothed results obtained by the combinations of the numerous parameters. For particular cases, where all parameters are given specific values, reference should be made to the detailed graphs presented in the various Quarterly Progress Reports.

CHAPTER III – SYSTEM CHARACTERISTICS

INTRODUCTION

This chapter reviews the general characteristics of the main physical components of the system which were the subject of this study: the interceptor aircraft, the air-borne electronic equipment, and the target aircraft. An attempt has been made to give the latest performance figures but, since the system was still in the development stage, the values in this chapter may differ somewhat from figures appearing elsewhere. As far as the study was concerned, the actual values chosen did not greatly affect the course of the work because it was understood at the beginning that since equipment performance figures were subject to change, ranges of values of the various parameters would be taken.

THE CF-105 ARROW AIRCRAFT

The Avro Arrow was intended to be a supersonic fighter with characteristics especially suited to Canadian needs. It was a two-seater, all-weather, day-and-night interceptor designed for a five-minute combat at 50,000 feet and Mach 1.5, but capable of speeds a little beyond Mach 2 for short lengths of time. Power was to be supplied by two Orenda Iroquois engines, with maximum net thrust of 21,700 pounds per engine at sea level.

AIRCRAFT GEOMETRY

The Arrow had a delta-wing planform with negative camber and 4-degree anhedral. Five-per-cent chord notches and ten-per-cent chord drooped extensions on the outboard sections of the wings improved the pitch-up and buffet characteristics and the static lateral stability. A three-view drawing of the aircraft is shown in *Figure 3.*

AIRCRAFT PERFORMANCE

The performance data reproduced here are based on the latest Avro estimates extracted from Avro's Periodic Performance Report, Number 15 (Nov. 19/58).

Figure 4 shows the variation of altitude and Mach number for different steady state normal accelerations at combat weight with afterburners lit, and *Figure 5* the maximum level speed as a function of altitude. The loading and performance under standard atmospheric conditions are summarized below.

WEIGHT

Take-off weight (with maximum internal fuel)	67,505	Lb.
Operation weight empty	45,892	Lb.
Combat weight (½ maximum internal fuel weight)	56,699	Lb.
Normal design landing gross weight AIR 7-4 – MIL-S-5701	49,958	Lb.
Wing loading at gross take-off weight	55.2	Lb/Sq. Ft.
Power loading at gross take-off weight	1.55	Lb/Lb. Thrust

SPEED

True airspeed in level flight at sea level at combat weight

Maximum thrust A/B lit	700	Kt.*
Maximum thrust A/B not lit	675	Kt.

True airspeed in level flight at 50,000 ft. at combat weight

Maximum thrust A/B lit	1,147	Kt.*

CEILING

Combat ceiling at combat weight, rate of climb = 500 F.P.M.

Maximum thrust at optimum Mach No. = 1.8, A/B lit	61,050	Ft.

RATE OF CLIMB

1) Steady rate of climb at sea level, combat weight

Maximum thrust at Mach No. = .92, A/B lit	44,600	F.P.M.
Maximum thrust at 527 kt. T.A.S. A/B not lit	18,600	F.P.M.

2) Steady rate of climb at 50,000 ft., combat weight

Maximum thrust at Mach No. = 1.8, A/B lit	10,330	F.P.M.

TIME TO HEIGHT

Time to 50,000 ft. Mach No. = 1.5 from engine start at gross take-off weight

Maximum thrust A/B lit	4.8	Min.

MANOEUVRABILITY

Load factor at combat weight

Maximum thrust at Mach No. = 1.5 at 50,000 ft. A/B lit	1.62
Maximum thrust at Mach No. = 1.8 at 50,000 ft. A/B lit	1.77

★ AIR 7-4 PLACARD SPEED

TAKE-OFF DISTANCE

Take-off distance over 50 ft. obstacle at sea level at gross take-off weight (67,505 lb.)

Maximum thrust A/B lit, standard day (+ 15°C)	4,000 Ft.
Maximum thrust A/B not lit, standard day (+ 15°C)	5,070 Ft.
Maximum thrust A/B lit, hot day (+38°C)	4,870 Ft.

LANDING DISTANCE

Landing distance over 50 ft. obstacle at sea level at normal design landing gross weight — 5,260 Ft.

STALLING SPEED

True stalling speed in landing configuration at combat weight at sea level — 117 Kt.

RANGE

1) **Subsonic High-Altitude Mission - Subsonic Combat**

Start weight 67,505 lb.
Climb at 527 kt. T.A.S. to 35,000 ft.
Cruise out at Mach No. = 0.905 at 35,000 ft.
Climb at Mach No. = 0.92 to 50,000 ft.
Combat for 5 minutes at Mach No. = 0.92
Cruise back at Mach No. = 0.905 at 39,000 ft.
Loiter at 39,000 ft. for 15 minutes
Land with 5 minute fuel reserve.

Range 589 nautical miles

2) **Subsonic High-Altitude Mission - Supersonic Combat**

Start weight 67,505 lb.
Climb at 527 kt. T.A.S. to 35,000 ft.
Cruise out at Mach No. = 0.905 at 35,000 ft.
Accelerate to Mach No. = 1.5 at 35,000 ft.
Climb to 50,000 ft. at Mach No. = 1.5
Combat for 5 minutes at Mach No. = 1.5
Cruise back at Mach No. = 0.905 at 39,000 ft.
Loiter at 39,000 ft. for 15 minutes
Land with 5 minute fuel reserve

Range 506 nautical miles

3) **Supersonic (Mach No. = 1.5) High-Altitude Mission - Supersonic (Mach No. = 1.5) Combat**

Start weight 67,505 lb.
Climb at Mach No. = 0.92 to 35,000 ft.
Accelerate to Mach No. = 1.5 at 35,000 ft.
Climb at Mach No. = 1.5 to 50,000 ft.
Cruise out at Mach No. = 1.5 and 50,000 ft.
Combat for 5 minutes at Mach No. = 1.5
Cruise back at Mach No. = 0.905 at 39,000 ft.
Loiter at 39,000 ft. for 15 minutes
Land with 5 minute fuel reserve

Range 358 nautical miles

4) **Supersonic (Mach No. = 1.8) High-Altitude Mission - Supersonic (Mach No. = 1.8) Combat**

Same as 3 except:
Accelerate to Mach No. = 1.8 at 35,000 ft.
Climb at Mach No. = 1.8 to 53,000 ft.
Cruise out at Mach No. = 1.8 at 53,000 ft.
Combat at Mach No. = 1.8 at 53,000 ft.

Range 338 nautical miles

5) **Combat Air Patrol - Supersonic Combat (M = 1.5)**

Same as 2, except that an extra 3,900 lb. of fuel carried in ventral drop-tank (weight 342 lb.) which is jettisoned just before acceleration to Mach No. = 1.5 at 35,000 ft.

Range 623 nautical miles

6) **Subsonic Low Level Mission (10,000 ft.) - Subsonic Combat**

Start weight 67,505 lb.
Climb at 527 kt. T.A.S. to 10,000 ft.
Cruise at Mach No. = 0.7 at 10,000 ft.
Accelerate to Mach No. = 0.92 at 10,000 ft.
Combat for 5 minutes at Mach No. = 0.92
Climb to 39,000 ft. at 527 kt. T.A.S.
Cruise back at Mach No. = 0.905 at 39,000 ft.
Loiter for 15 minutes at 39,000 ft.
Land with 5 minute fuel reserve.

Range 396 nautical miles

7) **Ferry Mission (No armament)**

Start weight 70,411 lb. (ventral tank carried throughout)
Climb to 35,000 ft. at 527 kt.
Cruise climb to 40,000 ft. at Mach No. = 0.905
Loiter over base at 40,000 ft. for 15 minutes
Land with 5 minute fuel reserve

Range 1,500 nautical miles

Fuel density 7.8 lb/gal.

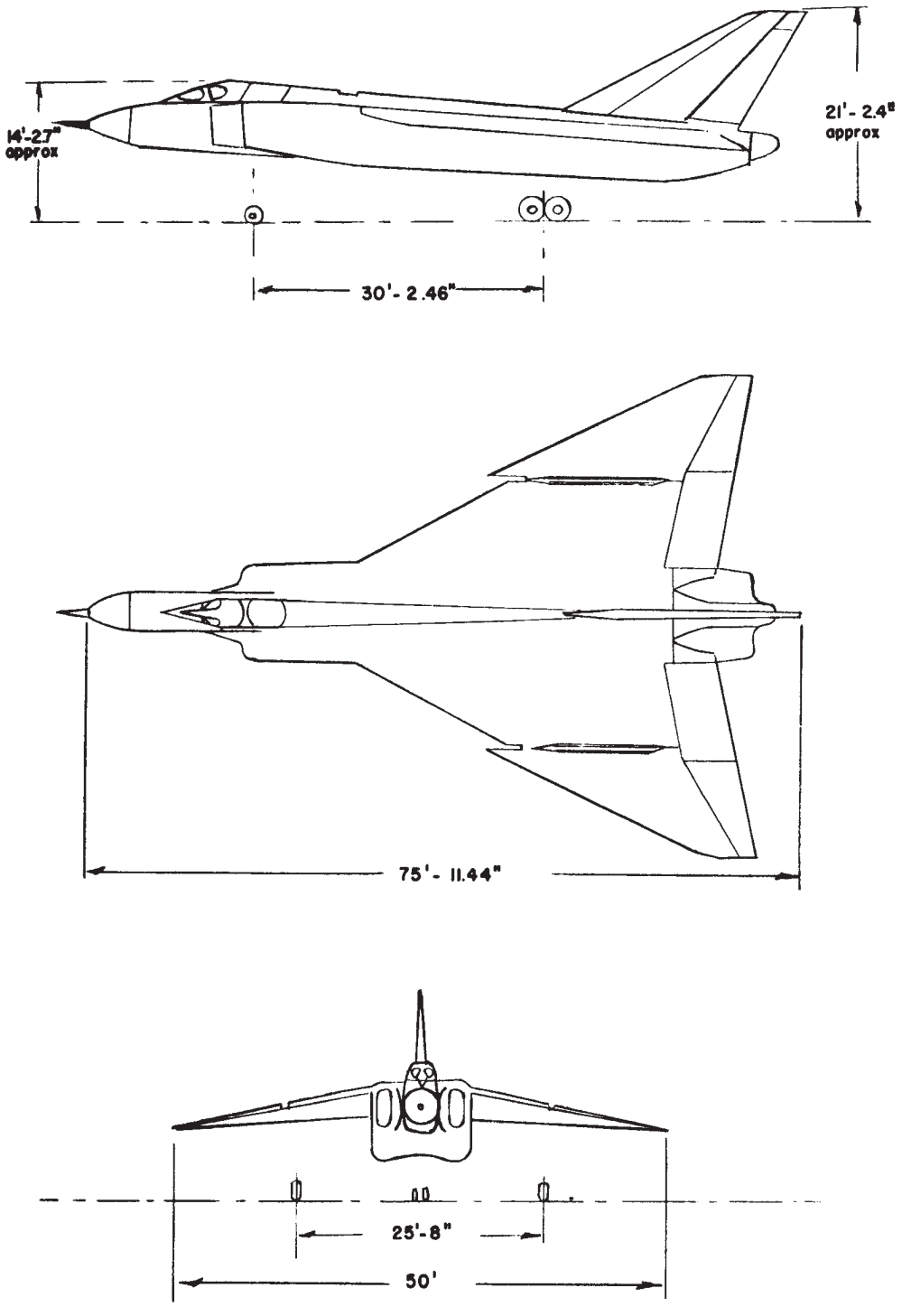

FIGURE 3 – The CF 105 Interceptor

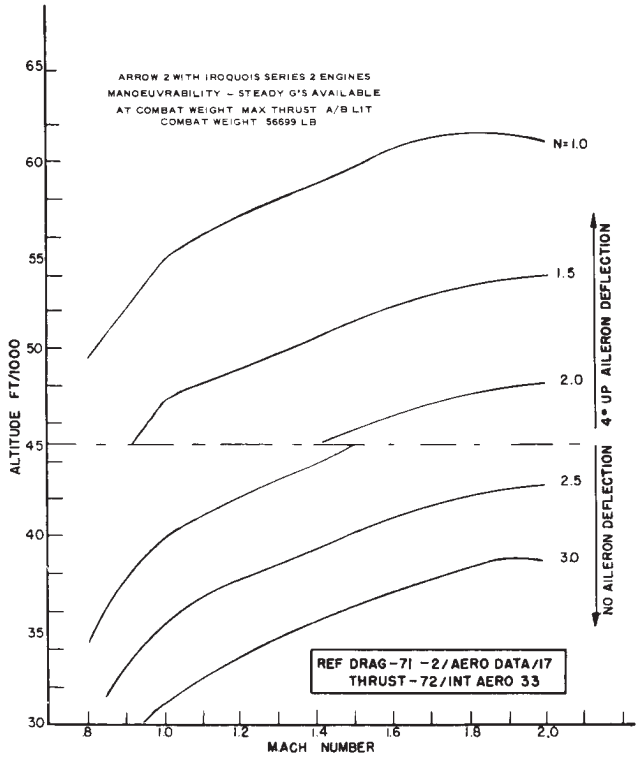

FIGURE 4

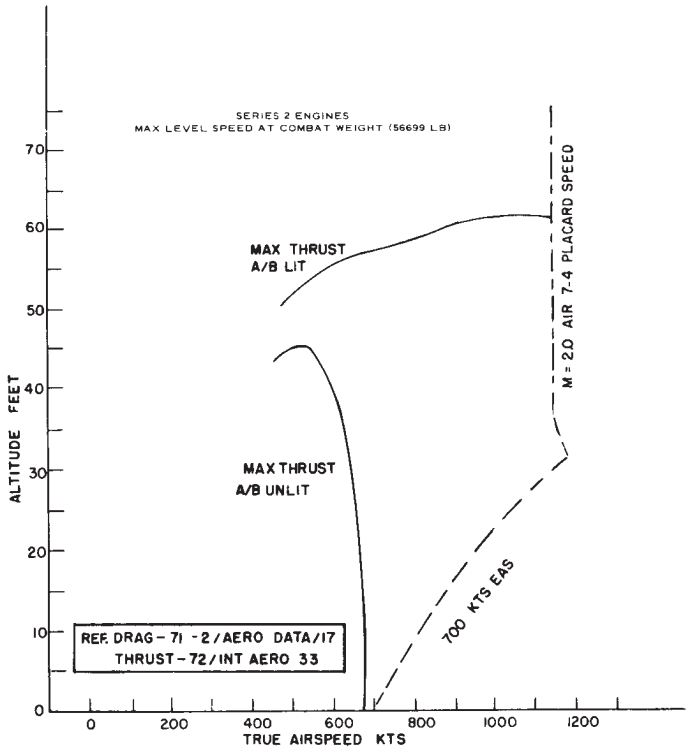

FIGURE 5

THE ASTRA I ELECTRONIC SYSTEM

The electronic system for the Arrow aircraft was to be designed and developed by the Radio Corporation of America and was to be called the ASTRA I. In concept it was to be a modern electronic control system in which flight controls, navigation, target detection and tracking devices, armament firing functions, communications, and airframe were one integrated system.

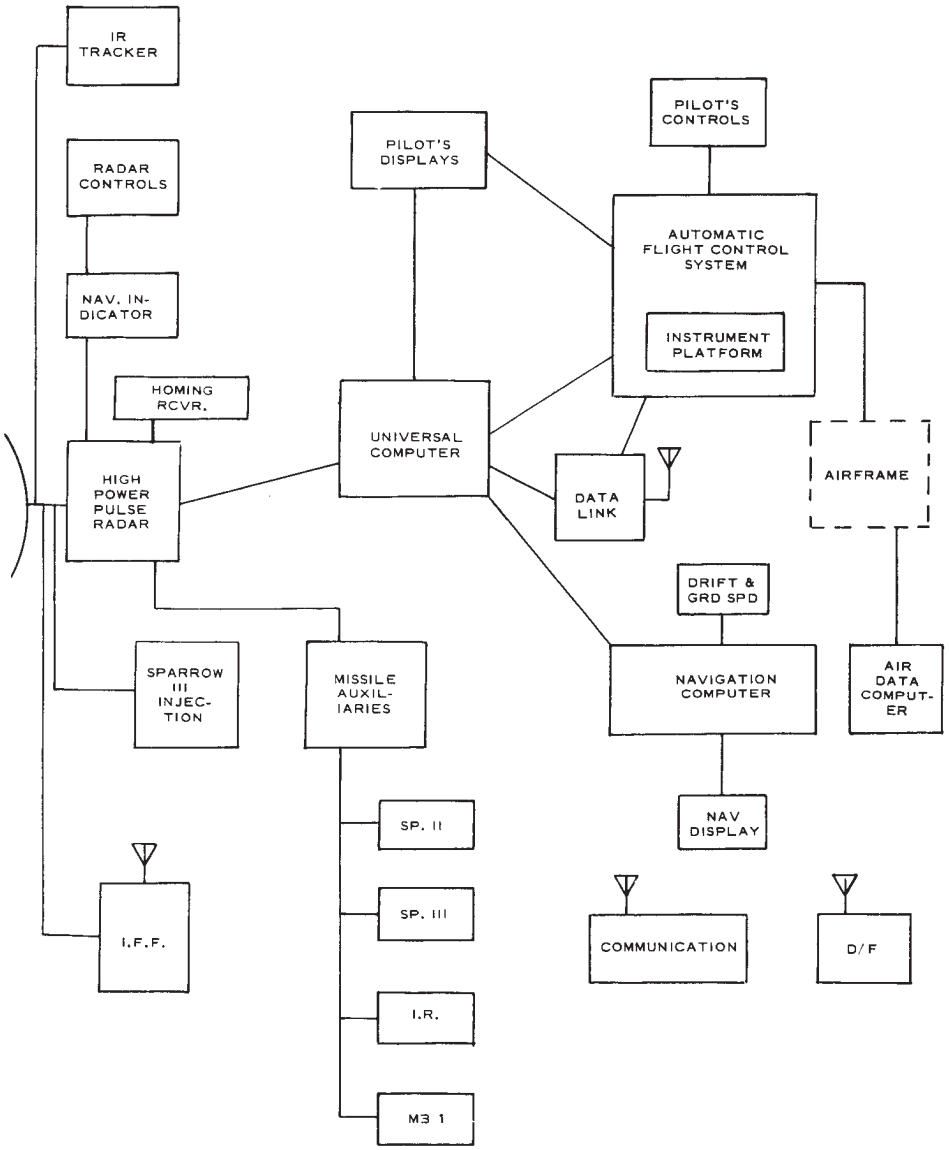

FIGURE 6 – Simplified Block Diagram of Electronic System

A simplified block diagram showing the principal system components appears in *Figure 6.* The RCAF specification to which the ASTRA I system was designed, required a detection range of 25 miles on a target of 5 square meter radar cross-section. This was to be provided by a high power pulsed X-band radar. The principal characteristics of the radar and the antenna were as follows:

Magnetron peak power output 1 megawatt

Frequency range 8800 – 9400 Mc/s

Search Mode P.R.F. 330, Pulse width 2.5μs

Track Mode P.R.F. 1000, Pulse width 0.5μs

AMTI P.R.F. 4000, Pulse width 0.5 μs

Antenna Diameter 32 in.

Antenna Gain 35 db

Antenna Beamwidth 2.7 degrees

Polarization completely variable

Tracking rate limits 0.1 to 228 degrees/second

Search Scan 140 x 13 degrees

Azimuth Limits ± 70 degrees
Elevation Limits + 75, – 45 degrees
} Rectangular field

Track Scan-Conical with 75 cps nutation rate, and 1.5db crossover

Max. Tracking Range 50,000 yd.

Receiver Overall Noise Figure 10 db

Variable frequency with random frequency programming to be used in the quasi-passive ranging mode.

The tracking circuits feature refinements such as Pulse Edge Tracking and Video pregating.

Hydraulically driven antenna

Range tracking accuracy of 20 yd. ± 1%

Max. opening rate 2,000 knots

Space-stabilized antenna

Snap-up mode.

In addition to active detection and tracking of targets, provision was made for passive tracking on ECM transmissions using a homing receiver, and for infra-red tracking using an infra-red detector slaved to the AI antenna.

Provision was also made in the missile auxiliary and fire control sub-systems for the use of Sparrow II and long range unguided rockets as armament. Both lead collision and lead pursuit attack modes were provided by the universal computer.

Automatic or manual interceptor control would be permitted at all times by the automatic flight control system which could combine inputs from the fire control computer, the air data computer, the data link, and manual controls. Appropriate filtering and limiting action was provided.

Using data from TACAN, the air data computer, data link or manual inputs, the navigation computer would be able at all times to determine the geographic position and the heading of the aircraft and to provide this information to the fire control computer, the navigator's display and the automatic flight control system.

TARGETS

Two classes of target, the high-subsonic swept-wing bomber and the supersonic bomber, were studied in the CARDE Assessment since both were considered as realistic threats for the operational period of the Arrow, which was assumed to terminate in 1970. The subsonic bomber should exist in large numbers until 1965 whereas the supersonic bomber may begin to appear in 1960. Other bomber threats of higher performance may also exist during this same period of time. These could be air-breathing unmanned aircraft of higher speed and altitude capability than the manned bombers studied in this evaluation. The sketch in *Figure 7* illustrates the time scale of various bomber threats which may have to be faced.

PERFORMANCE CHARACTERISTICS

(a) Subsonic Target – The subsonic bomber considered in the CARDE work was the Bear swept-wing turbo-prop bomber. Its salient characteristics are given in *Figure 8.*

(b) Supersonic Targets – No definite supersonic bomber has been designated to CARDE as representing a typical threat. Two basic types of high-speed bombers, having the same performance but different configurations have been proposed (see *Figures 9 and 10).*

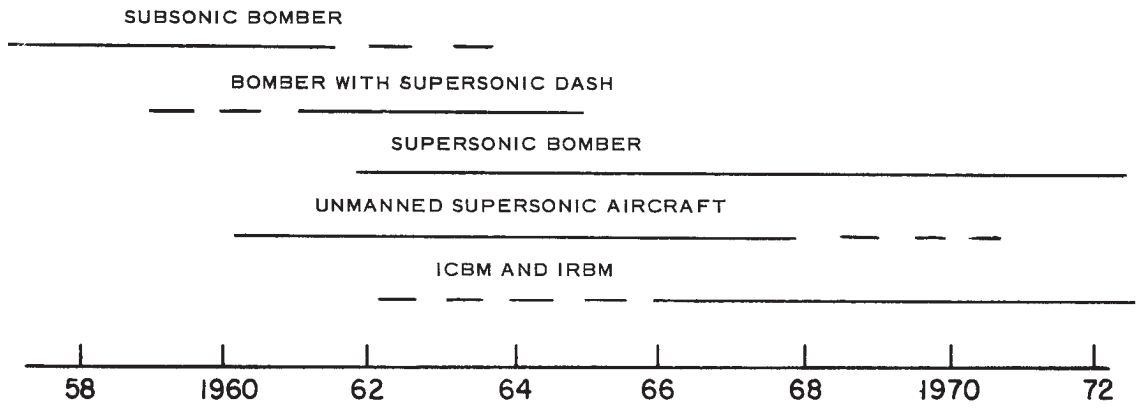

FIGURE 7 – Time Scale of Threat

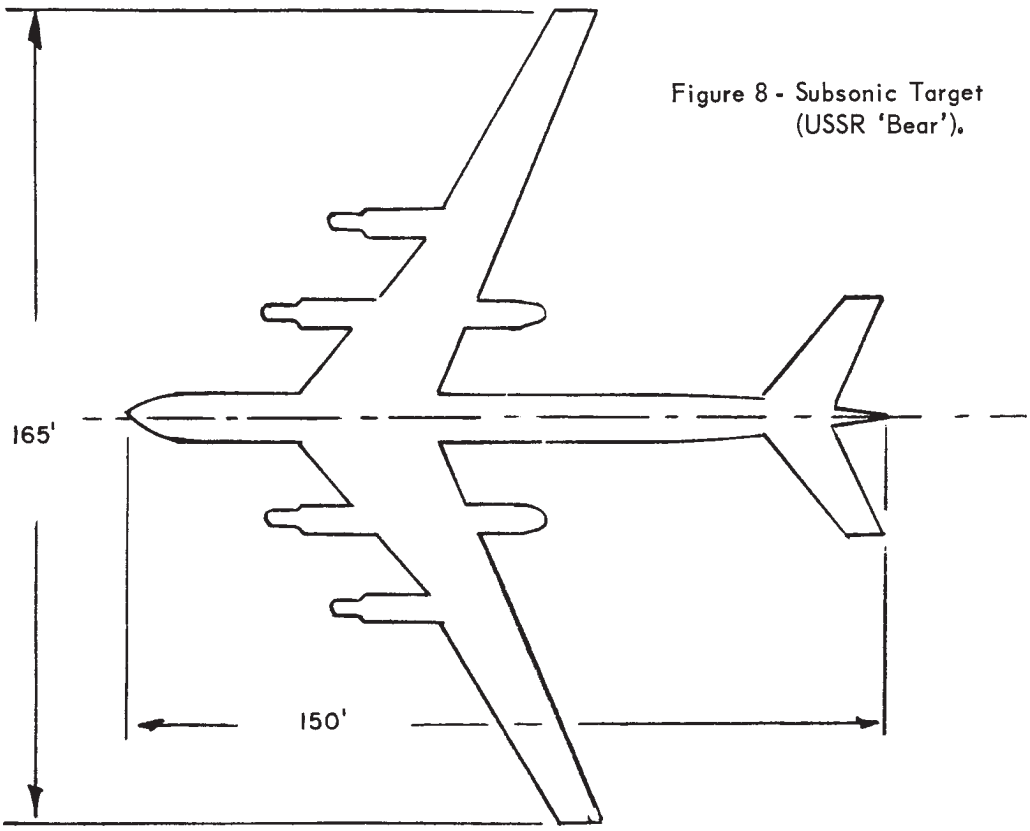

Figure 8 - Subsonic Target (USSR 'Bear').

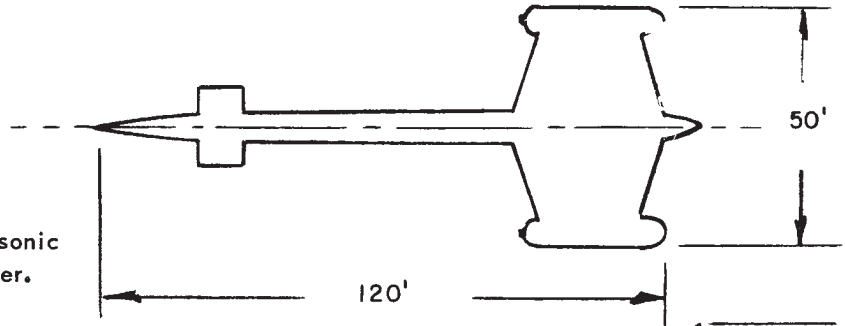

Figure 9 - Hypothetical Supersonic Straight Wing Bomber.

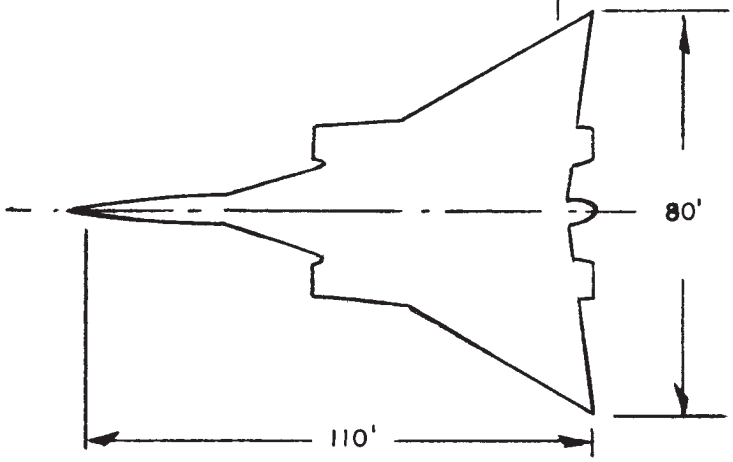

Figure 10 - Hypothetical Supersonic Delta Wing Bomber.

GROUND ENVIRONMENT

The ground environment in which the CF-105 interceptor would function was indeterminate at the time of the study. It could be similar to the present-day system which uses manual ground tracking of the target and voice link communication. Such a system can function with close or broadcast control, depending on the navigation capability of the interceptor. It was more probable that a semi-automatic or automatic system such as SAGE, BADGE or CAGE, where automatic tracking and data link for communication are used, would become available.

The CARDE assessment was not concerned with studies of possible ground environments. However, ground control accuracy was retained as a parameter so that, when the nature of the system and its performance were known, these data could be combined with the results of the CARDE study to determine the overall system effectiveness. Conversely, the CARDE results could be used as a basis for defining the ground control accuracy which would be required for the operation of the CF-105 interceptor system.

The measure of ground control accuracy used in this study is standard deviation, σ, of the displacement of the interceptor track, relative to the target, from the attempted line of approach. The component of position error along the interceptor track can only affect the time of interception and is not considered. Assuming that errors about the ideal line are symmetrical, σ is the half-width of the corridor in target space in which 68% of interceptors will be placed. This concept is illustrated graphically in *Figure 11*.

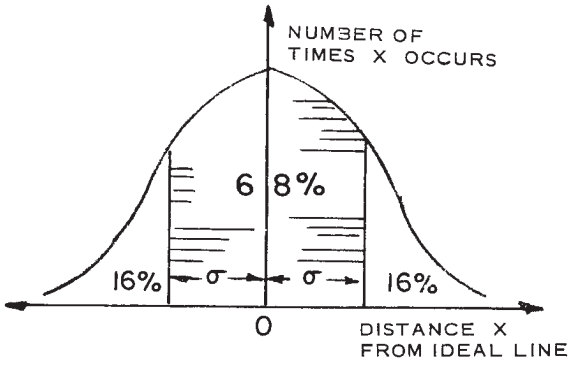

FIGURE 11 – Distribution of Interceptor Tracks.

The range of values assumed for σ throughout the CARDE study is from 1.5 to 9 nautical miles. Present-day ground environment can achieve a placement accuracy of about 3 miles for subsonic interceptors and bombers. As aircraft speed increases accurate placement becomes more difficult; more automatic methods should, however, reduce time delays and errors in ground control. It is felt that the range of values used during the CARDE study is realistic for the operational period of the CF-105.

ARMAMENT FOR THE CF-105

Provisions were made in the electronic system for launching MB-1 rockets, SPARROW II, and possibly an infra-red version of SPARROW.

Although the performance of these missiles for subsonic launch against subsonic targets is well known, little information is available concerning their behaviour when launched at supersonic speeds against supersonic targets at high altitudes. However, as will be pointed out in chapter VI, the reasonable approximations which have been made should yield fairly accurate results.

CHAPTER IV – METHOD OF STUDY

INTRODUCTION

This chapter describes in some detail the method by which the results of the CARDE study were obtained. Particular attention is given to both hand and computer techniques by which the placement charts were derived. The methods by which the placement charts are reduced to placement probability and those of presenting the overall results derived from these charts are also described. In this chapter, the discussion of techniques is concerned only with the Al phase of the attack. Special methods used in studying the Weapon system and ECM are presented in Chapters VI and VIII respectively.

DERIVATION OF PLACEMENT CHARTS

The Al phase of the attack is conveniently studied by dividing space into regions

i) from which attacks can succeed,

ii) from which attacks cannot succeed.

These regions can be displayed on a placement chart. The chart is drawn in target co-ordinates for a given set of values of a large number of parameters. Quantities that must be defined before the positioning diagram may be drawn are:

a) Target Mach Number

b) Interceptor Mach Number

c) Initial interceptor course difference relative to target

d) Target evasion (lateral acceleration)

e) Interceptor lateral acceleration capabilities

f) Al radar look angle limits

g) Missile launch zone (allowable launch heading error, proper launch heading, and allowable launch range, functions of target aspect)

h) Steering law

The system of barriers obtained for one set of values of the parameters may appear as in *Figure 12*. The vector A indicates the initial heading of the interceptor, and T represents the target, with the launch zone of the missile drawn around it. The point P on the launch zone is that point at which the missile may be launched with the given initial heading – there is a region along the launch zone for which this heading is usable when the launch heading error allowance is taken into account. The line L is a relative approach line passing through the offset target, along which the interceptor may progress and arrive at this allowable region of the launch zone without turning. It may thus be called an ideal approach line, along which the ground controller tries to place the interceptor.

If the original fighter approach line L_1 is behind the correct line L and if the fighter is to enter the launch zone at a correct heading for some more astern aspect than P, a turn to starboard must be made. The barrier (a) is the locus of the last points at which the turn may be started if the fighter is to reach an allowable launch position. The turn may be started sooner, but not later: in this sense, the locus is a 'barrier'. A typical trajectory is shown for a fighter progressing along L_1.

Similarly, if the original fighter approach line is L_2, ahead of L, a port turn must be made to provide the correct final heading of the aircraft when it reaches an allowable launch range at some more forward aspect than P. The barrier for the port turn in *Figure 12* is (b), and a typical trajectory is shown for a fighter vectored so as to approach along L_2.

The extension to the rear barrier (a) is (c), which is a composite of three effects: AI look angle limit, relative speeds and allowable target penetration. The fighter which is approaching at the given course difference, far enough from L_1 to cross this line, must make a starboard turn before crossing it. This is necessary in order to keep the target in view throughout the turn and, also, in case of fighter speed disadvantage, to avoid passing the time barrier line (e) which is called a "Speed ratio" barrier. (The speed ratio barrier is a line behind which a fighter can never enter the launch zone because of speed limitations). This boundary (c) may be composed of a third barrier which is determined by the target penetration limit. In a sense this is a time barrier, in that the bomber must be intercepted in a certain time or it will penetrate an unacceptable distance into the defended zone.

The extension to the forward barrier (b) is (d) which is a line below which the fighter will not see the target with its AI radar. To keep the target in view, the interceptor must make a port turn before reaching this line.

Therefore, the curves (d), (b), (a) and (c) enclose a region in space in which the interceptor must be placed if its initial heading is A, to be able to launch its missiles. A similar zone can be outlined, then, for any initial course difference of the fighter relative to the target. *Figure 13* shows a typical family of barriers for several initial course differences, representative values of which are marked on the barrier systems. To determine the length of barrier which is of interest, i.e., to complete the closure, the radar range must be considered. This is a range limitation superimposed on the placement zone restrictions. See Section on AI Acquisition Range.

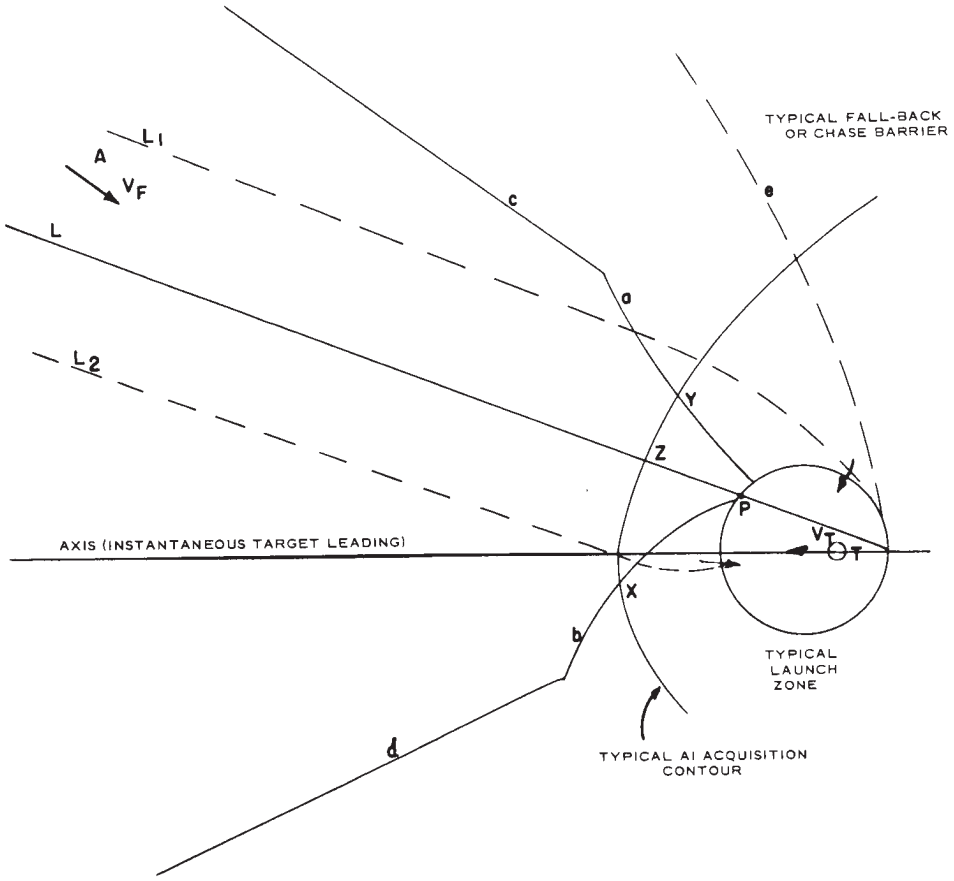

FIGURE 12 – Composite Barriers

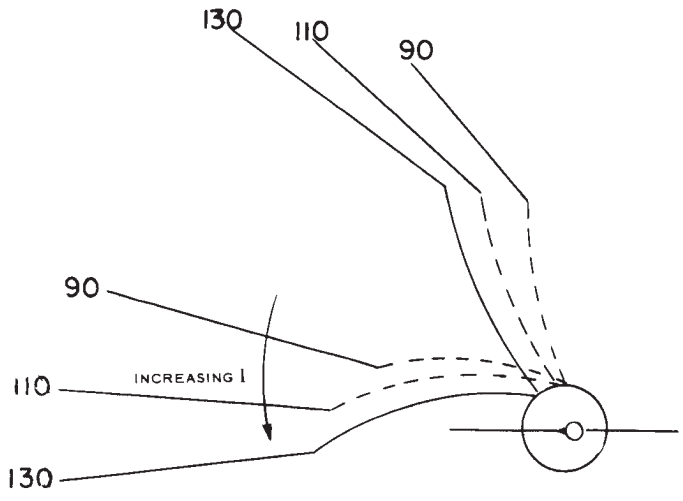

FIGURE 13 – System of Barriers for Different Course Differences Γ

PLACEMENT PROBABILITY

Although the ground control may roughly position the interceptor for its attack on the target, the final approach run must be made under the guidance of the aircraft's own AI radar; thus the correcting turn can only be made if the target is seen on the AI screen. The turn may be started with the AI on its search mode, or may be delayed until the AI is locked on to the target for automatic tracking, at the discretion of the pilot. Consequently, the width of the permissible placement zone inside the obtainable AI range determines the required GCI placement accuracy for a given probability of conversion from approach into attack.

The procedure for determining the probability of success in conversion is discussed in this paragraph . The AI detection range contour for the 50-per-cent level of probability of detection is drawn on the kinematic barrier system. A parallel contour, allowing for delay of the operator recognizing the blip or for delay in its appearance due to the AI scan time and for pilot reaction time, is drawn closer to the target. The separation of these two contours may represent the relative distance travelled by the fighter in 3 or 6 seconds flight time. Such a delayed AI contour has been drawn in *Figure 12* to illustrate the method. It represents average range at which corrective turn is initiated. It cuts the barriers and the ideal approach line at the points x, y and z. The half-widths xz and xy of the approach zones are measured, and these widths are compared to the standard deviation σ of the GCI placement errors which are assumed to be Gaussian. The ratios xy/σ and yz/σ are computed and, from a table of the probability integral, the corresponding probability of placement is found.

METHODS OF OBTAINING PLACEMENT CHARTS

The method of drawing placement charts for constant speed fighter and a non-evading target was outlined by Rand Corporation and other agencies. It was developed quite extensively in a CARDE study of the CF-100 and described in some detail in the report on that study (see Reference 27). This procedure will not be discussed here. However, most of the results in this report are based on a variable speed fighter and include manoeuvring targets. Different methods of obtaining the charts had to be devised and are described below.

The major portion of the placement work was done on a REAC Analogue computer. Some results were obtained by graphical means for a non-evading target and the procedure for drawing placement zone for these cases is first described. In the constant speed case, the fighter will turn in a circle and the relative trajectory as seen by the target will be a trochoid. A fighter like the Arrow decelerates in a high-g turn and the relative trajectory is a different spiral depending upon the fighter drag characteristics. These spirals were drawn by means of the REAC for various initial course differences with maximum permissible fighter turn rates. By course difference is meant the angle between the fighter and target velocity vectors, wherein a tail approach is taken as 0 degree course difference. A segment of a spiral is illustrated in *Figure 14.*

In this particular example the initial course difference is assumed to have been 160 degrees, and the fighter turned to reduce this angle. The course differences at various points on the path are marked along the top of the curve and the corresponding Mach numbers are indicated along the bottom. These spirals must be used in conjunction with an approximation to the missile launch zone in order to derive a placement chart.

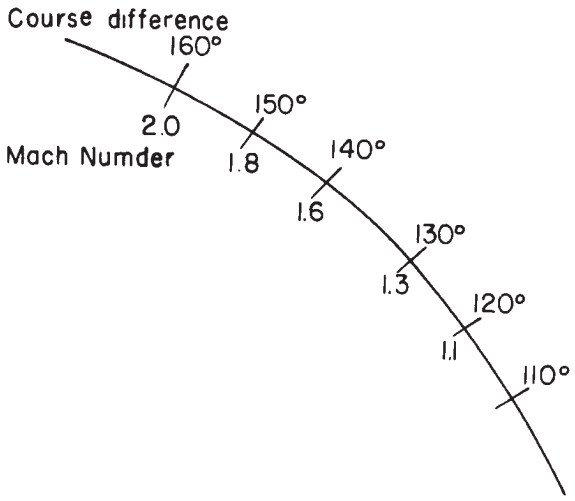

FIGURE 14

The concept of launch zone is described in some detail in Chapter VI. In deriving a placement zone by the method outlined here, it is advantageous to approximate the launch zone by a firing circle. This is a circle of radius $F + V_f T_f$ centered a distance $V_t T_f$ ahead of the target. Kinematically, the fighter is in an ideal firing position anywhere on this circle, if its speed is V_f, if it is heading towards the centre, and if T_f is the time the missile will take to travel a distance F relative to the fighter. In approximating the launch zone by means of such firing circles, circles are chosen which fit the maximum and minimum ranges of the actual launch zone. Actually, in constructing the placement charts, a series of concentric circles is required corresponding to various values of V_f. The ideal course difference at any point on these circles must also be known. A family of these circles is illustrated in *Figure 15*.

When constructing the placement chart, a point on the family of launch circles must be chosen such that the course difference of the fighter and target is just within the allowable launch error of the missile and the speed of the fighter is as indicated on this launch circle. These points are shown as squares in *Figure 15*. The point on the spiral corresponding to this Mach number and course difference is placed on the circle so that the course difference indicated on the spiral differs from that of the launch circle by an amount equal to the missile's heading allowance. If the point on the spiral corresponding to the initial course difference is noted, a point on the manoeuvre barrier is obtained. By choosing different values of missile heading, a corresponding fighter heading and speed can be found and one can work back along the spiral to the initial course difference and Mach number. This point on the spiral is also a point on the manoeuvre barrier. Look angle and fallback barriers are obtained in a similar way to that of the constant speed case except that the spiral trajectories must be used and attention paid to final Mach number and fighter heading. Families of these spirals for various initial course differences and Mach numbers have been published in Progress Report No. 2, (see Reference 14).

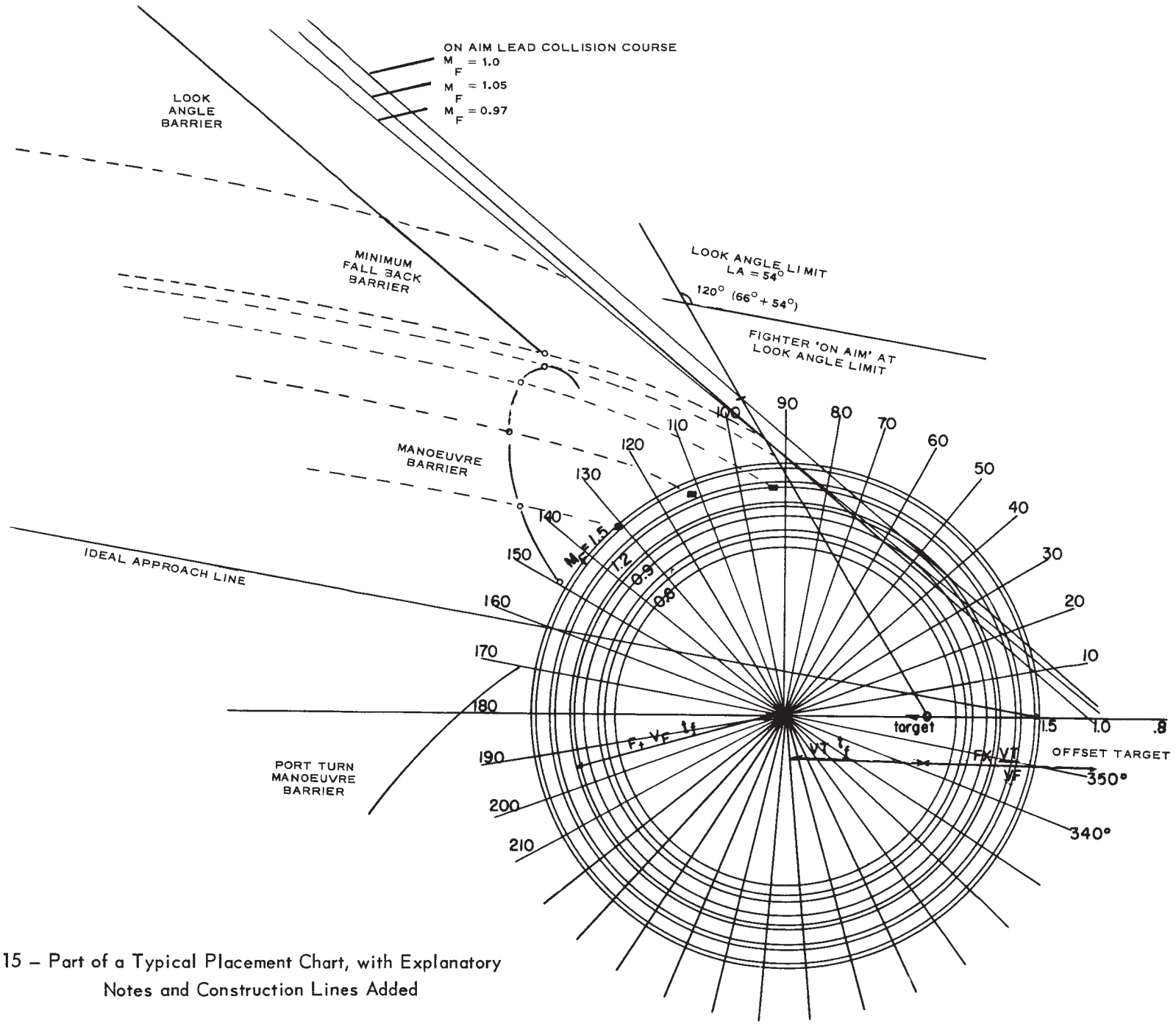

FIGURE 15 – Part of a Typical Placement Chart, with Explanatory Notes and Construction Lines Added

COMPUTER METHODS

Much of the work in deriving placement charts was done on the REAC Analogue Computer. The method was essentially a hit-and-miss process. In some ways it was the reverse of the paper-and-pencil method in that one started at a point somewhere in the placement zone and worked in towards the firing circle. For a given initial course difference and fighter speed some point in the placement zone was chosen, and the trajectory of the fighter, proceeding under lead collision control, was drawn. If the fighter reached the launch zone with the correct heading and speed, and if at no time during the flight the look angle limits of the radar were exceeded, then this flight was considered a success. A new initial point with the same range from target but different aspect angle was chosen and another run made. This procedure was continued until failure occurred and, in this way, the boundaries of the placement zone could be established. With some practice a fair choice of initial conditions could be chosen to limit the amount of runs. This REAC simulation included the following features:

a) Radar look angle limits, including the variation in the form of the antenna limits with bank angle
b) Blinding of the missiles by the fighter aircraft
c) Fighter drag and thrust characteristics
d) Choice of navigation laws
e) Target manoeuvre
f) Interceptor manoeuvre capabilities as a function of Mach number.

There was no attempt to simulate the dynamic response of either the interceptor or the fire control system. At first a single time lag was employed to cover pilot response time, system lags and aerodynamic lags. As high a gain as possible was desired because it was assumed that this case would most closely resemble the paper and pencil results which were thought to be near optimum. However, when a gain of 4 degrees/sec/degree error was used some compensating phase lead had to be introduced into the control loop in order to prevent oscillations about the ideal course. In practice, more complex time lags occur for which simple compensation cannot be made and a much lower value of gain (about 1/3 degree/sec/degree error) is used. In later simulation work, it was decided to leave out all time lags since those chosen were more or less arbitrary and added nothing to the representation of the true system. The simulated system with a gain of 4 degrees/sec/degree error and all time delays neglected is stable.

Ironically, checks made with a lower value of loop gain (about 1/3 degree/sec/degree error) gave higher values for placement probability, because smaller accelerations are required at critical points of the attack.

The fact that the interceptor slowed down during the manoeuvre was at first expected to cause some difficulties with the launch zones because the launching requirements depend on the interceptor speed. However, it was soon established that small differences in launch zone affect allowable placement zone boundaries very little provided the fire-control system and launch zone are compatible.

Simulation in the first year of the study was confined to co-altitude attacks. In the second year, a three-dimensional analogue computer model was built up to study climbing and snap-up attacks and a few more complex tactics. It was used to study navigation modes in the presence of ECM and also with infra-red guidance for the missile and for the interceptor. Look angle limits corresponding to the actual infra-red hardware limits were used; for example, the infra-red seeker mounted on the CF-105 vertical stabilizer could not be used if the target were below the interceptor because of airframe screening. The three-dimensional simulation is more fully discussed in Chapter VII.

AI ACQUISITION RANGE

The preceding section which discussed placement probability indicated the way in which AI acquisition range is used in conjunction with a placement chart to yield a probability of placement. Acquisition range is that range at which the AI radar, after detection of the target, may be locked onto it to provide steering instructions. In a track-while-scan or manual tracking mode, it would be defined as that range at which steering instructions can commence after detection of the target. It has been assumed in this study that the median value of acquisition range is equivalent to the range for 80-per-cent probability of detection. This assumption is illustrated in *Figure 16.*

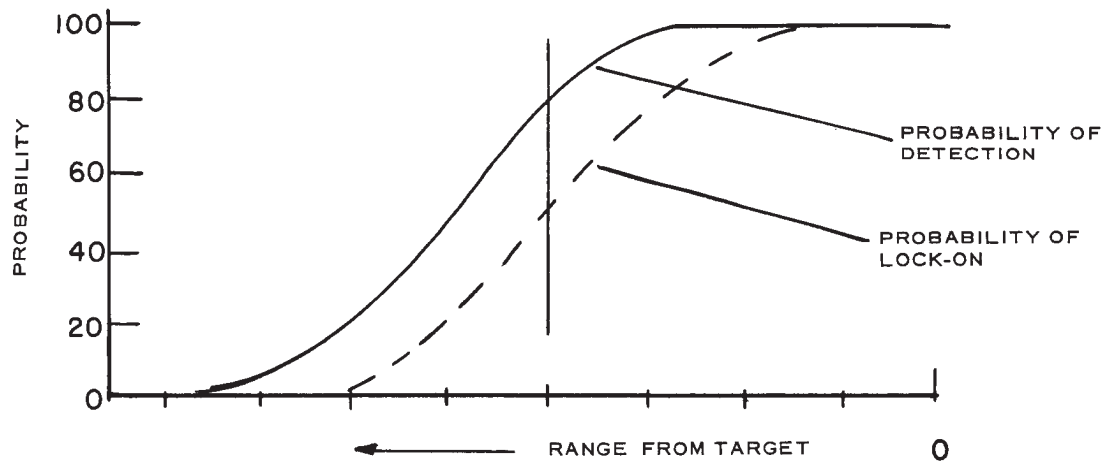

FIGURE 16

The actual range at which detection occurs depends on the equivalent radar cross-section of the target and, therefore, varies with the aspect angle at which the target is viewed. However, with an aspect of between 110 and 250 degrees the median acquisition range contours are roughly circular for all targets. *Figures 17, 18* and *19* show polar graphs of the expected acquisition range for three targets. The RCAF Specification for the ASTRA I requires a range of 25 nautical miles for 80-per-cent probability of detection of a target having a five-square-meter reflection area at X-band. The values of S shown on the polar charts represent the range that such a specification set would have on the particular target. This distance is assumed to be the average (50%) range for initiation of corrective manoeuvre. Interpretations for other values of range are as follows:

S: Range required by RCAF Specification.

1.92S: Range proposed by RCA for final development.
1.28S: Range proposed by RCA for the degraded system.

.85S: Various degradations of the specification which may be due to
6 S: maintenance, enemy countermeasures, atmospheric conditions,
.4 S: operator inexperience, or may represent range actually obtainable if the target has a smaller radar cross-section than that proposed here.

Semicircles are drawn on the graphs to indicate the 30-nautical-mile lock-on range capability demanded by the specification, and the 60-nautical-mile limit of the search presentation. The head-on values of lock-on range S for the two supersonic targets are 34 nautical miles for the delta wing and 21 nautical miles for the straight wing. Thus the range obtainable on the straight-wing target is about 0.6 of that for the delta, for the same radar performance.

The values for the B-52 aircraft are derived in part from those given in University of Michigan reports on Radar Cross-Sections. Any sharp peaks have been reduced or eliminated since such peaks, if only a few degrees wide, are of no use in positioning an aircraft by ground control because of the obtainable accuracy in placement and the variability in the position of these peaks due to pitch and yaw of the target.

Radar cross-section values used for the delta-winged aircraft are those for the Avro Vulcan medium bomber, taken from RRE reports. The median values were used.

Reflection area values for a straight-winged supersonic aircraft are purely hypothetical and represent a possible case. DRTE was consulted in establishing likely values.

The dependence of acquisition range on closing rate is not quoted in the RCAF specification. The value of closing rate, for the target and interceptor speeds considered in this study, varies from 3000 to 4000 feet/second only, so that the resulting uncertainty in the actual value of S in any case is not great.

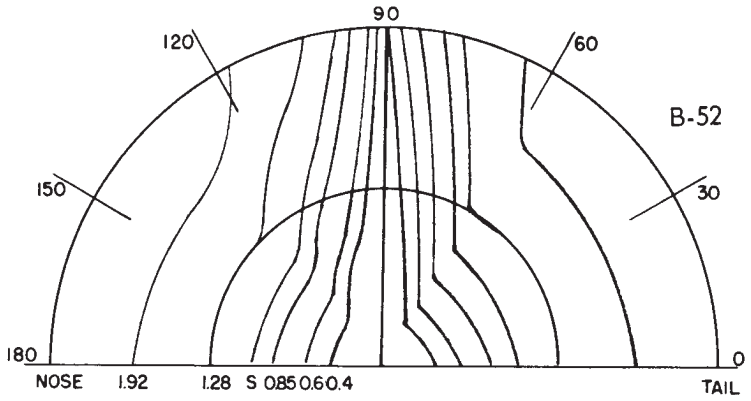

FIGURE 17

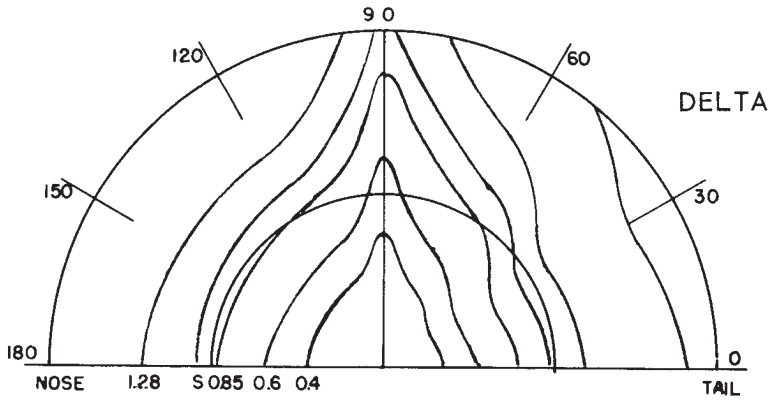

FIGURE 18

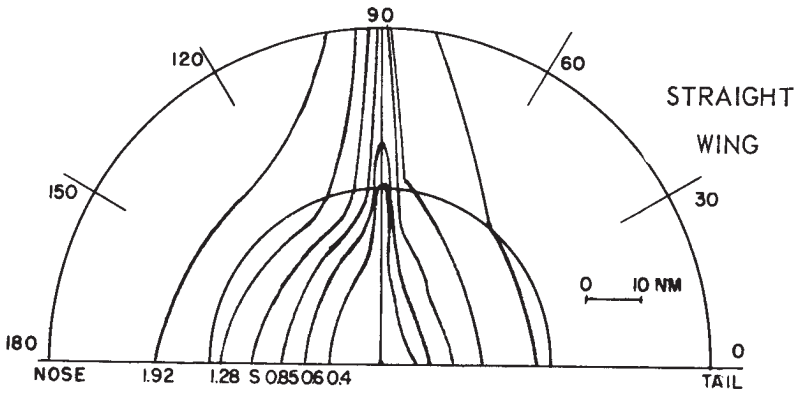

FIGURE 19

CHAPTER V – SYSTEM PARAMETERS

INTRODUCTION

This chapter reviews in some detail the effects on placement of the more important parameters of the system. The discussion in most instances is limited to two-dimensional considerations. Three-dimensional aspects of interception are discussed in Chapter VII. All results and discussions in this chapter are pertaining to supersonic bomber targets. The Arrow system has a high capability against subsonic targets. This threat is reviewed briefly in Chapter X.

Figure 20 is a representation of the many parameters which enter the study of interceptor placement. The parameters are arranged in a circle to stress the fact that no one factor can be considered by itself, and that the value of one parameter influences those required of all the others in order to obtain a desired system effectiveness. Statements in this report must therefore take a conditional form: if certain parameters have given values, certain conclusions can be stated. Where possible, expected values of the parameters are indicated. However, in most cases, a range of values was chosen so that if the situation changed, the results of the study would not be invalidated. This method of procedure indicates the sensitive and critical parameters of the system.

The parameters illustrated in *Figure 20* are considered individually in this chapter and in subsequent ones. Where possible a basic case was chosen for primary study and the effects of one variation at a time of parametric values, were investigated. Occasionally, two parameters were varied at once to find if there were cross coupling effects but, because of the considerable work involved, this effort had to be kept to a minimum.

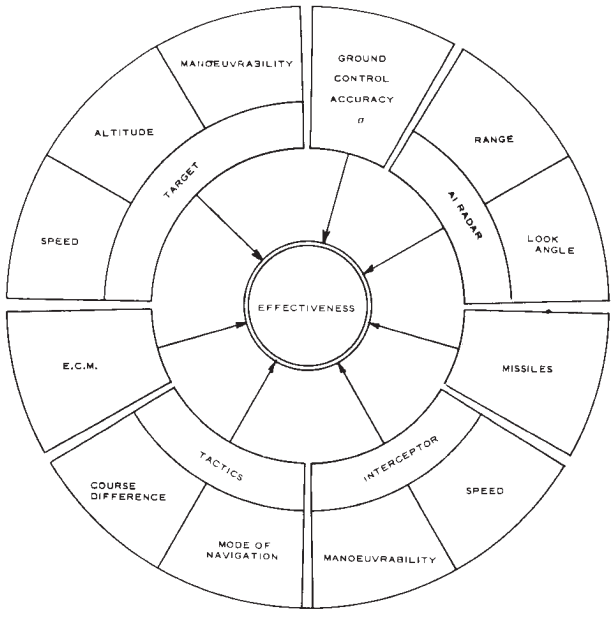

FIGURE 20 – Principal Parameters of the Interception Problem

The parameters which received the greatest attention in the study were AI range and ground environment accuracy (σ). The discussion in Chapter IV on the manner in which these parameters were derived and expressed should be consulted when reviewing the results in this chapter.

STANDARD VALUES

The basic case was essentially a tactical condition defined by altitude and velocity of target and interceptor. This case may be specified as follows:

Target – Speed: Mach 2
Evasion: Nil
Altitude: 60,000 feet
Configuration: Delta Wing
Nominal Radar Cross Section on Nose: 17.5 square meters

Interceptor – Initial Speed: Mach 2
Altitude: 60,000 feet

Treatment of this case was mainly concerned with the study of parameters AI range and σ and their contribution in producing (or failing to produce) high probabilities of placement. It should be emphasized that AI range was not in fact known with certainty, nor was the degradation to be expected from ECM definite. Hence a range of σ's and AI performances was taken.

PROBABLE VALUES OF σ

Information supplied by DSE indicated that, with a SAGE environment and no ECM, a vectoring error measured normal to the attempted approach path of 1.5 nautical miles may be achieved. Under ECM conditions, if good angle information is available, vectoring may be accomplished within 3 nautical miles. When the ground environment cannot supply angle information, the fighters have to proceed under broadcast control, being given only the general direction and heading of the threat. Although the largest vectoring error investigated in the CARDE study was 9 nautical miles, this is not to be taken as any indication of the accuracy to be expected under broadcast control.

DESIRED PLACEMENT PROBABILITY

The various probabilities that must be taken into account in determining overall interception potential are discussed in Chapter II. In order to get an acceptable figure of overall effectiveness all these probabilities must be high. As a working criterion in this study it is generally taken that a placement probability of 95% is required.

RESULTS FOR THE BASIC CASE

A summary of the results for the basic case is given in *Table I*. There are several ways in which comparisons of various situations may be made, such as

a) Values of parameter to give $P_p = 95\%$

b) Actual values of P_p

c) Allowable AI degradation

d) Permissible values of course difference

e) AI range required.

The method of evaluation used varied. *Table I* indicates values of placement probability to be expected. When this probability is essentially 100%, the allowable AI degradation which may be tolerated and still retain $P_p = 100\%$ is shown. Results are for three values of σ, with no target evasion.

TABLE I

PLACEMENT RESULTS IN THE BASIC CASE

Target — Configuration: Delta Wing
Speed: Mach 2
Altitude: 60,000 ft.
Nose aspect cross-section: 17.5 sq.m.
Evasion: nil

Interceptor — Initial speed: Mach 2
AI radar performance: Specification

Course Difference (degrees)	$\sigma = 1.5$		$\sigma = 3.0$		$\sigma = 9.0$	
	P_p (%)	Allowable AI Degradation (%)	P_p (%)	Allowable AI Degradation (%)	P_p (%)	Allowable AI Degradation (%)
180	100	60	100	42	88	None
135	100	60	100	37	82	None
110	100	32	93	None	62	None
75	68	None	59	None	42	None

The figures quoted in the main column of *Table 1* are for an unjammed AI radar. The degradation allowable for the value of P_p shown may be due to very mild ECM, equipment deterioration, or low value of target radar cross-section.

Whenever allowable degradation is greater than 40%, placement probability against the smaller cross-section straight-wing target is also greater than 95%. Typical values are shown in *Table II.*

TABLE II

STRAIGHT-WING TARGET

Target — Configuration: Straight Wing
Speed: Mach 2
Altitude: 60,000 ft.
Nose aspect cross-section: 2.5 sq.m.
Evasion: nil

Interceptor — Initial speed: Mach 2
AI radar performance: specification

Course Difference (degrees)	P_p for $\sigma = 3.0$ n.m. (%)	P_p for $\sigma = 9.0$ n.m. (%)
180	96	53
135	94	50
110	86	45
75	53	29

Conclusions that may be drawn on this basic case with no target evasion are listed below.

1. Provided the AI and the ground environment function, (σ = 3 nautical miles) the interceptor system is capable of intercepting the basic threat with a high-placement probability (greater than 95%).
2. Attacks may be made with course differences from 180 to 110 degrees.
3. For ($180° \leq \Gamma \leq 135°$) conversion is practically a certainty for either a Delta (nose cross-section 17.5 square meters) or a straight-wing (nose cross-section 2.5 square meters) target.
4. Under jamming of the AI radar the system has an unacceptable placement probability if only crossover techniques are used (See Chapter VIII).

AI RANGE

One of the more important parameters of an interceptor system is the acquisition range obtainable on the target. This parameter was taken as the basic variable in the study. In general, the raw data obtained from the placement charts were presented in graphical form as placement probability plotted against AI range. Families of curves for various values of vectoring accuracy of ground environment were plotted together. Other parameters are assumed constant. A few specific cases are illustrated and discussed in this section. Compilation of these graphs will be found in the Quarterly Progress Reports. For particular cases and for the data on which the material herein is based, the reader is referred to these reports. An attempt has been made therein to give a complete listing of individual cases.

Against a non-evading target probability of placement always increases with increasing AI range. *Figures 21* and *22* show typical graphs of P_p as a function of R. Usually the curve starts with a very steep slope, followed by a knee, and then a "plateau" or gradual increase to some maximum value.

It will be noted that in the case of a head-on attack this maximum is essentially 100%. The position of the knee on the curve is important since, in general, probabilities are good above the knee but critical below.

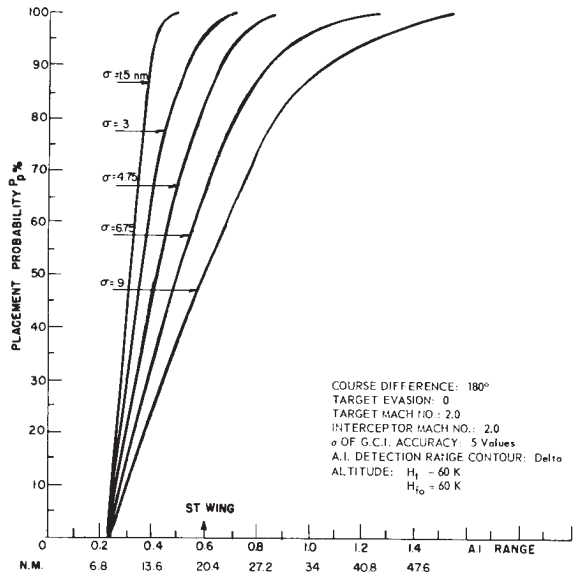

FIGURE 21

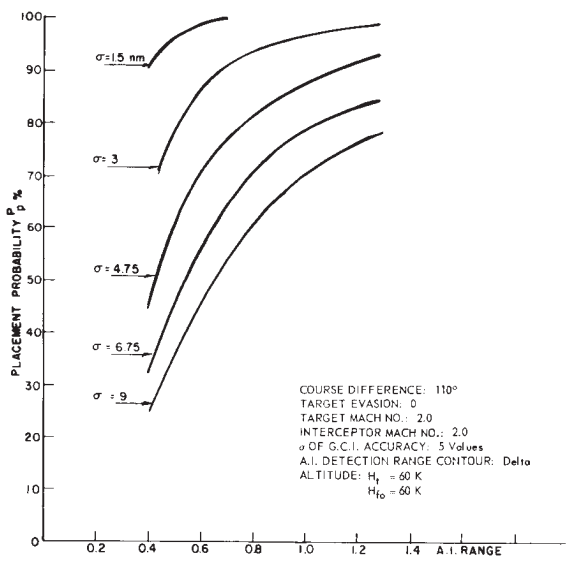

FIGURE 22

As an aid in visualizing the actual range a second scale in nautical miles has been placed on *Figure 21*. This procedure could be followed for a course difference of 180 degrees since the detection contour around the nose of the target aircraft is roughly circular. However, the actual ranges at near beam aspects change too rapidly for an average value to be taken. Therefore no second scale could be put on *Figure 22*.

The graphs shown are for a delta target. The results for a straight-wing target may be obtained by reading values at .6S as equivalent to S on the straight wing.

GROUND ENVIRONMENT ACCURACY (σ)

Ground environment or vectoring accuracy has been defined in Chapter III. It may be thought of as the second major variable employed in the study. Results were usually presented as in *Figure 21* where σ enters only as a running parameter. However, to illustrate the effect of this variable, graphs are plotted in *Figures 23* and *24* wherein σ is the abscissa. The results are for a head-on and a beam attack.

As would be expected, the placement probability improves with GCI accuracy (i.e., as σ becomes smaller). As noted above, it is assumed that the value of σ expected will be between 1.5 and 3 nautical miles. It should be observed, however, that the value of σ for any particular radar set is a function of target speed and increases linearly with target velocity.

ARROW SYSTEM REQUIREMENTS FOR AI RANGE AND GROUND CONTROL ACCURACY

The values of AI range performance and ground control accuracy, which are required to operate the Arrow interceptor adequately, are summarized graphically in *Figures 25* and *26*, which display "isoprobs" for the 95-per-cent level of placement for selected course differences and two-target speeds. Arrows indicate the expected ranges for delta and straight-wing targets and a probable value of σ.

It should again be stressed that the graphs shown in *Figure 25* are intended for illustration only and are chosen from the case taken as basic in this study. The actual values vary widely with interception conditions, and Progress Reports should be consulted for specific situations. Trends and results given in this report are to be considered as smoothed averages.

INTERDEPENDENCE OF PARAMETERS

In the first section of this chapter, it was pointed out that the numerous system parameters are interdependent and cannot be viewed in isolation, one from the other. Certain topics are more closely related than others. In particular, the factors of missile launch range, AI acquisition range, and interceptor manoeuvre capability must frequently be thought of together. *Figure 27* illustrates the regions of influence of these parameters in terms of range from the target. It is an attempt to show where the influences of the various parameters blend, and is to be considered as a descriptive item rather than quantitative data.

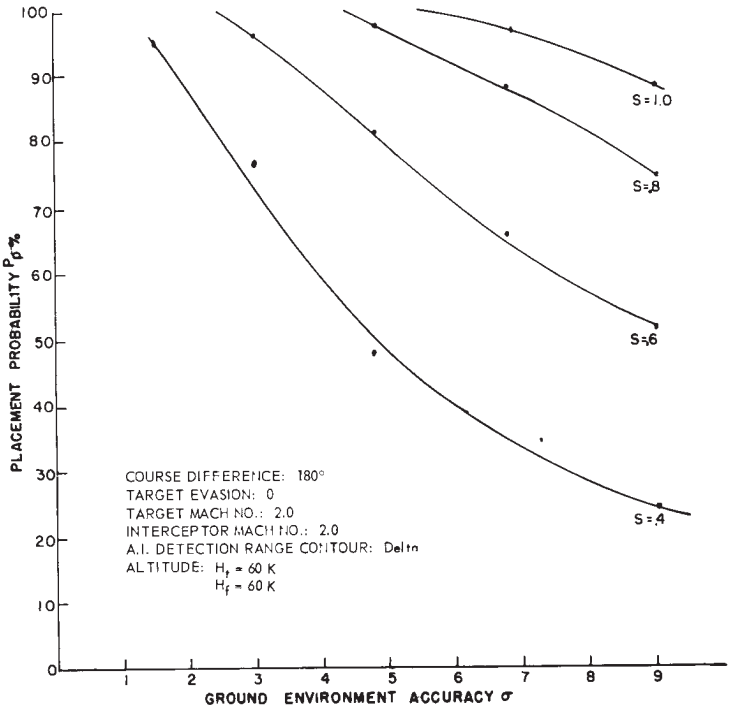

FIGURE 23

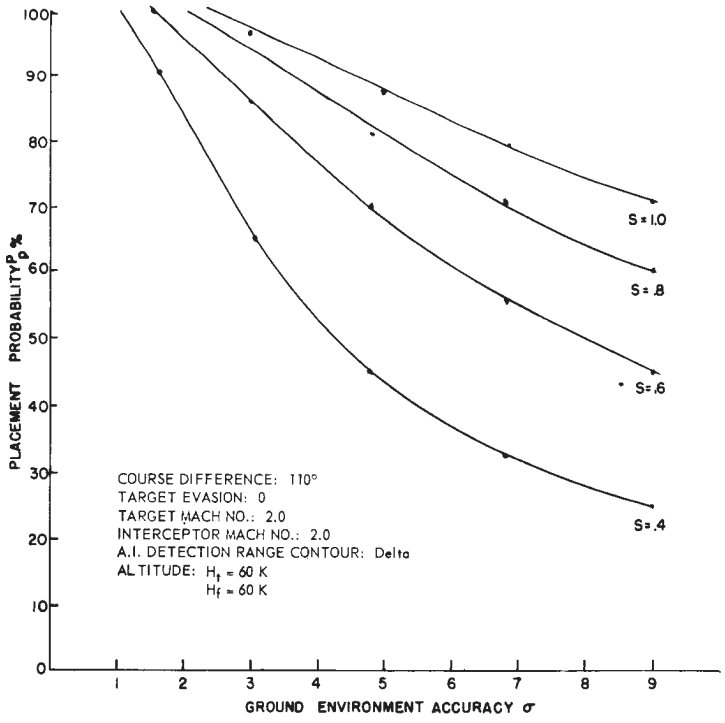

FIGURE 24

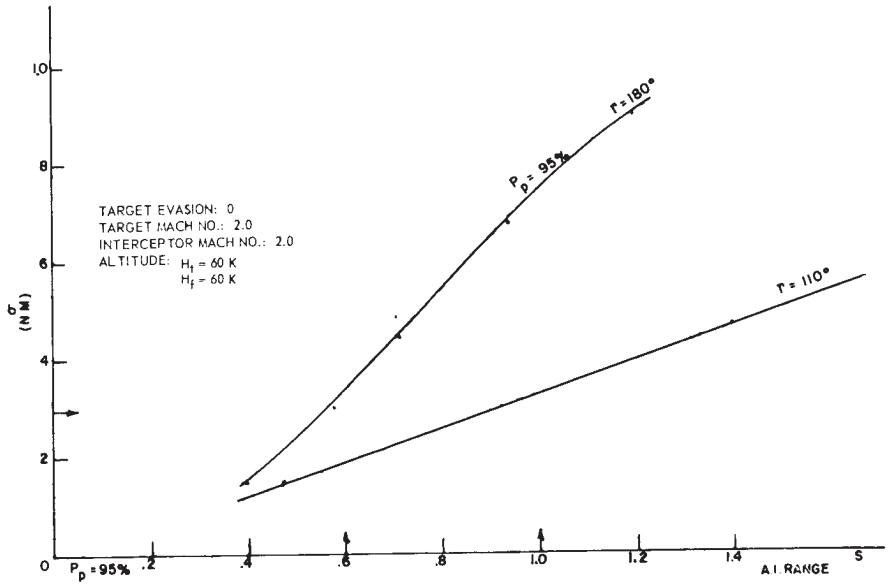

FIGURE 25

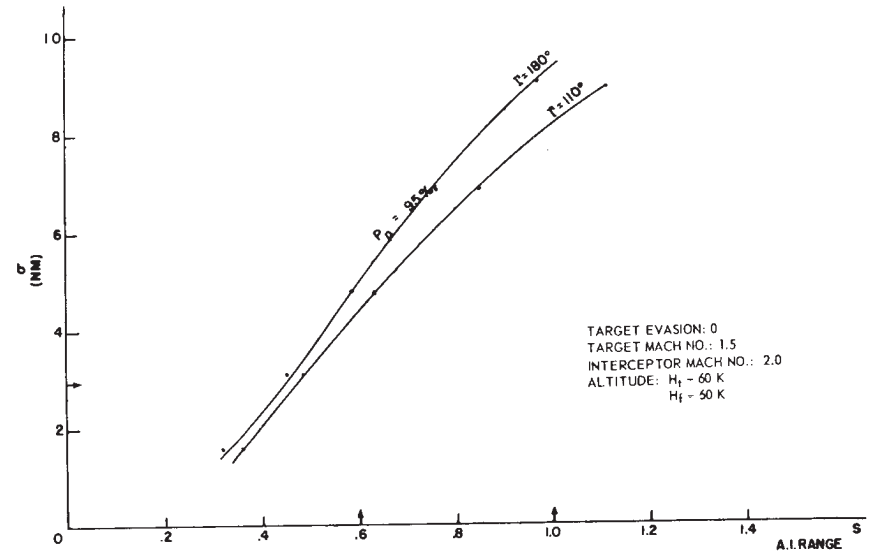

FIGURE 26

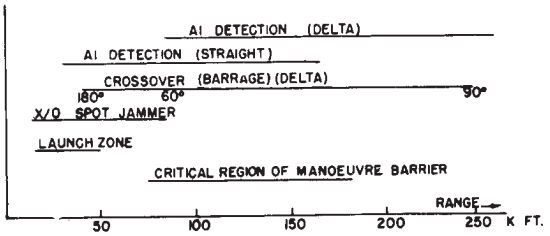

FIGURE 27 – Range Relationships

COURSE DIFFERENCE (Γ)

One of the main parameters in interception from the point of view of tactics is that of course difference. By course difference is meant the angle between the interceptor's velocity vector and the target's velocity vector. A tail attack is taken as a 0-degree course difference and a head-on attack as a 180-degree. The symbol for course difference is Γ. This parameter is especially important when the interceptor has a speed disadvantage compared to the target.

Talbe III summarizes the permissible course differences for the basic case, if a placement probability of 95% is required.

TABLE III

VALUES OF COURSE DIFFERENCE GIVING $P_p > 95\%$

Target — Configuration: Delta Wing
Speed: Mach 2
Altitude: 60,000 ft.

Interceptor — Speed: Mach 2
AI radar performance: specification

σ	Acceptable Course Difference
3 n.m.	$180^\circ - 110^\circ$
9 n.m.	None

Satisfactory results cannot be obtained with a course difference of less than 110 degrees unless the interceptor has a speed advantage. Referring again to *Figures 25* and *26*, one may use the contours of constant probability to examine the variation in required range and ground environment accuracy that is due to changes in course difference.

It will be seen that in all cases attacks at higher course difference require smaller values of AI range. Similarly, for a fixed value of AI performance, the placement probability is higher for head-on attacks. Comparing *Figures 25* and *26*, it will be seen that the amount by which P_p varies with Γ depends on the interceptor tactics used, attacks at higher initial closing speeds showing the least degradation for beam approaches.

Figure 28 summarizes the region of desirable and less desirable course differences. It also indicates that for course differences near head-on the aircraft operates in a region ahead of the bomber which is relatively free from the effects of chaff.

It should be noted that these conclusions are based on desirable course differences from the placement point of view only. They could be modified by the following considerations:

(i) The penalty of complicating the vectoring phase problem by demanding a given course difference.
(ii) The optimum missile attack direction based on lethality studies may be different.

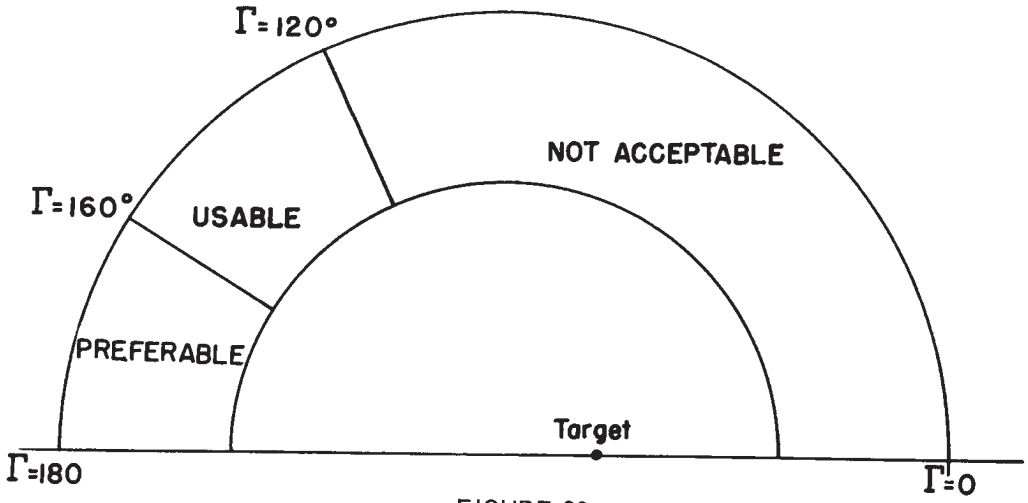

FIGURE 28

EFFECT OF ALTITUDE

Targets flying at lower altitudes than the basic case of 60,000 feet allow a better probability of placement, at least for the ranges considered. These included 40,000 feet, as the lowest value. Very low altitudes were not studied. Typical values of placement probability and allowable AI degradation are given in *Table IV* for equal speed, co-altitude attacks on a Mach 2 target at 50,000 feet.

TABLE IV

Course Difference (degrees)	$\sigma = 1.5$		$\sigma = 3.0$		$\sigma = 9.0$	
	P_p (%)	Allowable AI Degradation (%)	P_p (%)	Allowable AI Degradation (%)	P_p (%)	Allowable AI Degradation (%)
180	100	50	100	40	95	None
135	100	45	100	20	90	None
110	100	40	96	5	85	None

Similar results are obtained tor co-altitude, equal speed attacks on a Mach 2 target at 40,000 feet. Generally some 5% more AI degradation is allowable.

Figures 29 and *30* give contours of constant probability for co-altitude interceptions at different altitudes. These curves are interpolated values obtained from data derived from several forms of aerodynamics. In comparing *Figures 29* and *30*, a comment may be made that holds for many such situations, namely: if the particular condition is very bad from a placement point of view, variations of the parameter do not greatly improve the situation.

Targets above 60,000 feet cannot be attacked co-altitude but must be met by a snap-up or a climbing attack. These tactics are discussed in Chapter VII.

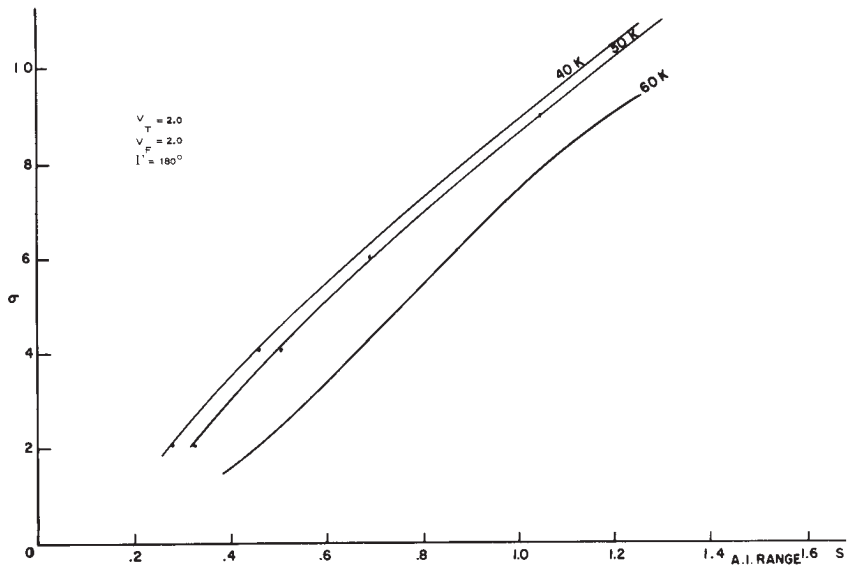

FIGURE 29

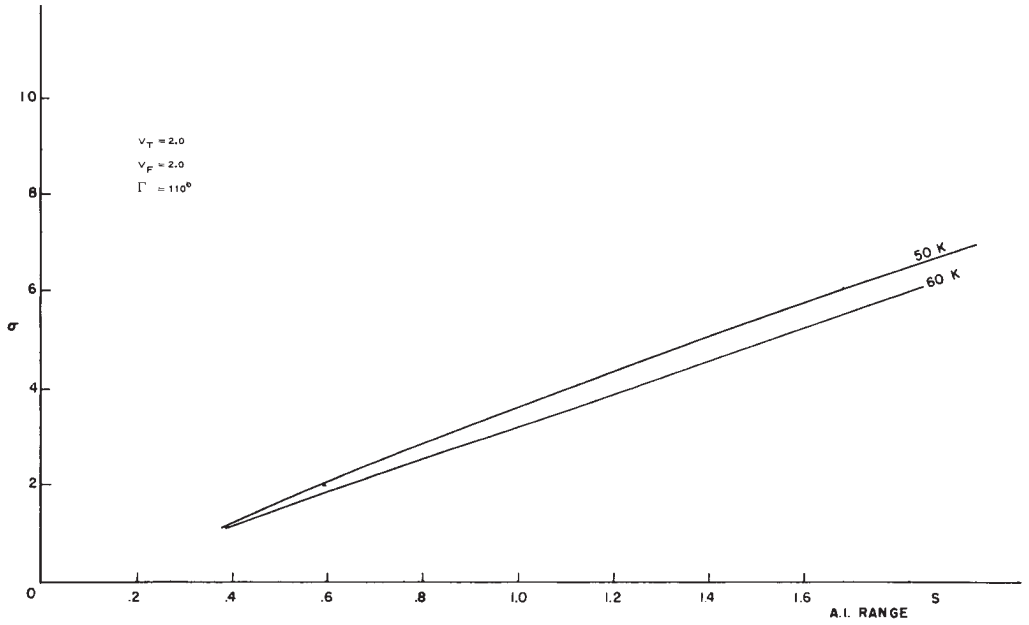

FIGURE 30

LOWER INTERCEPTOR SPEED

If the basic target (Mach 2 at 60,000 feet) is attacked by the Arrow with only Mach 1.5 initial speed, a definite degradation in placement chance is incurred. For a 95-per-cent placement probability the following circumstances are required.

σ = 1.5

AI range = .6S

Course difference = 180° – 110°

When the initial speed of the interceptor is low compared to the target, commencing manoeuvre at an extremely long range at a 60,000-foot altitude will lower the placement chance, since loss of speed in the turn causes the fighter to fall too far behind the target.

If co-altitude attacks are made at a 50,000-foot altitude, the reduction of initial interceptor speed to Mach 1.5 against a Mach 2.0 target does not degrade deplacement probability to the same extent as at 60,000 feet. Near head-on attacks a value of σ of 4.75 nautical miles allows a degradation in AI range of some 40% for a P_p = 95%.

For smaller course differences better vectoring accuracy is required so that at Γ = 110 degrees a value of σ = 3 nautical miles is required.

LOWER TARGET SPEED

If the Mach 2 interceptor makes a co-altitude attack on a Mach 1.5 target at 60,000 feet, placement chance is improved for smaller course differences. The situation is summarized in *Table V*.

TABLE V

MACH 2 INTERCEPTOR VS MACH 1.5 TARGET

Course Difference (degrees)	σ = 4.75 (%)	σ = 9.0 (%)
180 – 135	P_p = 100	P_p 95
110	P_p = 100	P_p 92
75	P_p = 98	P_p 83

INTERCEPTOR PERFORMANCE

The values of the aerodynamic coefficients changed from time to time, since the Arrow airframe was still under development when this study was being carried out. This factor allowed some comparison of aerodynamic data and their effect on overall system performance. Actually load factor and drag were the only aerodynamic factors employed. Quantities pertaining to the dynamic stability of the aircraft were not used.

The most important aspect of aerodynamics that is to be observed in placement studies of supersonic aircraft is that these vehicles slow down when they manoeuvre, i.e., a constant speed, constant load factor interceptor cannot be assumed. This fact was probably the most important single item that made this study somewhat different from other placement studies. It must be emphasized that the fighter's slowing down has a marked effect on placement probability, especially on beam attacks against a relatively fast target.

The actual difference in placement probability due to different aerodynamic estimates e.g., a change in overall load factor of .2 or .3 was not great. Usually the change was about 5% in absolute value of P_p. The effect became more marked when the value of AI range was small (e.g. .3 or .4S). This may be accounted for from two points of view. Considering the graphs of AI range versus P_p *(Figure 21)*, it will be seen that as AI range decreases, the slopes of these graphs increase, so that a small shift in the curve, the normal result of a change in aerodynamics, can cause a fairly large change, say 10 to 15% absolute in P_p at the lower end of the scale.

Another way of observing the same problem is to consider the actual placement zone. If AI range is large the fighter will turn far from the manoeuvre barrier and the effects of aerodynamics will not be very great. However, the actual manoeuvre barriers are determined by the interceptor's performance and, at low values of AI range, they are the predominant factor.

Some study was done on the effects produced on placement probability, by having the interceptor turn at less than the maximum available g's. The Arrow was assumed limited to 4 g's maximum load factor; however, turns at this rate cause considerable deceleration. In some cases, limiting of the interceptors g's to some lower value improves placement chance. Conclusions must be based on such information that is available to the interceptor, as follows:

1. The course difference is known, then the pilot could use the rule:

   180° – 135° – Pull maximum g's.

   110° – 90° – Pull less than g limit (about 2 g's).

2. If polarity of the steering signal is known, more improvement could be obtained by:

   a) pulling maximum g's if the lead angle is too great;

   b) pulling less than maximum (about 2 g's) if the lead angle is too small.

3. If information is not available for (1) or (2), it is usually better to always pull full g's.

If tactics (1) and (2) can be used at course differences equal to 90 degrees, some unacceptable cases of P_p equal to 70% can be brought up to 90%.

AI LOOK ANGLE

The AI look angle was taken as 70 degrees in most of the two-dimensional placement work and very little study was done on changing its value. Look angle barriers in the placement zone are described in Chapter IV. The comments presented in the preceding section on limiting the interceptor's lateral acceleration are closely tied with look angle, since a slower fighter more often will loose sight of the target. The required value of the angle between the direction of the interceptor track and the line of sight to the target, called the lead angle, is a function of the interceptor and target speeds, their instantaneous position and the attack mode. If the interceptor has a considerable speed advantage the lead angle need never be very large; for example, for a speed ratio of 3:2 it will never exceed 45 degrees. However, with equal speed interceptions, or with a speed disadvantage, the required lead angle may exceed the look angle limits of the AI radar.

The ideal approach line for lead collision courses is often situated towards the rear of the placement zone. Vectoring the fighter ahead of this ideal line often allows more room for manoeuvre, and placement probability is raised without serious effects arising from deceleration.

A more detailed discussion on the effects of the shape of the AI look angle pattern is given in Chapter VII.

CHAPTER VI – WEAPONS

INTRODUCTION

In evaluations of the placement probability during the AI phase, the effects of the aircraft armament enter through launch zone characteristics. In studying the probability of successful conversion, the launch zone may be considered as the target to which the interceptor must manoeuvre. For a rocket such as the MB-1, the launch zone is merely a firing circle determined by the relative velocity of the launch and target aircraft and the time of flight of the weapon.

In the case of a guided weapon, the missile launch zone is defined by the maximum and minimum ranges permitted for launch, and the allowable values of missile heading relative to the target course. These quantities for a given missile are functions of:

a) Target aspect

b) Target velocity

c) Target evasion

d) Target radar cross-section

e) Interceptor velocity at launch

f) Altitude of target and interceptor.

Launch zones may be drawn as a set of allowable values of relative heading which are a function of range, other parameters having fixed values. A typical allowable region is illustrated in *Figure 31*. In practice, a certain tolerance of missile launch headings will be required, say 5 or 10 degrees, and the maximum and minimum launch ranges used will be somewhat more restricted than the extreme values shown in the figure. The modified maximum and minimum range figures for different aspect angles from the target can be combined to give a polar launch zone as shown in *Figure 32*.

For determining the allowable heading error that is acceptable, a figure of approximately 10 degrees is usually taken, but this quantity actually varies with altitude, and the effects of this variation are discussed below.

These launch zones are defined primarily on a kinematic basis, but other factors may have a marked effect on the configuration. The maximum range may be restricted by insufficient seeker range while the minimum range may have to be increased by considerations of safety in interceptor breakaway.

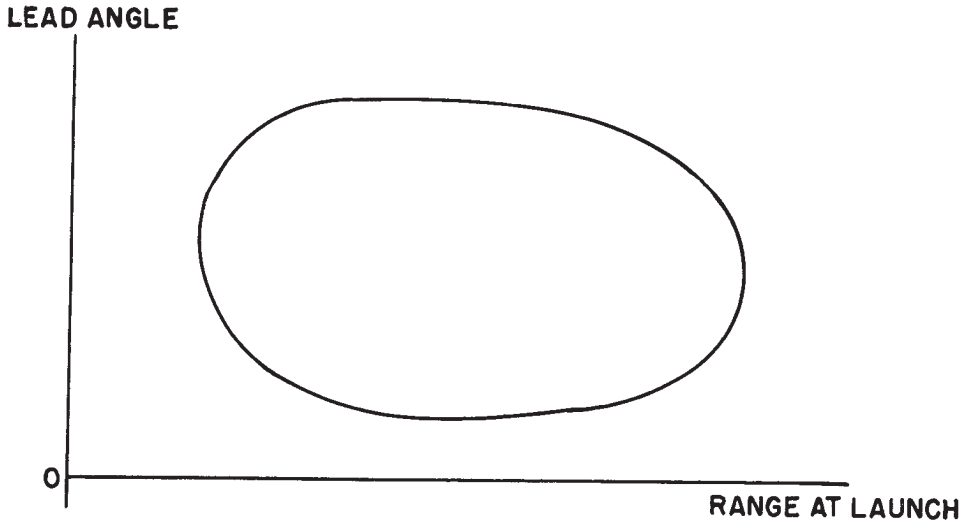

FIGURE 31 – Typical Allowable Launch Conditions for a Given Aspect

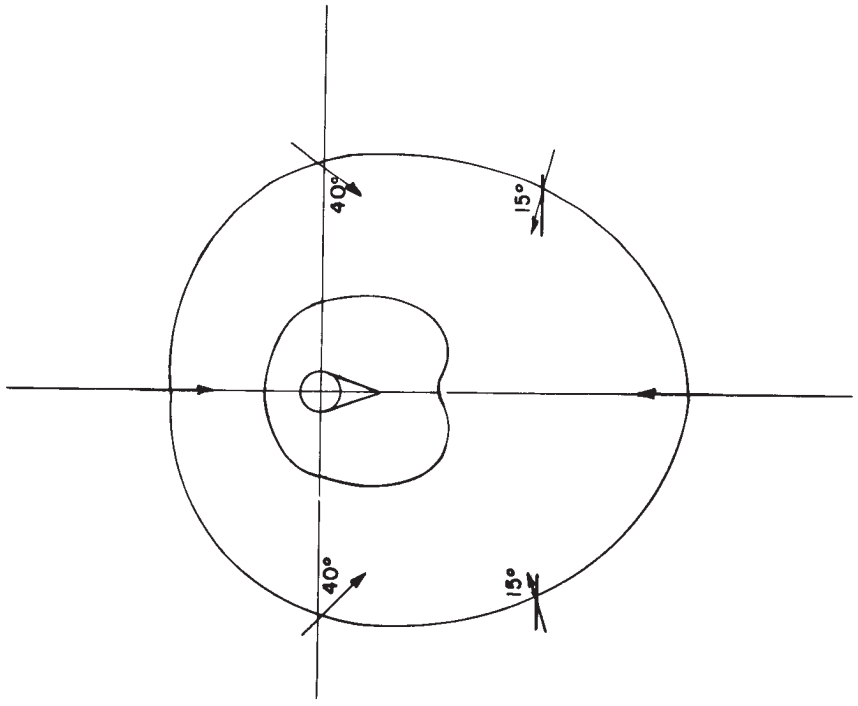

FIGURE 32 – Typical Polar Plot of Missile Launch Zone in Target Coordinates

The launch zones for a guided weapon are usually obtained by simulation of missile flights on an analog computer. The missile under consideration in this study was the Sparrow II. Sparrow III had been considered as an alternative in the early stages of the study, but was dropped later for two reasons:

a) It appeared that a firm decision had been made in favour of Sparrow II.
b) As outlined below, placement work is relatively insensitive to the weapon characteristics, and results in this study could not differentiate between Sparrow II and Sparrow III.

An alternate weapon which was considered in some detail was the MB-1 unguided rocket. The placement results for this weapon are given at the end of this chapter.

The emphasis of this study was placed on supersonic targets at high altitudes. In the beginning of the work, no information was available on the performance of Sparrow II under these conditions; therefore, an investigation was made on the REAC analog computer with a simplified model of the missile to determine typical launch zones. By running numerous trajectories, graphs of permissible heading error with range were obtained as illustrated in *Figure 31.* The boundary of the region depicted divides launch conditions into two zones: acceptable and unacceptable conditions. The criterion employed in determining acceptability requires some discussion.

Whether a given simulated run is classified successful or not depends on four factors:

a) Miss-distance

b) Time of flight

c) Closing speed

d) Absolute Mach number

A given simulated run can be classified as successful only if the terminal miss-distance is small enough for the fuse-warhead combination to destroy the target. However, full and accurate lethality data against the expected targets were not available and it was assumed, rather than proved, that 20 to 30 foot centre of gravity to centre of gravity miss-distances would be necessary for kill.

Large miss-distances may result from various conditions:

a) Inability of the missile to correct excessive launch heading errors.
b) Time of flight too long so that the supply of hydraulic fluid for wing deflection is exhausted before intercept.
c) Final closing speed so small that the time spent inside the blind range of the radar guidance is large enough for large errors to build up.
d) Missile speed is so small that control moment cannot provide sufficient manoeuvrability to correct heading error.

Each of these effects was taken into account in the missile simulation work.

The miss-distance obtained from any given launch condition will vary from run to run because of noise, radar scintillation, receiver noise, etc. For this reason, it is more meaningful to talk about miss-distance distributions than about values of miss-distance. For a missile like Sparrow II, simulator runs with noise indicate that the miss-distance distribution remains uniform and acceptable as launch heading is varied about the optimum until too large a value of heading error is reached, when the dispersion displays a marked change for the worse. One criterion for acceptable miss-distance is that the conditions at launch are satisfactory as long as this uniform distribution is obtained. Douglas Aircraft have, in fact, used such a criterion in two-dimensional simulation of Sparrow II, demanding that 10 out of 10 runs from given launch conditions yield miss-distances of less than 15 feet. Another way of approximating these results is to establish a zone wherein the miss-distance is less than 25 feet without noise and to reduce the width of this zone by about 3 degrees to allow for the effects of noise. Studies by Douglas have indicated that this procedure was acceptable and it was used in CARDE REAC work. Both the Douglas Aircraft Company and CARDE employed a two-dimensional simulation to obtain launch zones, and it was felt that, to as close an approximation as is required in placement work, the two-dimensional launch zones could be used for three-dimensional attacks and this was verbally confirmed by Douglas.

Placement studies of constant speed interceptors against non-evading targets can be done by pencil and ruler methods. For such work actual polar launch zone contours of maximum and minimum range could be used.

For placement zone work on the REAC, lead-collision navigation of the interceptor was simulated, and to optimize the lead-collision courses flown, it was necessary to know missile flight time, t_f, and flight distance relative to the launching aircraft F. For any given set of the parameters, aspect angle, target velocity, interceptor velocity, altitude, etc., values of t_f and F can be chosen which will give a lead-collision course terminating in launch from the centre of the corresponding launch zone. Unfortunately, for the best results, the t_f and F values used should be functions of the above set of parameters. Again, if the values of F and t_f are chosen to give the ideal heading at the centre of the launch zone, launch heading errors will occur at launch ranges greater or smaller than the optimum however well the interceptor is controlled. Two questions arise: (i) is it better to launch immediately upon entering any part of the launch zone, or would it be preferable to wait for a few seconds until conditions are nearer the ideal?, and (ii) should there be modification of the lead-collision steering inside the launch zone to ensure nearly ideal heading from maximum to minimum launch range?

When the study was being carried out, no method of overcoming these problems in the weapon system itself had been definitively adopted. Therefore, some broad simplifying assumptions about the form of launch zones were made for the majority of the REAC placement studies and these were justified by a limited series of more detailed studies.

The following assumptions were made:

i) The missile would always be launched for constant time of flight, t_f

ii) The missile relative flight distance F, was assumed to be constant. Therefore, the ideal launch heading angle can easily be computed as

$$\theta = \sin^{-1} \frac{V_t}{V_f + F/t_f} \text{ Sin A}$$

where V_f = Fighter velocity

V_t = Target velocity

F = Flight distance of missile relative to fighter

t_f = Time of flight of missile to impact

A = Aspect angle measured from target

θ_i = Ideal interceptor lead angle

$V_f + F/t_f$ = Ideal Average missile velocity

F/t_f = Ideal average velocity of missile relative to fighter

T = t_f and the suitability of interceptor heading examined at this point.

The launch contour takes the form of a circle, called the F circle. *(See Figure 33).* This circle is centered at the intended collision point, which is a distance $V_t\ t_f$ ahead of the target's position at launch, and has a radius $F + V_f\ t_f$ (the fighter is at a distance F away from the collision point when the impact occurs).

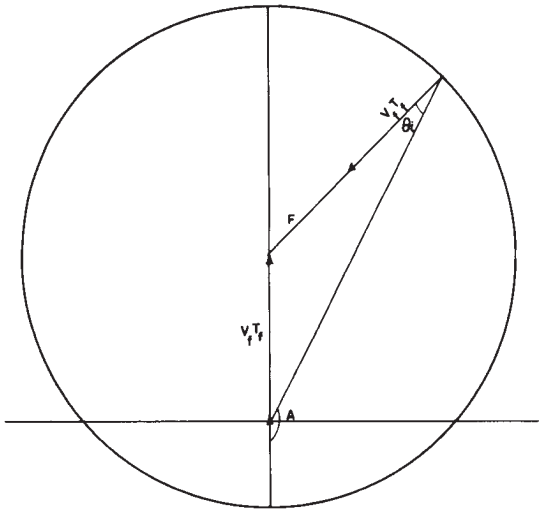

V_M = AVERAGE MISSILE VELOCITY

V_f = FIGHTER VELOCITY

V_t = TARGET VELOCITY

ΔV_M = INCREMENTAL MISSILE VELOCITY

FIGURE 33

EFFECT OF LAUNCH ZONE CHARACTERISTICS ON PLACEMENT PROBABILITY

In early work on constant speed fighters, the actual maximum and minimum range contours were used. These ranges were varied by rather wide amounts. It was found that placement probability was relatively insensitive to variations in launch zone parameters. The missile launch range was allowed to vary from 15,000 to 55,000 feet and the heading error from 5 to 20 degrees. *Figures 34* and *35* illustrate to what extent P_p is affected by these launch zone variations. In these graphs the R – σ plane is divided into regions. The absolute variation, which results from variations in launch conditions is shown for each region. This absolute value is expressed as a percentage of placement probability. Comparison of the two graphs shows that launch characteristics are more critical for course differences near 90 degrees than for those near 180 degrees.

These graphs indicate that if the system is operating very well in regard to AI range and vectoring accuracy, little is gained or lost by changing missile performance. If both AI range performance and GCI accuracy are poor, the situation cannot be saved by a moderate variation in missile kinematic capability. Only when the AI range is greatly degraded but the GCI accuracy is high, can the missile performance influence greatly the overall result. This may occur if the AI is jammed but the GCI is not. The manner in which the launch zone parameters affect placement probability for this case is described in the following paragraphs. The effects are greatest for values of σ between 2 and 4 nautical miles and for R = .4 S.

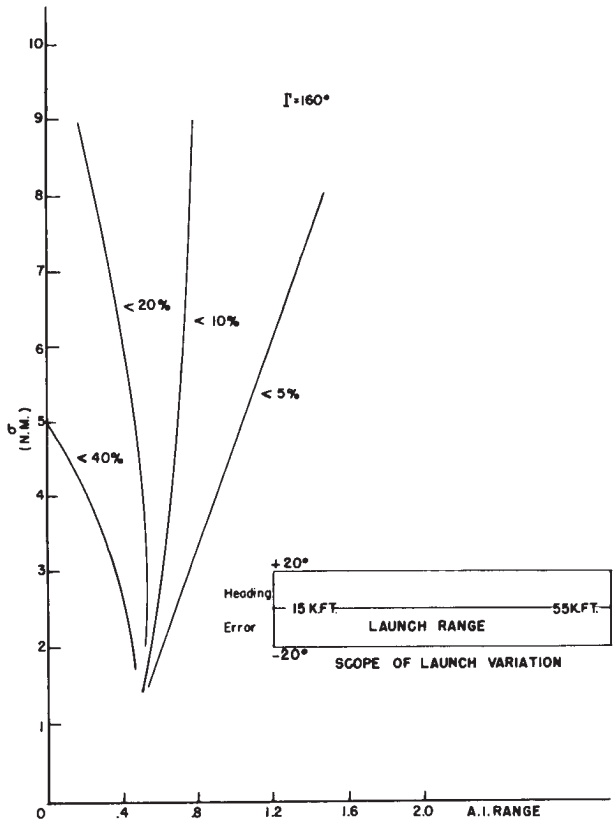

FIGURE 34 – Regions of Changes in P_p Due to Launch Zone Variation

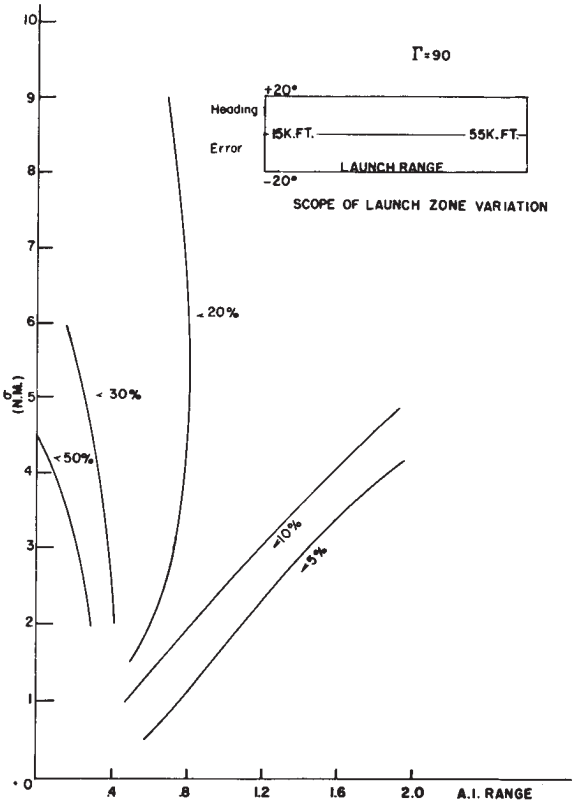

FIGURE 35 – Regions of % Change in P_p Due to Launch Zone Variation

HEADING ERROR

Changes in heading error allowance affect only the manoeuvre barrier of the placement zone. If the permitted error is greater, the manoeuvre barrier moves closer to the target and P_p increases for AI acquisition ranges within this region. The trend is still more pronounced for manoeuvring targets. *Figure 36* shows the magnitude of variations in P_p for typical cases for values of heading error between 5 and 20 degrees. These cases should be considered as illustrative only since they employ a constant fighter speed and are not comparable to the standard cases. From work done at Hughes Aircraft Company and a brief check at CARDE, it appears that increasing the heading error allowance above 20 degrees has little effect.

LAUNCH RANGE

A change in missile launch range affects the manoeuvre and the fall-back barriers. When the AI acquisition contour intersects the manoeuvre barriers, decreasing the missile launch range increases the placement probability. For an evading target, this effect is reversed: an increase in launch range increases placement probability. In the results obtained in the study, the effect of launch zone parameters is so interwoven with effects of target evasion, that it is difficult to assign a definite magnitude to each one separately. In a typical case, with a target load factor 1.25, a change of 25,000 feet in launch range produces a variation of 20% in P_p for values of σ and R in the initial region being considered.

There is a rather pronounced decrease in P_p if the launch range approaches the AI acquisition range. As a rough estimate, for a 40-degree turn, a 50,000-foot separation between the AI contour and the launch range contour is sufficient to complete the conversion manoeuvre.

Greatest values of P_p for both evading and non-evading targets are obtained for a launch zone of greatest allowable depth between maximum and minimum range. However, this result may be of little practical utility. In paper-and-pencil methods, the use of a navigation law to guide the interceptor is very much in the background. It would require a rather complex navigation system to allow the interceptor to take advantage of the breadth and depth of the launch zone.

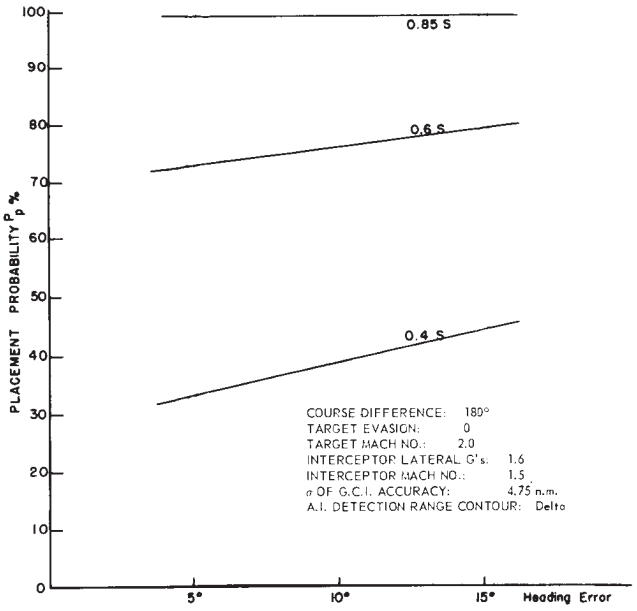

FIGURE – 36

VARIATION OF F CIRCLE

A change in the value of F-pole from 15,000 to 25,000 feet increased P_p by about 2% absolute. The larger F-pole was slightly better in all cases. For course differences of 110 degrees the results were not as definite when AI range was varied but, in general, they lay between plus and minus 4% absolute.

DEPTH OF LAUNCH ZONE

The concept of an F circle essentially means that the weapon is to be fired at one range only. The effect of introducing a maximum and a minimum range, that is, a launch zone with depth, is to increase the placement probability by about 2% for head-on attacks and by about 10% for beam attacks. See remarks at the end of the previous section.

MISSILE HEADING ERROR

It was stated earlier that the allowable missile heading error at launch was a function of altitude, although in some work it was taken as a constant e = ± 10 degrees. The difference between using a constant error and one that is a function of altitude was negligible for head-on attacks, except at AI ranges less than .5 S, when the difference may be of the order of 25%. The results are essentially the same for beam attacks but the difference is less marked for degraded AI ranges.

RESTRICTIONS ON THE LAUNCH ZONE

The probability of positioning an interceptor for missile launch is seriously affected if certain target aspects, or sectors, are prohibited. A typical example of such a restricted launch zone is that of a first generation infra-red missile, or of the Velvet Glove type fixed guidance head missile. If the permissible cone of attack is small, target evasion can produce nearly zero placement probability.

The Sparrow type missile has all-round launch capabilities. However, this requires that the missile seeker have sufficient range. If this guidance range is less than the minimum launch range as defined by dynamic considerations, the missile cannot be launched. This seeker range deficiency may exist at forward aspects for high interceptor and target speeds. The effect on the placement zone is illustrated in *Figure 37*. The central position of the zone is now forbidden, only the shaded portions being permissible initial interceptor positions. The typical resulting effect on P_p for a non-evading target is shown in *Figure 38*. For an evading target, the placement probability falls to zero if the front aspects are forbidden.

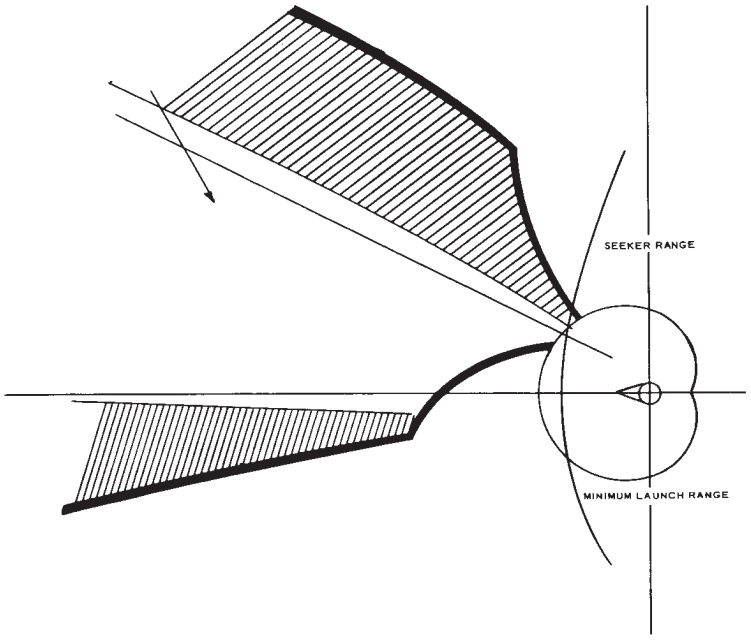

FIGURE 37 – Effect of Poor Seeker Range on Nose

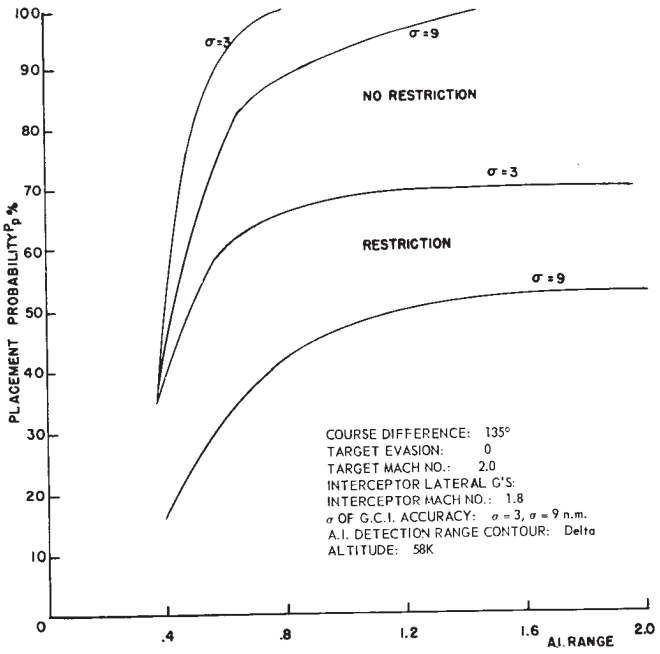

FIGURE 38 – Case wherein Missile Seeker Range is Limited on Bomber Nose

SUMMARY OF CONCLUSIONS ON LAUNCH ZONE EFFECTS

a) P_p is relatively insensitive to variations in launch zone parameters.

b) Consequently, the fact that only approximations to the Sparrow missile launch zones were used in the CARDE study does not invalidate the results.

c) If AI range is degraded but GCI accuracy remains good, a short launch range and a large heading error allowance increases P_p appreciably.

d) Increase in allowable missile heading error beyond 20 degrees does not increase the placement probability.

e) P_p is more sensitive to launch zone parameters for evading targets than for straight-flying targets.

f) P_p is more sensitive to launch zone parameters for beam attacks than for head-on attacks.

g) Variation in the value of F-pole used in lead collision navigation has little effect on P_p.

h) It would seem useful to have a missile with great depth of launch zone, where the maximum range is large and the minimum range is small. This will provide optimum launch range for both evading and non-evading targets. A change in navigation law from lead collision to lead pursuit at R_{max} would permit the fire control computor to use this depth.

i) It is most important that there be sufficient seeker range at all aspects.

INFRA-RED MISSILES

Some work was done on the effects of using an infra-red missile. The best information that could be obtained on the required launch zone indicated that it would be similar to that of the radar case, except that a 30-degree cone must be deleted from the nose portion of the zone. This 30-degree restriction is both vertical and lateral. Placement results for this case indicated that for co-altitude attacks, placement probability is very low, except for near beam-attacks ($\Gamma = 110°$). Here, for $P_p = 95\%$, σ of 1.5 nautical miles is required. Differential altitude of 10,000 feet does not improve the situation for either snap-up or climbing attacks. For differential altitude equal to 20,000 feet, snap-up attacks gave results which were as good as those for the radar missile because the launch took place outside the 30-degree restricted cone on the nose of the target. However, climbing attacks with a 20,000-foot altitude difference still gave poor placement probability.

SUMMARY

1. Co-altitude – low probability

2. $\Delta h = 10{,}000$ feet – no improvement

3. $\Delta h = 20{,}000$ feet climbing – low probability

4. $\Delta h = 20{,}000$ feet snap-up – high probability

PLACEMENT WITH MB-1 LONG-RANGE ROCKET

When considering the MB-1 rocket from a placement point of view, the only difference between this weapon and a guided missile is that allowable heading error is essentially 0 degree. However, placement probability does not vary too greatly with heading error so that placement results for the rocket are essentially the same as for Sparrow II. For the subsonic case of a target Mach number of .95, results in P_p are within 1% of the missile case, both co-altitude and snap-up attacks. Only at very low AI ranges (less than .2S) are changes more noticeable. Then, for σ = 1.5, degradation is about 5% and for σ = 3, degradation is about 10%. Placement probabilities for supersonic cases are outlined in *Tables VI* to *VIII*. Except for AI ranges less than .6S, they are identical with the missile case.

TABLE VI

$\Gamma = 135°$ $\Delta h = 0$

AI Range / σ	.2S		.4S		.8S		1.0	
	Missile	MB-1	Missile	MB-1	Missile	MB-1	Missile	MB-1
1.5	95	90	100	100	100	100	100	100
3.0	70	65	98	98	100	100	100	100
4.75	45	40	90	91	99	100	100	100
6.75	35	30	76	79	95	96	97	98
9.0	25	20	65	66	90	90	93	95

TABLE VII

$\Gamma = 110°$ $\Delta h = 0$

AI Range / σ	.4S		.5S	
	Missile	MB-1	Missile	MB-1
1.5	91	83	96	96
3.0	64	51	89	72
4.75	55	34	61	49
6.75	34	25	45	46
9.0	25	18	35	28

TABLE VIII

$\Gamma = 110°$ $\Delta h = 10{,}000$

AI Range / σ	.4S		.5S	
	Missile	MB-1	Missile	MB-1
1.5	95	85	98	95
3.0	75	55	84	84
4.75	56	35	70	65
6.75	41	25	68	49
9.0	34	20	48	38

The MB-1 does not present a placement problem. However, if allowable heading errors are very small, the stability of the fire control in maintaining the correct heading may be important. This aspect has not been studied at CARDE. Methods of homing under ECM conditions are discussed in Chapter VIII.

CONCLUSIONS

1. Under favourable conditions, placement probability for Arrow with MB-1 is as high as for Arrow with Sparrow.
2. Because of degradation under ECM conditions, tactical usefulness of MB-1 is doubtful.

CHAPTER VII – THREE-DIMENSIONAL ATTACKS

INTRODUCTION

So far the discussion has been mainly concerned with interception in a plane. However, an actual interception usually takes place in three-dimensions, and certain peculiarities may arise from the introduction of the third dimension which could have a marked effect on the attack. A fairly extensive study of the Al phase was made of the situation wherein the interceptor was assumed to be manoeuvring in three-space. The approach to the problem was essentially the same as in two-dimensions in that placement charts were constructed and reduced to probability estimates. All placement charts for this portion of the work were generated on the REAC.

The study was far from being exhaustive. Generally, it was considered that the interceptor started the attack from an altitude below that of the target and either pulled up or climbed to a suitable launch altitude. Attacks of this nature had received very little previous study, and therefore considerable exploratory work had to be done before the study proper could commence. Numerous situations in which the fighter performed complicated manoeuvres, such as diving turns, were not studied or were given only superficial consideration.

However, it is felt that the basic cases studied give greater understanding on aspects of an attack which heretofore have received very little detailed attention.

Some consideration was given to very high-altitude and very high-speed targets. It was assumed that if such targets were attacked, the interceptor could be equipped with weapons capable of operating at these altitudes and speeds. It must be emphasized that, to date, there is no assurance that such weapons do or could exist. However, limited studies were carried out to show what extrapolations of the system might be expected.

RESULTS FOR THE BASIC CASE

Since the number of parameters in three-dimensions is even greater than in a plane, economy had to be exercised in the variety of cases to be studied. A specific situation was taken and parameters were varied, usually one at a time, from this norm. The basic case which was chosen for analysis is the same as in Chapter V, i.e., one in which a Mach 2 interceptor attacks a Mach 2 delta-wing target flying at 60,000 feet. The capability of the Arrow system will be reviewed for this case and the effects of altitude and speed variations will then be discussed and compared. The original results were presented as families of graphs of placement probability as described in Chapter V. The general picture is illustrated here by means of tables which give placement probability that may be achieved in specific cases and the percentage of Al degradation that would be allowable and would still maintain the placement probability. *Table IX* summarizes the placement probability for the basic case for three values of σ with no target evasion. This table shows values for co-altitude attacks, which are the same as in Chapter V, and for snap-up attacks from 40,000 feet.

TABLE IX

PLACEMENT RESULTS IN THE BASIC CASE

Target — Configuration: Delta Wing
Speed: Mach 2
Altitude: 60,000 ft.
Nose aspect cross-section: 17.5 sq.m.
Evasion: nil

Interceptor — Initial speed: Mach 2 in level flight
AI radar performance: specification

Course Difference (degrees)	$\sigma = 1.5$		$\sigma = 3.0$		$\sigma = 9.0$	
	P_p (%)	Allowable AI Degradation (%)	P_p (%)	Allowable AI Degradation (%)	P_p (%)	Allowable AI Degradation (%)
180	100 100 SU	60 63 SU	100 100 SU	42 56 SU	88 96 SU	None 14 SU
135	100 100 SU	60 64 SU	100 100 SU	37 55 SU	82 94 SU	None None
110	100 100 SU	32 63 SU	93 99 SU	None 44 SU	62 81 SU	None None
75	68 54 SU	None None	59 52 SU	None None	42 40 SU	None None

SU — Signifies snap-up attacks from an initial altitude of 40,000 feet.
All other figures are for co-altitude attacks at 60,000 feet.

For a Mach 2 target at 60,000 feet, the probability of placement for the Mach 2 Arrow for differential altitude is as good as, or better than, for co-altitude attacks. When the AI range on the delta target is within the specification, the gain is slight at forward aspects, but when the AI is degraded to 0.5 of specification, an absolute gain of 10% may be obtained. Increases in beam attacks are even more striking. For example, when $\Gamma = 75$ degrees and $\sigma = 1.5$, P_p is 65% for a co-altitude attack, and 95% in a climbing attack from 40,000 feet.

One of the basic questions to be answered by the three-dimensional studies was whether it would be better to use a snap-up or a climbing attack. In a snap-up attack the interceptor is initially at a lower altitude than the target, and its tactic consists in first manoeuvring to achieve the correct lead angle while still at the initial altitude. The fighter is then pulled up to an acceptable angle for launching the weapon. In other words, the azimuth errors are first eliminated and, then, the vertical errors.

In a climbing attack, the interceptor immediately attempts to fly a lead-collision course if that is the desired mode. Initial manoeuvres are, therefore, carried out in three dimensions and the aircraft is steadily climbing.

The basic case indicates that improvements in placement zone width can be achieved by using snap-up rather than climbing attacks from 40,000 feet for Γ = 180 to 110 degrees. For reasonable σ's the P_p's are high in either case.

For Γ = 75 degrees snap-up is worse; P_p's are considerably worse; e.g. for specification AI range, and σ = 1.5 nautical miles,

Climb from 40,000 feet P_p = 98%

Snap-up from 40,000 feet P_p = 54%

This fall off in P_p is caused by severe encroachment of the AI radar look angle barrier which becomes almost coincident with the ideal approach line for Γ = 75 degrees and thus halves the P_p values.

When employing snap-up tactics the increase in probability over the co-altitude case is not so dependent on AI range capability as in the climbing case. For snap-up, improvement can be expected from specification range down to .4S. For climb, improvement is greater if manoeuvre starts at about .6S and is less for longer and shorter AI ranges. *Figure 39a* illustrates how the improvement in P_p, over co-altitude results, varies with AI range capability for climbing and snap-up attacks. *Figure 39b* shows how the improvement in P_p for snap-up attack varies for two different values of σ.

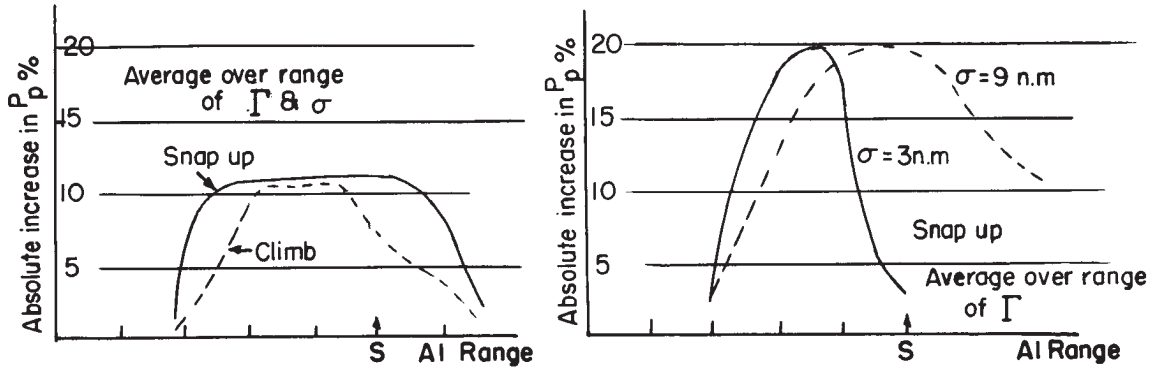

FIGURE 39

Implementation of a snap-up attack requires knowledge of the proper time to snap the interceptor up to the required launch elevation. It was found that the requirement is not too critical. The time chosen was 20% longer than the time-to-go corresponding to the minimum successful range for the climbing attack. This time-to-go varies with the launch requirement of the missile, speed and altitude of the interceptor, and altitude of the target. It is independent of initial course difference between interceptor and target.

In the case of the snap-up attack, satisfactory time-to-go-to-impact was found to be 20 seconds for an interceptor at 40,000 feet altitude, and 16 seconds at 50,000 feet against a 60,000-foot target. For an interceptor at 40,000 feet altitude the time was 30 seconds against a 70,000-foot target.

Details of placement probability for a straight-wing target are given in *Table X*.

TABLE X

Target — Configuration: Straight Wing
Speed: Mach 2
Altitude: 60,000 ft.
Nose aspect cross-section: 2.5 sq.m.
Evasion: nil

Interceptor — Initial speed: Mach 2
AI radar performance: specification

Course Difference (degrees)	P_p for $\sigma = 3.0$		P_p for $\sigma = 9.0$	
	Co-altitude Attack (%)	Snap-up from 40,000 ft. (%)	Co-altitude Attack (%)	Snap-up from 40,000 ft. (%)
180	96	100	53	80
135	94	99	50	72
110	86	97	45	67
75	53	54 (73 climbing)	29	30 (37 climbing)

The general conclusions which may be drawn from the studies of the basic case are outlined below.

Conclusions

1. Differential-altitude attacks from 40,000 feet with the Mach 2 Arrow are always preferred to a co-altitude attack on a 60,000-foot Mach 2 target.
2. For cases of most interest (σ = 1.5 to 3 nautical miles), the results of climb and snap-up attacks are similar, except for very short AI range (.5S).
3. In general, it is better to use snap-up if Γ is greater than 110 degrees, and climb if Γ is less than 110 degrees.
4. Under poorest GCI conditions (σ = 9.0), acceptable placement is accomplished only by snap-up for head-on attacks on a delta target.

EFFECTS OF COURSE DIFFERENCE IN BASIC CASE

The effects of course difference are summarized in *Table XI* which gives permissible course differences for achieving a placement probability of 95%.

TABLE XI

BASIC CASE: VALUES OF COURSE DIFFERENCE GIVING $P_p > 95\%$

Target — Configuration: Delta Wing
Speed: Mach 2
Altitude: 60,000 ft.
Evasion: nil

Interceptor — Initial speed: Mach 2
AI radar performance: specification

σ	Climbing Attack from 40,000 ft.	Snap-up Attack from 40,000 ft.	Co-altitude Attack
3 n.m.	$180^\circ - 100^\circ$	$180^\circ - 100^\circ$	$180^\circ - 110^\circ$
9 n.m.	None	$180^\circ - 160^\circ$	None

In a climbing attack at $\sigma = 9$ nautical miles, the P_p never rises above 92%. For $\Gamma = 145$ degrees, P_p is between 85 and 92%. Generally, satisfactory results cannot be obtained with a course difference of less than 110 degrees. If a very small course difference (75 degrees) must be used, then a σ of 1.5 nautical miles is required and a climbing attack from 40,000 feet must be made.

EFFECT OF INCREASE IN TARGET ALTITUDE

As indicated above, the main purpose in studying high-altitude and high-speed targets was to determine the possible extended capabilities of the system, and the comments on weapons that were made in the opening section of this chapter should be noted.

Table XII summarizes the cases where placement probability is greater than 95% for a Mach 2 target flying at 70,000 feet and the Arrow intercepts by climbing from initial speed of Mach 2 and an initial altitude of 50,000 feet.

TABLE XII

Target — Configuration: Delta Wing
Speed: Mach 2
Altitude: 70,000 ft.
Evasion: nil

Interceptor — Initial speed: Mach 2
Altitude: 50,000 ft.
AI radar performance: specification
Climbing attacks

Course Difference (degrees)	$\sigma = 1.5$		$\sigma = 4.75$		$\sigma = 9.0$	
	P_p (%)	Allowable AI Degradation (%)	P_p (%)	Allowable AI Degradation (%)	P_p (%)	Allowable AI Degradation (%)
180	100	48 20 SU	95 75	None None SU	71 45	None None SU
135	100	48	95	None	68	None
110	100	45	86	None	61	None
75	45	None	48	None	38	None

A similar set of results is given in *Table XIII* for the case wherein the initial interceptor altitude is 40,000 feet.

It should be noted that for attacks from 50,000 feet, which is an altitude difference of 20,000 feet, the snap-up tactic gives poorer results than a climbing attack. However, if the fighter starts at 40,000 feet, snap-up is better than climbing for $\Gamma = 180$ to 110 degrees. Generally, if P_p is good ($\geq 95\%$) for a 60,000-foot target, it will also be good ($\geq 95\%$) for a 70,000-foot target; however, less degradation in AI range will be permissible, about 12% less for the head-on case, ($\sigma = 1.5$ nautical miles).

Invariably it may be said that if conditions are unfavourable at 60,000 feet, the increase in target altitude has a much worse effect than if the conditions were favourable.

The 70,000-foot target case bears out the conclusion that snap-up is better than climb for large Γ's, especially from 40,000 feet, but P_p's are not significantly different. The same encroachment of the look angle barrier causes snap-up to become inferior to climb at the smaller course differences with the change at about $\Gamma = 100$ degrees.

TABLE XIII

Target – Configuration: Delta Wing
Speed: Mach 2
Altitude: 70,000 ft.
Evasion: nil

Interceptor – Initial speed: Mach 2
Altitude: 40,000 ft.
AI radar performance: specification

Course Difference (degrees)	$\sigma = 1.5$		$\sigma = 4.75$		$\sigma = 9.0$	
	P_p (%)	Allowable AI Degradation (%)	P_p (%)	Allowable AI Degradation (%)	P_p (%)	Allowable AI Degradation (%)
180	100	50 40 SU	100	20 30 SU	85 96	None None SU
135	100	40 50 SU	100	10 20 SU	80 86	None None SU
110	100	40	95 98	None 10 SU	75 80	None None SU
75	97 15	None None SU	73 30	None None SU	51 30	None None SU

Climbing attacks except where nqted.

Conclusions that may be stated for attacks against a Mach 2, 70,000-foot target are outlined below.

Conclusions

1. Under favourable conditions high-placement probabilities against large Mach 2 targets at 70,000 feet can be obtained.
2. If AI range is less than that for the delta target, placement probability will be considerably degraded unless σ is good.
3. If an attack is to be made under marginal conditions of target speed and altitude, ground control judgment of target altitude is critical.
4. A brief set of rules may be given for attack on 70,000-foot target:

   a) if fighter is at 60,000 feet – climb

   b) if fighter is at 50,000 feet – climb

   c) if fighter is at 40,000 feet – snap-up

   d) if Γ is smaller than 110 degrees – always climb

This bears out RCA's rules to climb if Δ h is smaller than 30,000 feet and to snap-up if Δ h is greater than 30,000 feet. CARDE's work indicates that snap-up is usually better, but in cases where Δ h is small the difference is negligible.

HIGHER SPEED TARGET

As a further extension to the demands that might be made upon the system, a very high-speed target at a 70,000-foot altitude was investigated. For attacks on a Mach 3.5 target at 70,000 feet, the conditions for satisfactory placement are more restrictive. They are summarized in *Table XIV*. Results are essentially the same for climbing and snap-up attacks.

TABLE XIV

CONDITIONS FOR 95% P_p, (HIGH SPEED, HIGH ALTITUDE)

AI radar performance: specification

No target evasion

Course Difference	Δ h = 10,000 ft.	Δ h = 30,000 ft.
180°	σ = 1.5 – 3.75 n.m.	σ = 1.5 – 4.5 n.m.
135°	σ = 1.5 – 2.5 n.m.	σ = 1.5 – 3.0 n.m.

In general, if the placement probability is high (near 100%) for a Mach 2 target, the degradation is relatively small for increasing the speed to Mach 3.5 (0 to 15% Abs.). When P_p is poor (75 to 80%) for Mach 2, then degradation is much more severe for a Mach 3.5 target; (it may be of the order of 30%).

The above figures are those for specification AI performance on the delta target. If the AI is degraded, or target radar cross-section small, the situation is more critical. If vectoring accuracy is 1.5 nautical miles, and AI range is .6S, P_p is 90% but drops rapidly to zero at .5S. Thus, if the AI is somewhat below specification and if the target is small, there is practically no placement chance.

Conclusions that may be stated for attacks against a Mach 3.5 target at 70,000 feet are presented below.

Conclusions

1. Good vectoring accuracy is required.
2. Attack should be as near head-on as possible.
3. AI range must be at least specification.
4. There must be a weapon which works at these altitudes.
5. Better results are obtained from initial fighter altitude of 40,000 feet.
6. For $\Gamma = 180$ degrees it is better to snap-up, but for $\Gamma = 135$ degrees it is better to climb.

It should again be stressed that the accuracy of ground environment equipment is a function of target speed, so that a piece of equipment which gives $\sigma = 1.5$ on a Mach 2 target will have a larger value of σ on a Mach 3.5 target.

VERY HIGH-ALTITUDE TARGETS

The most severe threat which was investigated was that of a Mach 3.5 target flying at an altitude of 80,000 feet. As would be expected, the requirements for obtaining a value of 95% for P_p are even more stringent in this case than in those reported above. *Table XV* illustrates the results for a course difference of 180 degrees.

TABLE XV

CONDITIONS FOR 95% P_p FOR A MACH 3.5 TARGET AT 80,000 FEET

Course difference 180 degrees

No target evasion

σ	Minimum AI Range
1.5	.65 S
4.75	1.0 S
6.75	1.30 S

If the course difference is reduced to 135 degrees, placement chance of 95% cannot be achieved unless σ is smaller than 1.5 nautical miles. For specification Al range on a delta target, P_p ranges from 85% at 1.5 to 60% at 4.75, and to 40% at 9.

These results are for snap-up attacks from 40,000 feet. Climbing attacks from 40,000 feet are definitely inferior to snap-up in this case, since range at which the climb may begin is very critical.

Conclusions that may be drawn for attacks against a Mach 3.5 target at 80,000 feet are outlined below.

Conclusions

1. Within a very restricted set of conditions, placement may be accomplished.
2. Snap-up attacks must be used commencing at 40,000 feet.
3. For targets of smaller radar cross-section than the delta, P_p may be unsatisfactorily low.
4. Any evasion would highly degrade the situation.

LOWER INTERCEPTOR SPEED

If the basic target (Mach 2 at 60,000 feet) is attacked by the Arrow with Mach 1.5 initial speed only, a definite degradation in placement chance is incurred. For a 95-per-cent placement probability with $\sigma = 1.5$ nautical miles the following circumstances are required:

Al range 0.6S or better.

Course difference 180 to 110 degrees.

In this situation differential altitude is harmful. As Δ h increases Al detection range values required increase. For Δ h = 20,000 feet and Γ = 180 degrees, Specification range is necessary for $P_p = 95\%$.

If the course difference is 110 degrees, commencing interceptor manoeuvre at an extremely long range will lower the placement chance since loss of speed in the turn makes the fighter fall too far behind. The ability of the Arrow to maintain altitude at Mach 1.5 at 60,000 feet is questionable.

LOWER TARGET SPEED

If the Mach 2 interceptor makes a co-altitude attack on a Mach 1.5 delta-wing target at 60,000 feet, placement chance is improved for smaller course differences. *Table XVI* summarizes the situation.

TABLE XVI

MACH 2 INTERCEPTOR VS MACH 1.5 TARGET

Course Difference (degrees)	$\sigma = 4.75$ (%)	$\sigma = 9.0$ (%)
180 – 135	$P_p = 100$	$P_p > 95$
110	$P_p = 100$	$P_p > 92$
75	$P_p = 98$	$P_p > 83$

Climbing and snap-up attacks yield even better values for P_p. For example with $\Gamma = 75$ degrees, $\sigma = 9.0$ snap-up from 40,000 feet on a delta-wing target gives a placement probability of 97% and climbing gives $P_p = 96\%$.

Snap-up is more successful than climb at course differences from 180 to 75 degrees. With the reduced target speed, look angle barrier encroachment does not restrict snap-up too seriously even at $\Gamma = 75$ degrees. However, the difference is slight. Only for large σ's and small target radar cross section will there be any real advantage in using snap-up attacks.

TABLE XVII

STRAIGHT-WING MACH 1.5 TARGET, σ = 9 n.m.

ATTACK FROM 40,000 FEET

Γ (degrees)	P_p for Climbing Attack (%)	P_p for SU Attack (%)
180	80	97
135	77	93
110	80	91
75	84	85

It should be noted that the advantage of snap-up over climbing falls off as P_p becomes smaller.

LOOK ANGLE LIMIT PATTERN

Some work was done on the shape of limits that might be imposed on the look angle capabilities of the AI radar: the types investigated were rectangular and elliptic. The results obtained did not prove one to be better than the other. The rectangular may be better in some cases, but most of the time when the fighter was in a steep bank, the radar was centered at the bottom.

LOOP GAIN

In preliminary considerations of three-dimension interception problems, it was felt that a high-loop gain would imply maximum utilization of the fighter's manoeuvre capabilities, and that it would also give the most optimistic placement results. It was assumed that the fighter's navigation computer would have the highest gain consistent with a stable operation. This line of reasoning is true for a constant speed investigation; unfortunately, in a supersonic fighter, a sustained high "g" produces serious deceleration. In addition, high gain means that a high bank angle is maintained until the fighter is almost on course. With a small permissible negative deflection of the radar elevation gimbal, this causes serious encroachment of the look angle barrier. A study was therefore carried out to determine the effects of varying loop gain, and the following facts emerged:

a) When the placement probability is limited by look angle or fallback barriers, the width of the placement zone increases with reduced gain because when the turning rate is reduced, bank angles are small and deceleration less.
b) When the placement zone is bounded by manoeuvre barriers, probability is reduced when the gain is reduced, but only after a special value is passed. This value corresponds to the interceptor turning at a maximum rate when the heading error is equal to the maximum tolerated by the missile and is the maximum value of loop gain which need be considered.

Most of the studies herein are based on a loop gain of 4 degrees/second/degree heading error. These produce somewhat pessimistic placement probabilities. The value of $K = 1/3$ degree/second/degree heading error, as incorporated in the intended ASTRA I system, would seem to be more suitable and would give better values for placement probability.

CHAPTER VIII – ARROW EFFECTIVENESS IN ECM

INTRODUCTION

A considerable portion of the CARDE study has been devoted to the operation of a single Arrow against a single target in an ECM-free environment. This work was necessary to gain familiarity with the weapon system. However, the numerical probabilities obtained do not represent real system capability since they are derived from an unrealistic combat situation. ECM cannot be neglected for reasons of analytical difficulty, nor can it be fairly dismissed with the statement that it will "seriously degrade" our estimates of effectiveness. As will be seen in the threat statement below, ECM represents the normal environment for the Arrow weapon system. It must operate in ECM or not operate at all.

This chapter is a summary of studies carried out at CARDE to determine and improve the effectiveness of the Arrow in ECM. Although they were not fully successful in subjecting the complex countermeasure situation to numerical treatment, several advances in this direction were made.

NORAD ELECTRONIC ENVIRONMENT

Before a model of the ECM threat can be formulated, a description of the NORAD environment is required. Although the CARDE study is concentrated on the AI phase, it is necessary to consider the whole environment in order to ensure that the jamming allocated to X-band is realistic. This is described in References 28 and 29. The frequency bands are summarized in *Table XVIII* which includes the Canadian K-band and the new bands of the frequency diversity program. Canadian conversion to UHF communications is anticipated. Only the Sparrow II and Nike missiles are listed, as other NORAD missile radars use frequencies included in the surveillance or AI coverage.

The Nike Target Ranging Radar is described in Reference 33. It is a CCM device proposed by BTL, and its contractual status is uncertain.

An important difference must be noted between non-elevation-scanning surveillance radars and the height finders. The surveillance radars may not achieve "crossover" against jamming at any range because the jammer flies out of the lobe maxima of their elevation coverage at close ranges. Surveillance crossover ranges calculated on lobe maxima have little meaning unless accompanied by crossover range contours in the elevation plane.

TABLE XVIII

NORAD ENVIRONMENT

Type	Lower Frequency (mc)	Frequency Band (mc)
Interceptor	225	175
Communications		
Surveillance Radars		
FPS-24	214	20
FPS-35	400	50
FPS-28	510	80
FPS-7,20	250	100
FPS-27	2,000	300
FPS-14,16	2,700	200
FPS-26	5,400	500
Height Finders		
FPS-6	2,750	110
FPS-4	9,230	200
AI Radars	8,500	1,000
Missiles		
Nike TRR	15,500	2,000
Sparrow II	24,000	500

THE THREAT

No ready-made statement of the ECM threat was available to CARDE during the study. Since then the situation has clarified somewhat, and improved estimates (28 to 32) have been introduced into the analysis. It is stressed that the following is a tentative description of a variable environment, and represents only an average interpretation of various intelligence estimates. In most instances Russian ECM development is assumed to parallel that of the West. Reference 34 supports this assumption. Russia is assumed to have complete knowledge of our defence radar characteristics and locations. The period covered is approximately 1962 to 1967. During this period, the Russian long-range airforce will include a few tens of Bisons and Bears, and a few hundreds of Badgers and supersonic aircraft such as Blowlamp and Backfin.

RAID SIZE

The first attack will be directed against American SAC bases and will be composed of two parts: a small sneak raid to gain the advantage of surprise and, following closely, a mass raid to saturate the defences. The sneak raid aircraft will probably penetrate singly from several directions, using airline or low-altitude approaches and one-way missions. The mass raid will penetrate at one point as a roughly circular "clump" of aircraft spaced five to ten miles apart to avoid multiple kills by nuclear warheads.

JAMMER GAIN AND SPECIFIC OUTPUT

The gain of the jamming antennas is taken as five. However, plumbing loses and the requirement for omnipolarization, at least on X-band, are assumed to reduce the effective gain to one.

The specific output of barrage or spot jammers in watts per pound is estimated in References 28 and 29. An average estimate for the period 1962 to 1968 is 2 watts/pound below 500 mcs, 3 1/2 watts/pound, from 500 to 6000 mcs, 1 1/2 watts/pound at X-band and 1/2 watt/pound at K-band. These figures include the passive receivers associated with the jamming equipment.

The specific output of repeater jammers was derived from examination of Reference 35 which describes some 40 jammers of various types now being produced or operated in the U.S.A. The repeater jammers showed specific outputs from 3 to 170 watts per pound (peak), the spread apparently arising from differing development stages and duty cycles. A reasonable figure for the 1963 to 1968 time period appears to be 10 watts per pound (peak) with a maximum duty cycle of about 0.01(sufficient to handle four radars at once). This performance is about twice that of the ALQ 16, which reached the engineering model stage in 1955.

CHAFF

The introduction of aluminized glass and mylar chaff will provide about a tenfold decrease in volume and a fourfold decrease in weight for the same echoing area as compared to present chaff packages (36). Thus a supply of 1000 eight-ounce packages of the new chaff, considered adequate for unlocking purposes, will weigh about 650 pounds including the dispenser. It will cover P, L, S, X, and K-bands. Owing to its lower density and improved methods of dispensing, gravity-launched chaff will be assumed to disperse effectively to equal the radar area of the aircraft at X-band with zero time delay. This effect may also be achieved by using cartridge launching, if necessary, and may be enhanced by the combined action of the AGC and RTU video limiter, which will be described later. Dispensing rates up to 5 packages per second will be assumed.

Two other methods of chaff dispensing may be encountered if Russian development parallels that of the West. The first involves chaff-sowing rockets, such as those developed by BU Ships or WADC (36). These rockets fly ahead of the target aircraft dispensing from 5 to 15 packages of chaff at intervals of approximately 150 feet. Their launching is usually accompanied by target manoeuvre. The rockets weigh about 25 pounds and it is assumed that 20 can be carried. The second dispenser consists of a series of rockets carrying single chaff packages; this is conventionally known as forward fired chaff and is exemplified by WADC's ALE-9.

ABSORBENT COATING

The state of the art is represented by a resonant coating developed for RADC (36), which reflects less than 5% of the incident power over a frequency range of 6.4 to 13.3 kmc (presumably at normal incidence) and which has a thickness of 0.2 inch. Reference 37 indicates similar performance for materials developed by NRL, including a .218-inch coating for L-band with a bandwidth of 28%. Trials of X-band materials on the Canberra (32, 38) indicate reductions in echoing area for non-specular reflections by a factor of 5 for a weight of 2,000 pounds of material. Specular reflections are reduced by much larger factors, of the order of 100, so that the large peak in echoing area at the beam aspect is removed. Slight structural modifications to the engine intakes and outlets can reduce their contribution to echoing area by a factor of 5. In view of this, Soviet capability will be represented by an echoing-area reduction of 5 at head and tail aspect and 50 at beam aspect, over a 50-per-cent bandwidth at X-band, S-band or L-band (one band only) for a total weight of 2,000 pounds. The residual echoing area will be assumed constant with aspect angle and equal to 1, 3.5 and 0.5 m^2 for the B-52, delta, and straight-wing aircraft types, respectively.

ECM LOADS

The total weight of countermeasure equipment carried will be about 8,000 pounds for the Bisons and Bears, and 5,000 pounds for the Badgers and supersonic bombers. These figures reflect improvements in power plant and aerodynamic performance and a steady reduction in the weight per megaton of nuclear bombs. Since most of the bombers of the raid will have only 5,000 pounds ECM capacity, this figure is used in making up the ECM load. The types of jammers will be specified only in general terms, and the X-band threat will be discussed in more detail in the section on 'Hardware Duel'. The allocation of the ECM weight allowances to jamming devices will vary between the sneak and mass attacks. This allocation will now be discussed.

SELECTION OF COUNTERMEASURES FOR SNEAK ATTACK

The primary concern of the sneak raid is to avoid detection or, failing that, to avoid identification as hostile. Hence, it is assumed that the raid will not jam communication or surveillance radar frequencies and that L-band absorbent coatings will be used. Passive receivers will permit the attackers to delay turning on AI and missile ECM until it is essential to their immediate survival. Detection of AI lock-on is considered the decisive cue for initiation of countermeasures. These will include X-band chaff (and K-band if the target is a Canadian city – see next section) and pulsed repeater type jammers of about 1 kilowatt peak power. The repeaters may be gate stealers, conical scan inverters, or phase front spoilers (39). Repeaters are used in preference to barrage or spot jammers because their transmissions are more difficult to distinguish from normal AI transmissions.

Since jamming will be provided against the terminal defensive weapons only, there will be no weight limitations on the jammer complement. Adequate coverage (i.e. denying useful crossover ranges) of all terminal weapon frequencies can be provided within an ECM load of less than 2,000 pounds.

SELECTION OF COUNTERMEASURES FOR MASS ATTACK

The mass raid will be known to NORAD directly, via DEW line detection, and indirectly, via strategic warning or by detection of the sneak raid. The DEW line could be rendered useless through periodic jamming over several months, but the political implications of such an action make it unlikely. If one presumes that detection is certain without jamming (in the absence of jamming), the jamming of the DEW line will not affect the mass raid except that it will prevent the accurate assessment of its size and direction. The Mid-Canada line will probably not be jammed since it provides a warning function only. Jamming of surveillance frequencies will recommence shortly before the Pinetree radar horizon is reached and will be continuous thereafter. Sweep jamming is the most likely threat since it produces sidelobe strobes which make direction finding difficult. AI jamming will commence as soon as the first fighter lock-on is detected. There is some disagreement in the estimates regarding the type of AI jamming to be expected. References 32, 41 and 42 state that deception, or spot jammers, which require passive listening to the AI cannot be used in multiple aircraft raids since their passive receivers would be confused by neighboring jammer transmissions. Dr. Van Voorhis of W.S.E.G. disagrees with this view and states that the power received from the victim AI will be at least 20 db above that of neighboring jamming transmissions. The range ratio at which AI radar power exceeds jammer power by 20 db is given by:

$$\frac{R_R}{R_J} = \sqrt{\frac{P_R G_R}{100 P_J G_J}} \doteq 55 \text{ for Astra}$$

hence, the power received at the jammer from the AI will exceed that from neighboring repeater jammers by 20 db or more, whenever the AI is less than 55 bomber spacings from the jammer receiver. A similar ratio is obtained for spot jammers. On this basis, CARDE retains the spot and repeater jammers as possible threats in the mass raid. Other factors influencing the enemies' choice between deception and spot or barrage jamming are the state of the art (deception jammers are not as fully developed as barrage jammers), the jammer weight required (deception and spot jammers are lighter), and the relative jamming effectiveness (see section on "Hardware Duel"). For the time being, the mass raid will be assumed to use either deception and spot jamming, or barrage jamming, against the AI and missile radar. These two models will be designated A and B respectively.

Before allocating the ECM load for the two models, the effect of specifically Canadian frequencies must be discussed, particularly K-band. It is assumed that bombers allocated specifically to Canadian targets will carry ECM coverage only for Canadian defence frequencies; hence, these aircraft will carry K-band jamming and chaff. It is improbable that the aircraft assigned to American targets will carry K-band chaff and jamming equipment since Reference 31 estimates that only 6 to 12% of all attacks against the raid will be made by Canadian air defence weapons. There seems little point in adding a thousand pounds of K-band chaff and jamming to every aircraft to ensure success against a small proportion of attacks, when reasonable success is achievable without it. It is assumed that none of the sneak raid aircraft, and only a few of the mass raid aircraft (about 2%), will be assigned to Canadian cities. These aircraft will not be distinguishable from the others. Since the maximum number of Canadian attacks against the raid is about thirty, the probability of even one Canadian intercept against a bomber assigned to a Canadian target in only approximately 60%. K-band chaff and jamming are therefore not representative of the average combat situation and are deleted from the model. If the Americans were to install a large number of other K-band devices in NORAD this conclusion would have to be revised.

Mass Raid Model A

There appears to be no need for each aircraft to provide coverage of the whole communications band. Each aircraft will be assumed to carry one 100-watt sweep jammer; thus a 200-aircraft raid can provide a total of 100 watts/mc over the UHF band. The GCI's are covered by sweep or spot jammers having 200-watt output over a 10-mc band. The FPS-6 height finder is singled out for special attention because of its obvious capability as a "burn-through" radar. X-band is covered by a pulsed deception repeater or a spot jammer, plus absorbent coating. The estimates of peak pulse power required for a deception jammer vary widely. Reference 42 states that 100 watts within the victim bandwidth is sufficient to exceed the echo pulse power at ranges of over two miles. Nearly all the deception jammers of Reference 8 have pulse powers of 1 kilowatt; Reference 32 suggests 10 kilowatts and Reference 40, up to 50 kilowatts. CARDE will use 1 kilowatt as this seems to provide adequate power margin over the echo to ensure control of the victim AGC. The Nike Target Range Radar on K_U band is allocated a range gate stealer. The jammer complement is given in *Table XIX*.

TABLE XIX

MASS RAID MODEL A

Use	Minimum Frequency	Watts*	lb/watt	lb
Interceptor Communications	UHF	100c	½	50
Surveillance Radars	214	200c	½	100
FPS-35	400	200c	½	100
FPS-28	510	200c	$\frac{1}{3.5}$	60
FPS-7,20	1,250	200c	$\frac{1}{3.5}$	60
FPS-27	2,000	200c	$\frac{1}{3.5}$	60
FPS-14,16	2,700	See FPS-6		
FPS-26	5,400	200c	$\frac{1}{3.5}$	60
FPS-6	2,750	1,000c	$\frac{1}{3.5}$	300
FPS-4	9,230	200c	$\frac{1}{1.5}$	135
AI Radars	8,500	1,000p	$\frac{1}{10}$	100
	OR	200c	$\frac{1}{1.5}$	135
		Plus X-band absorbent		2,000
Nike TRR	15,500	1,000p	$\frac{1}{10}$	100
			Total	3,125 or 3,160

*Subscript c indicates continuous output of spot or sweep jammers, p indicates peak pulse output of repeater jammers.

It appears that an adequate complement of jammers can be provided within the ECM capacity of the aircraft.

Mass Raid Model B

Again, concerted action in the UHF-band will be assumed with each aircraft contributing 100 watts or 0.5 watt/mc. Except for the FPS-6 height finder the GCI radars are allocated 2.5 watts/mc. This is adequate to deny crossover at any range, on any of the surveillance radars at any altitude above 30,000 feet. The FPS-6 finder is assigned 5 watts/mc, which reduces its effective range to 25 nautical miles. The FPS-4 height finder is assumed covered by the AI X-band jamming. Barrage of the Nike ranging radar is not possible because of its 2,000-mc frequency spread; it is assigned a gate-stealing repeater as in model A. A 10-per-cent allowance is made for Russian uncertainty regarding the NORAD frequency bands. The model assumes less GCI jamming than other estimates for the following reasons:

1) The GCI phase is an early stage in the interception chain. As indicated in References 43 and 44, it can degenerate to a form of loose control using triangulation of the whole raid mass without seriously degrading the defence system. Thus the GCI jamming payoff is low.
2) The ground environment is most amenable to the installation of bulky ECCM hardware. Thus the GCI jamming payoff is uncertain.

The weight breakdown for Model B is given in *Table XX*.

TABLE XX

BARRAGE JAMMING

MASS RAID

Type	Minimum Frequency	Frequency Band	Watts/ mc	lb/ watt	lb Needed	lb + 10% Allowance
Interceptor Communications	225	175	0.5	½	45	50
Surveillance Radars						
FPS-24	214	20	2.5	½	25	30
FPS-35	400	50	2.5	½	65	75
FPS-28	510	80	2.5	1/3.5	60	70
FPS-7,20	1,250	100	2.5	1/3.5	70	80
FPS-27	2,000	300	2.5	1/3.5	250	275
FPS-14,16	2,700	200	6 (See FPS-6)			
FPS-26	5,400	500	2.5	1/3.5	360	400
Height Finders						
FPS-6	2,700	200	6	1/3.5	340	375
FPS-4	9,230	200	4(See AIs)			
AI Radars	8,500	1,000	4	1/1.5	2,670	2,920
		OR	1	1/1.5	670	740
				+ absorbent coating		2,000
Missile						
Nike TRR	15,500	(Gate Stealer) 1000 W peak				100
					Total	4,375 or 4,195

The total weight of ECM equipment including chaff is thus 5,025 pounds for straight jamming in X-band, or 4,845 pounds for jamming plus absorbent coating. The absorbent coating alternative at X-band is preferable to straight jamming because it provides a reduction of 30-percent detection range in the absence of ECM, improves chaff effectiveness, takes up less space, and removes the long crossover ranges at beam aspect. It also halves the jammer waste power to be dissipated at high speeds. Since Neoprene has been used as an erosion coating on missile radomes, it is assumed that the absorbent coatings themselves can be made to withstand the high-temperature environment of supersonic flight.

SPECIAL TYPES OF JAMMING

ECM Aircraft

Reference 28 suggests that up to 10% of a mass raid might be composed of aircraft carrying only jamming equipment, possibly four times the normal complement. Reference 32 discounts this possibility. In order to be effective, the specialist jammer must be able to screen neighboring aircraft, which requires transmission into the side lobes of the defending radars. This would require an increase of transmitted power by a factor of 100, which appears impractical.

Area Sown Chaff

Reference 42 suggests that a small amount of chaff sown by the lead aircraft of a raid can create a confusing number of false targets. There are a number of counters to such a tactic which make it unlikely. These are discussed in the section on "Area Sown Chaff", on page 98.

Decoys

Reference 28 estimates that the Russians may use some decoys until 1963, but after this time their confusion effect will be provided more cheaply by advanced deception jammers. Reference 36 describes the Bull Goose 5,000-nautical-mile decoy, which is apparently being produced for the USAF. Reference 32 suggests that, if they are assumed to be effective, decoys should not be considered as an ECM threat, but rather as an increase in the number of targets which must be attacked.

THE "HARDWARE" DUEL BETWEEN ASTRA AND THE THREAT

The Astra radar circuitry is furnished with several ECCM features which should restore normal operation against some threats. These features and their performance will now be discussed.

ASTRA ECCM FEATURES

The ECCM features of the Astra are given in the following list. Items 1 to 10 are inherent in the normal operation of the set; items 8 to 19 are specially installed ECCM's.

1.	High transmitted power:	1 mw
2.	High antenna gain:	34 db
3.	Low antenna sidelobes:	20 db down
4.	Wide dynamic range:	120 db, including 30 db rf attenuation
5.	Narrow bandwidth:	1.5 mc search, 4 mc track
6.	Range rate memory:	Effective time constant: approximately ½ sec, can coast for 20 sec.
7.	Azimuth rate memory:	Effective time constant: approximately ½ sec, invariant with range.
8.	RTU video limiting:	Level unknown
9.	Video pregating:	0.5 usec. pregate
10.	Nose-tail tracking: —	0.25 usec. effective gate (Nav. chooses either 9 or 10)
11.	Magnetron tuning:	200 mc/sec^2
12.	Variable antenna polarization:	H,V, RC, LC; H and V non-space-stabilized.
13.	Jittered prf:	10% at 400 cps
14.	Intermittent (quasi-passive) ranging:	50 msec on, 2 sec off with random silent re-tune at 200 mcps^2. 6 sec. acquisition with ± 10 usec gates, tracking with 0.275 usec gate out to 25 miles at S/N exceeding 6 db.
15.	X-band passive angle tracking	
16.	S-band passive angle tracking:	ARD 501
17.	Infra-red search and angle tracking	Long wavelength (Used with QPR, also in an IR track-Al Range continuous mode).
18.	Aural display of radar video.	
19.	Optical sight.	

Only a few of these features require discussion.

The characteristics of the range tracking unit video limiting are not given in the RCA literature. Reference 45 states that it is incorporated in Astra but that its design is not yet finalized. It will probably be similar to that of the MG 2, which clips the 6 volt IF output to 1 volt in the RTU. This, combined with the 20-cps AGC bandwidth, means that chaff clouds having echoing areas from 1/6 to 6 times that of the aircraft are seen by the RTU as video pulses of identical height with that of the aircraft itself (assuming a square law detector). The implications of this will be discussed later.

Video pregating effectively clips the tails off the RTU discriminator curve, and ensures that chaff or ground echos, which fill the 240-foot pregate, will not cause error signals in the RTU.

The quasi-passive ranging mode derives its angular information from the infra-red tracker, since the QPR duty cycle is inadequate for radar angle tracking. The detection range capability of the infra-red sub-system is estimated by RCA to vary from 6 nautical miles head-on to 55 nautical miles tail-on. Range on a supersonic aircraft using afterburning is believed to be at least three times these figures in the forward hemisphere. Thus the infra-red ranges should permit the use of QPR for a few seconds before the missile launch in the rear hemisphere of subsonic targets, and in the forward hemisphere of supersonic targets. Its chief restriction is its limited field of view below horizontal; this effect is discussed on page 84.

Against a linearly polarized jammer RCA tests indicate that perfect cross-polarization provides better than 20 db jamming rejection. This reduces to 3 db at 45-degree polarization angle. However, it will be noted that the X-band threat includes omnipolarization so that no advantage is expected from the use of this ECCM feature. Even against the linearly polarized jamming source the feature must be used with care. Reception of a cross-polarized signal causes an inversion of the antenna gain pattern which reverses the slope of the angular discriminator curve. At some intermediate polarization angle the slope is zero. This condition may occur during manoeuvre since the polarization plane is not space-stabilized. Passive angle tracking is best done on one of the circular polarizations.

ASTRA VERSUS DECEPTION JAMMERS

The most likely deception jammer is the combined range gate stealer/conical scan inverter. Rf delays as low as 0.1 μsec and continuously variable up to 15 μsec are now available (35). During the 1963-1967 time period it is assumed that a multiple filter bank will be used to provide effectively instantaneous frequency set-on as in the ALQ5 and 15. The ground-based ULT2 can transpond on frequency in 2 msec. Jammers of this type can deny range and angle tracking to the Astra in its normal mode. The search display is not affected. The only ECCM for deception jamming is QPR, which within its infra-red range limitation will restore normal operation since, during each 50-msec transmission, there is insufficient time for the jammer to initiate the gate-stealing process against a rate-aided range gate. QPR may also induce an unattended repeater to remain silent, "thinking" that the AI is not yet locked on.

Another deception jammer is the false target generator, which produces false blips at various ranges around the true target. Prf jitter is an effective counter unless the jammer is a true repeater, i.e., unless it transponds on receipt of each AI pulse. In this case a series of false targets will appear during the search mode, which are aligned along the true target azimuth at ranges always exceeding true target range. This array will probably be detected by its distinctive arrangement on the scope. The jammer can be countered by locking on the nearest clearly defined blip.

ASTRA VERSUS SPOT JAMMERS

Sequential spot jammers which seek the AI frequency, jam for short period, and then move to the next victim, can break normal lock provided they remain on Astra frequency for about 1½ seconds. They can be countered by the QPR mode since its 0.025 duty cycle, combined with that of the jammer, makes detection of the Astra frequency unlikely. Even if detected, the 50-msec transmission period is less than the normal reaction time of the spot jammer. Random magnetron tuning should also be an effective counter since it moves the Astra frequency away from that of the jammer in approximately 0.02 second.

Continuous spot jamming can destroy normal lock. Passive X-band tracking can restore angular information against the small raid. However, in a large raid all target aircraft within or near the fighter's radar beam may spot jam on its frequency. RCA's criterion for successful passive tracking of one jammer is that its power exceeds the others in the beam by 6 db. This will occur when the fighter is within approximately two bomber spacings, i.e., 10 to 20 nautical miles from the nearest jammer.

Passive angle tracking of continuous spot or barrage jamming can be prevented if the jammer amplitude modulates its output at a frequency within ± 1 cps of 66 2/3 cps. This is the fixed conical scan frequency of every Astra radar. Stanford University's S440 jammer has an a.m. facility in addition to classical inverscan. The AN/APS 54 receiver installed in the B-52 displays victim conical scan rate. Hence the technique appears practical.

ASTRA VERSUS BARRAGE JAMMERS

Tuning and QPR are of no use against the barrage jammer since it more than covers the Astra frequency band. Jamming will be received via the image channel as well as the normal channel, thus doubling the vulnerable bandwidth of the radar.

If the Astra's large dynamic range prevents saturation, then angular information should be available during auto search on jammers on the edge of the raid formation. Passive angle tracking of more centrally located jammers will be possible when the range reduces to approximately two bomber spacings for X-band tracking, or four bomber spacings for infra-red tracking. Resolution of central jammers on auto search will occur at about three spacings by radar or, four spacings by infra red. (Reference 45).

DRML's tests of aural radar display indicate that propellor modulation can be heard through jamming. MIT project Buzzsaw reported similar aural signatures from jet engine blades. Thus aural ranging is a possibility. A program of flight trials has been proposed by CARDE to investigate this phenomenon.

As range decreases, the target echo power received by the AI increases as $1/R^4$, whereas the power from the jammer increases only as $1/R^2$. Hence at the "crossover" range the target blip will be seen through the jamming. The formula for "crossover" range is:

$$R_c = \sqrt{\frac{P_t G_t A_e L_{rj}}{4\pi P_j G_j B_r L_n K}}$$

where

R_c = crossover range in metres

P_t = Nominal Radar Transmitted power, watts

G_t = Radar antenna gain

A_e = Target echoing area, m^2

L_{rj} = Radar receiver losses for a jamming signal (numerical factor; not db)

L_n = Two-way losses for transmission and reception of aircraft echo in normal operation.

P_j = Jammer power output in watts/mc

G_j = Jammer antenna gain

B_r = Radar infra-red bandwidth, including image band, mc

K = Power ratio of $\frac{\text{signal}}{\text{jamming}}$ for detection or tracking.

Parameters for Astra are as follows:

P_t = 10^6 watts

G_t = 34 db (Ref. 47)

= 2,400

A_e = 1 m^2 for B-52

3.5 m^2 for Delta

½ m^2 for Straight Wing

Since targets are absorbent coated, A_e is constant with aspect angle (See Section on Raid Model B)

L_{ri} = 3 db, composed of radome loss 1 db (Ref. 45,46)
Receiver insertion loss 2 db (Ref. 46)

L_n = 7 db, composed of
Transmitter Insertion loss 2 db (Ref. 45)
2-way Radome 2 db (Ref. 45,46)
Receiver Insertion loss 2 db (Ref. 46)
Collapsing Loss (display) 1 db

Differential atmospheric absorption is neglected since crossover ranges are short. Field degradation is believed to be mainly in the crystals and is neglected as common to both signals.

P_j = 1 watt/mc

G_j = 0 db (to allow for plumbing, omnipolarization losses)

B_r = 2 x 1.5 mc on search,

2 x 4 mc on track.

K = 3 db (2.0) for detection on search,

7 db (5.0) for tracking.

Hence $R_c = 4.72 \sqrt{\frac{A_e}{K B_r}}$, n.m.

giving the ranges shown in *Table XXI.*

TABLE XXI

SINGLE JAMMER CROSSOVER RANGES

Aircraft Type	B-52	Delta	Straight Wing
R_c Search	1.93 n.m.	3.62 n.m. (3.3)*	1.36 n.m.
R_c Track	0.75 n.m.	1.49 n.m.	0.53 n.m.

* The crossover range on search for the Delta should be reduced by about 8% to allow for the effect of other more distant jammers in the raid transmitting into the Astra main beam and sidelobes. The reduction of the other entries in the table is negligible.

If the straight jamming threat at X-band had been used the table figures would increase 10% at nose and tail aspects, but would increase by a factor of 5 to 10 at beam aspects.

A cursory examination of the closing rates and minimum time delays indicates that the ranges given in the table are not sufficient to provide any missile launching capability whatsoever. Other information sources, such as passive ranging or missile seeker lock-on, must be used.

EFFECT OF ANGULAR LIMITS OF INFRA-RED COVERAGE

It will be noted that considerable reliance has been placed on the infra-red subsystem to supply angular information during quasi-passive ranging and to improve the angular discrimination capabilities of the AI when angle tracking multiple barrage jammers. With the infra-red seeker placed in the fin of the interceptor, the infra-red field of view below the horizon is limited to about 10 degrees head-on and to about 30 degrees at 60 degrees azimuth. This has a marked effect on the available placement zone, particularly for head-on attacks, and placement probability drops to about 60% at the expected infra-red detection range and a GCI σ of 3 nautical miles. As course difference decreases from 180 degrees, the degradation from the non infra-red placement zone is less; however, the zones become strongly lopsided relative to an ideal lead collision approach line, and GCI positioning procedure would have to be revised. By vectoring to an offset point about 10 nautical miles ahead of the target, probabilities very close to the non infra-red values can be obtained for all GCI σ's and all course differences less than 130 degrees.

Placement chance is also improved by using snap-up attacks from 20,000 feet below the target so as to provide an initial positive elevation angle.

In general, the passive homing courses seem less degraded than lead collision since they demand less lead angle than lead collision at long ranges (see page 99).

Target evasion aggravates the infra-red look-angle difficulties but, again, by using snap-up passive homing attacks, placement probability comparable to those for non infra-red lead collision can be achieved.

ASTRA ECCM VS CHAFF

The interaction of Astra and chaff is extremely complicated, and several distinctions must be made between gravity launched and rocket fired chaff, between single packet launches and continuous dispensing of multiple packets, and between aircraft with and without absorbent coating.

The following analysis differs from that of Reference 42 in several respects:

a) The range gate is considered a spherical shell in space rather than a flat slice as in Reference 42. This has a large effect in the critical beam areas at short ranges.
b) Since the Astra antenna is gyro-stabilized and rate-aided it has angular rate memory, whereas in Reference 42 it was assumed to have none.
c) The effective antenna beamwidth is taken as 6 degrees (including conical scan) for strong echoes and 5 degrees for weak echoes rather than the 4 degrees of Reference 42.
d) The approximate response functions of the range and angle tracking units were simulated on the REAC, whereas Reference 42 represents RTU response as a step function preceded by a time delay.

The chaff blossoming rate of *Figure 2* of Reference 42 for a 1-pound bundle is assumed here. Its growth in echoing area is shown in *Figure 40*.

The geometry of the chaff transient will be examined, then its effect on the RTU and the ATU separately and, finally, its effect on the RTU and ATU combined.

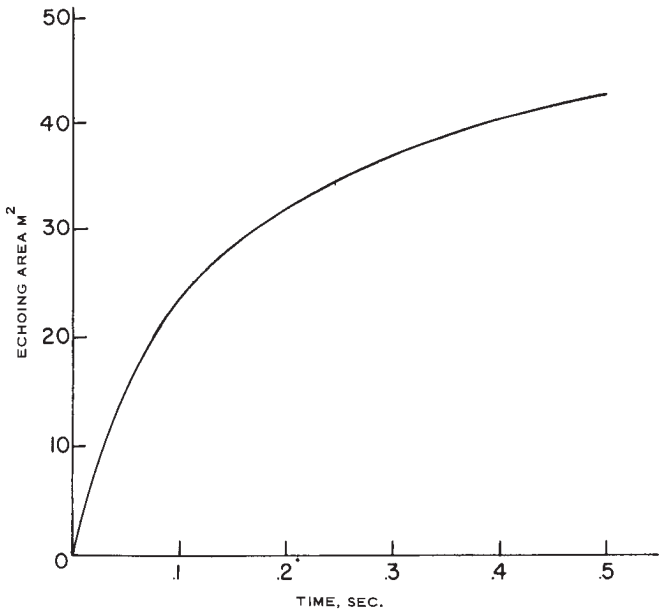

FIGURE 40 – Chaff Growth

Chaff Geometry

The kinematics of the chaff and target are shown in *Figure 41.* In this figure, the initial condition is assumed to be steady state tracking of the target, with the target centered in the edge gate. Upon this steady state the chaff imposes a transient, during which the position of the interceptor in target co-ordinates is considered fixed, since its relative motion is already included in the initial steady state tracking condition, and the duration of the chaff transient is usually less than two seconds.

The range difference between target and chaff is δ, where $\delta \equiv At^2 - Bt$, a quadratic function in time, and $A = \frac{V_T^2}{2R}$ and $B = V_T \cos a$.

Note that A is always positive and range dependent; B is positive or negative depending on aspect angle a.

$$\alpha = \frac{V_T (\sin a) t}{R}$$

$$= B_1 t, \text{ a ramp function.}$$

These expressions for δ and α represent the RTU and ATU inputs respectively whenever $\sigma_c > 6\sigma_t$ as in explosive chaff dispersal, or when σ_t is small (e.g. absorbent coated straight-wing target).

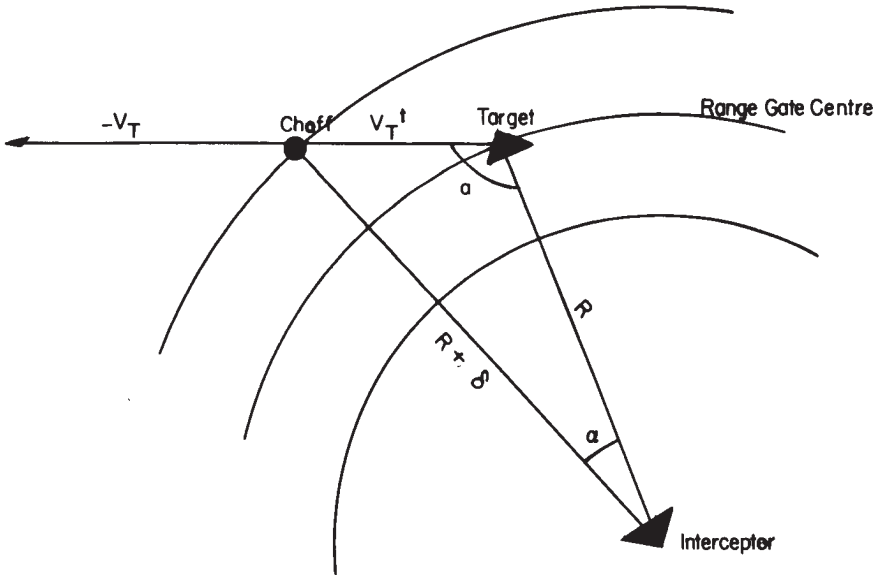

FIGURE 41 – Chaff Motion in Target Co-ordinates

By the cosine law

$$(R + \delta)^2 = R^2 + (V_T t)^2 - 2RV_T t \cos a.$$

Therefore,

$$\delta \approx \frac{(V_T t)^2}{2R} - V_T t \cos a \qquad \text{if } \delta << R$$

Delayed Blossom

Gravity dispensed chaff requires a finite time to blossom, and until it has an area large enough to overpower the RTU clipping feature, it has no effect on the RTU. Thus for the coated delta-wing target -the effective δ for about the first 1/6 second is zero. After that time it follows the same quadratic curve given above. For targets of large echoing area, the effective δ is always zero, since the target and chaff pulses are clipped to the same height in the RTU, and edge tracking follows the target. The input to the ATU is much more difficult to determine, since the ATU has neither signal clipping nor edge tracking features. The error signal can be derived by superimposing two ATU discriminator curves, one for the target, one for the chaff. Because of the fast AGC action, the maximum error signal voltage is taken as constant. Thus at first, the peak of the target discriminator curve has this maximum value and the chaff curve is lower; within less than .05 second the chaff curve takes control of AGC and the target curve diminishes.

The two discriminator curves are displaced from each other in angle according to the equation given above. It is evident that the error signal in the ATU is a complex function of the angular position of the antenna centreline relative to the combined discriminator pattern. It is theoretically possible, under certain conditions, to have three angular positions of equilibrium (zero error signal) – a stable one on the target, one at the geometric mean position which may be stable or unstable, and another stable one on the chaff. However, for all cases of interest it has been found permissible to assume that the ATU input is equal to $\left(\frac{K}{1+K}\right)\alpha$ where $K = \frac{\sigma_c}{\sigma_T}$, and that the error signal is proportional to the antenna pointing error measured from this position.

Forward Firing

The chaff is assumed to blossom instantaneously by explosive dispersal at some distance f directly ahead of the target.

Let

$$\tau = \frac{f}{V_T}$$

Then $\delta = At^2 + (B - 2A\tau)\, t + \tau^2 - B\tau$

Where δ, A and B are defined as before,
and

$$\alpha = \frac{V_T(\sin a)\, t}{R} - \frac{f \sin a}{R}$$

Note that if f and a are such that the chaff blossoms initially outside the range gate, it will have no effect until it enters the gate. An analogous restriction is true for the angle tracking unit.

Multiple Bundles

Each bundle follows the δ and α relations given above, therefore a series of bundles creates a series of these curves, spaced in time by the dispensing period.

Chaff Rocket

The rocket creates a series of chaff curves of the forward-fired type but with successively increasing f.

The inputs to the RTU and ATU for these cases are illustrated in *Figure 42* in which δ and α are plotted vs time, for positive and negative B.

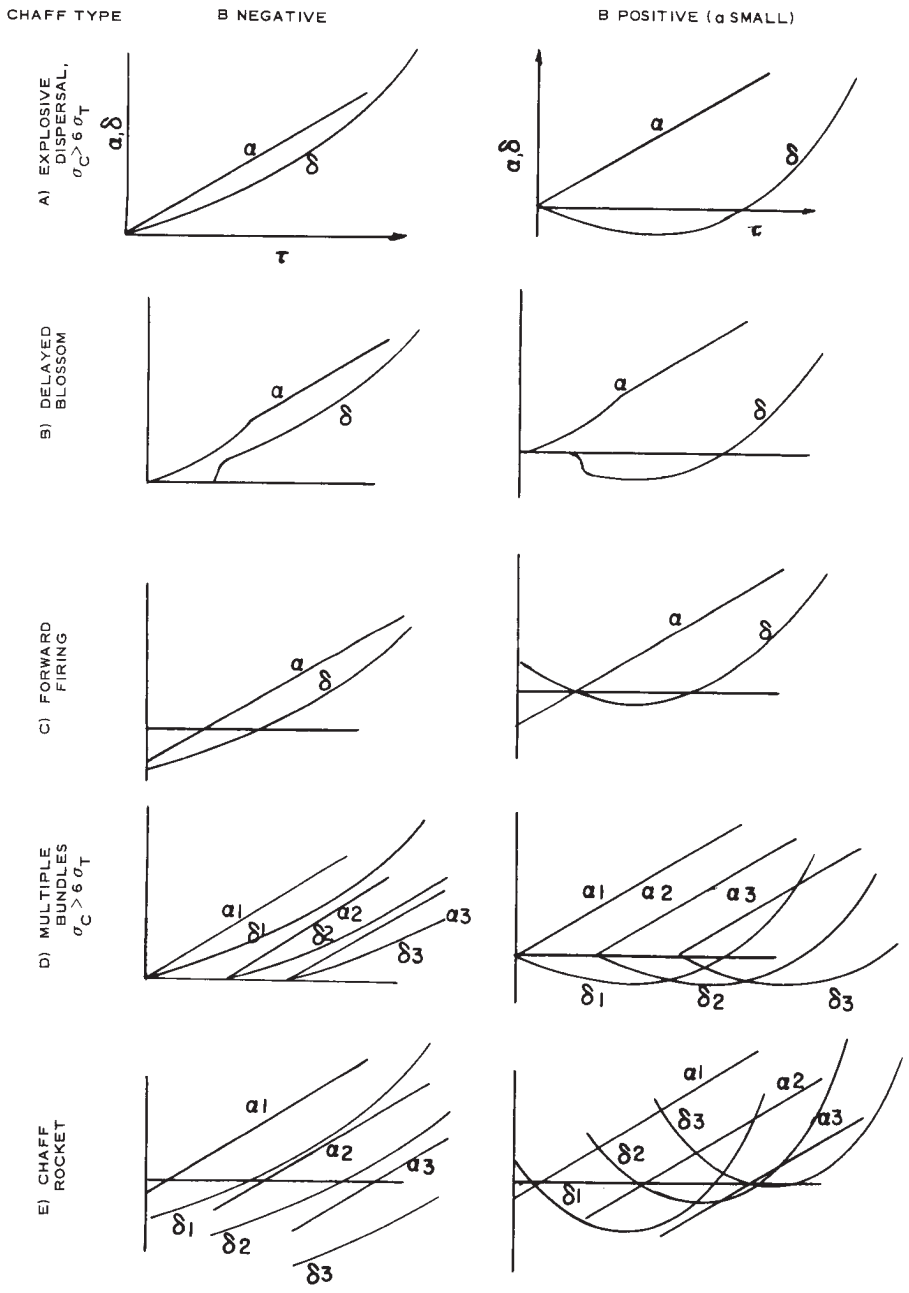

FIGURE 42 – Chaff Inputs to RTU, ATU

Effect on Astra Range Tracking

The Astra RTU was assumed to be operating in its edge tracking mode. The range gate response was simulated on the REAC by a quadratic function of the form $\frac{P}{QS^2 + RS + 1}$ chosen to provide adequate edge tracking in the presence of 5 g's of range acceleration. This gate was subjected to various combinations of A and B transients to find the limiting combinations for successful range tracking of the target. The condition of $\sigma_c > 6\ \sigma_T$ was assumed for most of the study. A typical response sequence is shown in *Figure 43*.

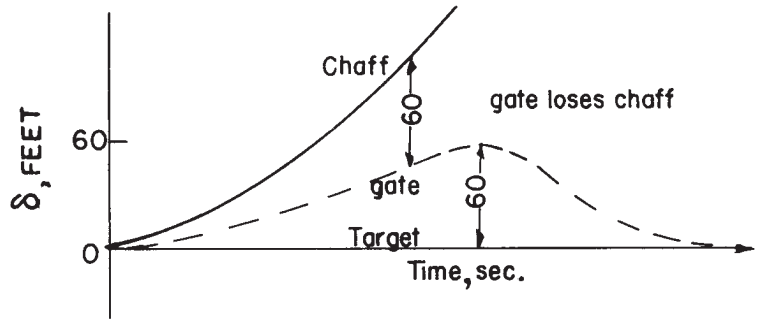

FIGURE 43 – Marginal RTU Tracking

The chaff is assumed lost when it leads the edge gate centreline by 60 feet. After losing the chaff the gate pulls back on the target, provided the gate centreline does not, at any time, coast from the target more than 60 feet; if it does, both the chaff and the target are lost. The A – B contour of chaff vulnerability is shown in *Figure 44*.

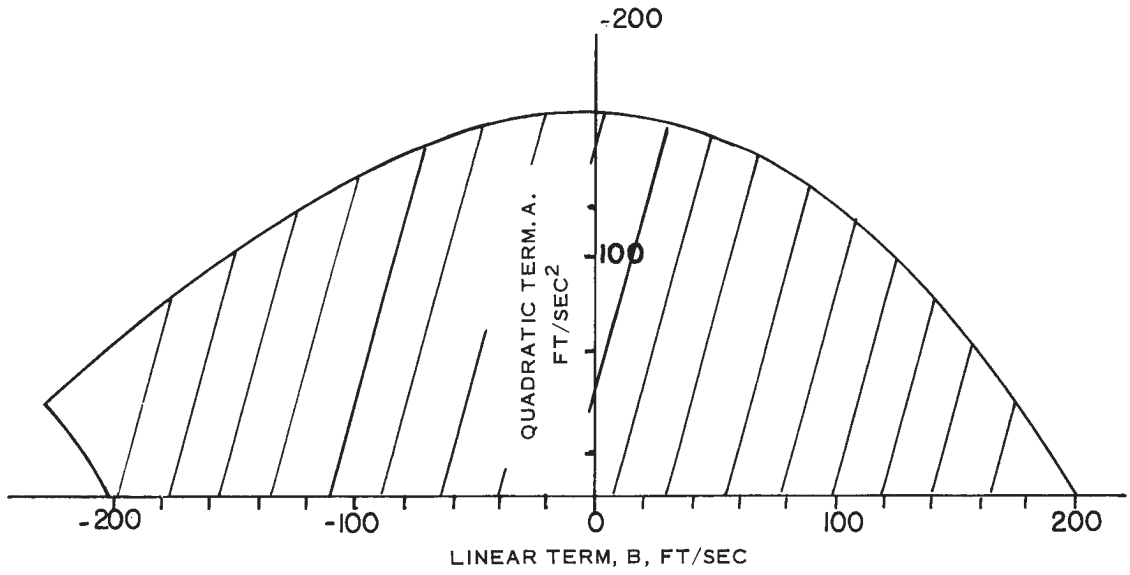

FIGURE 44 – RTU Chaff Vulnerability Zone in A–B Space,
Single Bundle, $\sigma_c > 6\ \sigma_T$, f = 9

The corresponding region of chaff vulnerability in target co-ordinates is shown in *Figure 45* for target speeds of Mach 0.8 and 2.

The B axis intercepts (A = 0) on *Figure 44* are symmetrical about zero, and represent the angular width of the chaff zone at R = ∞. The zone width at R = ∞ was found to be proportional to the square root of the range acceleration which the gate is designed to track, and inversely proportional to target velocity. The precise form of the RTU transfer function appears to have little effect provided it has the specified acceleration, i.e., tracking capability.

Single-bundle chaff cases other than gravity launching were analysed only in respect to their effect on zone width at R = ∞. The results are shown in *Figures 46* and *47*.

Both forward firing and delayed blossom of a single chaff bundle increase the suddenness of the transient caused by the chaff and, hence, increase the ability of the RTU to reject it.

If the target is not absorbent coated, its echoing area is comparable with that of the chaff, $\frac{1}{6} < \frac{\sigma_c}{\sigma_t} < 6$ and RTU clipping reduces both pulses to equal height. Edge tracking then enables the RTU to hold onto the target pulse. There will probably be a momentary break lock if the interceptor crosses the target's beam aspect while the navigator switches the RTU from one pulse edge to the other.

The effect on the RTU of sequential launching of several chaff bundles is rather surprising, but can be clearly deduced by an examination of *Figures 42d* and *43*. (The chaff rocket illustrated in *Figure 42e* will be discussed later). Consider in *Figure 43* the effect of adding a second identical chaff transient at any time during the sequence shown. Immediately, or after a very short blossom delay, the second bundle provides a competing input lying closer to the true target than the previous chaff bundle. Since the two chaff bundles have comparable echoing areas (in the ratio 1/6 to 6) the RTU "sees" them as equal pulses, and the edge tracking feature pulls the gate back toward the target. The same argument holds for any sequence of bundles. Hence, the effect of a sequence of bundles is merely to produce an oscillation of the range gate with period equal to the dispensing rate and with amplitude and average values small compared with the range gate width. The RTU memory, therefore, makes the discontinuous chaff trail into the equivalent of a continuous one. At normal dispensing rates, in excess of 1 per second, the RTU vulnerability zone disappears entirely. At slow dispensing rates, down to about .3 per second, (an unlikely case) it will be reduced in size.

The above argument is not true of the chaff rocket illustrated in *Figure 42c*. The points of origin of the successive bundles now lie progressively further from the target. The kinematics of the sequence can easily be designed to be acceptable to the range gate, which will follow the successive points of origin, i.e., the rocket, away from the target and coast off the end of the sequence into breaklock. The only practical difficulty for the rocket is that to carry the gate off the target at the beam aspect, a rather long trail of chaff bundles must be laid. If F is the trail length and G is range gate width, F must exceed $\sqrt{RG}$, which at R = 100,000 feet is 3,500 feet. However, a trail length of only 1,500 feet provides protection at all aspects except for a 3-degree gap on the beam, which is considered adequate. Hence, the chaff rocket is a practicable means of defeating the Astra RTU. However, it should be noted that if the chaff rocket is designed for use against non-rate-aided range gates, it may not be effective against Astra except in the beam region. To be effective at all aspect angles, the opening rate between the target and the chaff rocket must not exceed 200 feet per second.

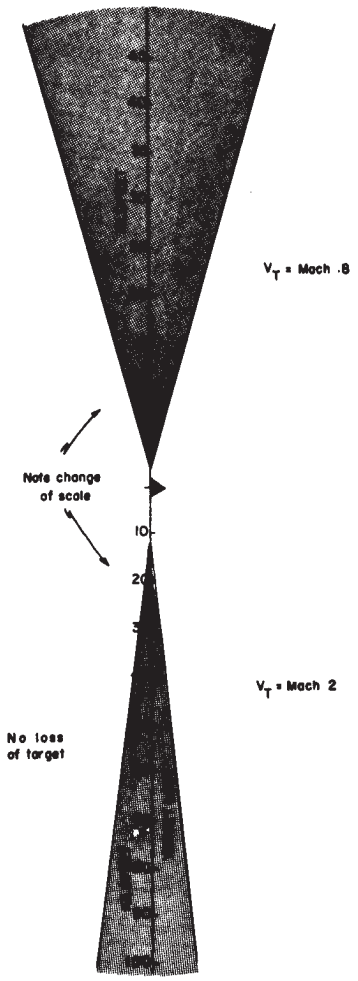

FIGURE 45 – RTU Chaff Vulnerability Zone in Target Coordinates

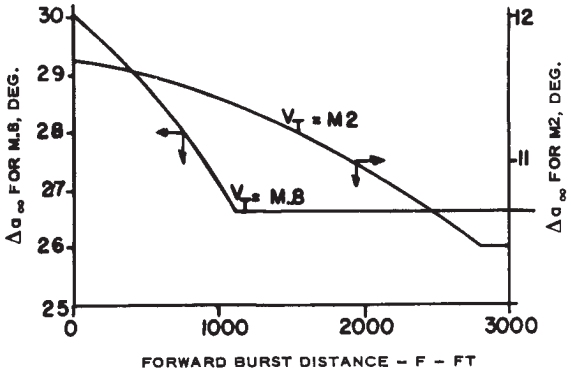

FIGURE 46 – Effect of Forward Firing on RTU, Single Bundles, $\sigma_c > 6\,\sigma_t$

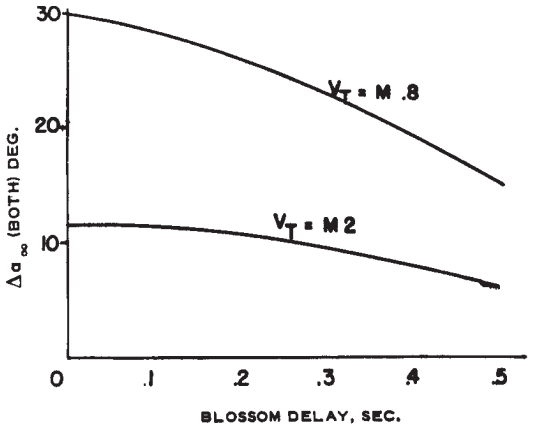

FIGURE 47 – Effect of Blossom Delay on RTU, Single Bundles

Effect on Astra Angle Tracking

The angle tracking response of the Astra was derived from the angle tracking circuits provided by RCA during CARDE visits to Camden. The open loop response was of the form $\frac{CS^2 + DS + E}{S^2 (FS + G)}$ with constants chosen to provide adequate angle tracking of an acceleration of 3 degrees per second^2, this being slightly greater than the maximum angular accelerations to be expected in non-chaff interceptions against Mach 2 targets. The tracker was subjected to ramp inputs to find the maximum chaff ramp it would track. Marginal angle tracking of the target was analogous to that of the RTU shown in *Figure 43*, except that the ATU response showed a sharp reversal in slope the instant the chaff was lost. The chaff was assumed lost if the angle between it and the antenna centreline exceeded 3 degrees. After losing the chaff the ATU reverses direction immediately and pulls back on the target, provided the antenna is not displaced more than 2.5 degrees at the instant of losing the chaff.

The limiting value of B_1 was found to be 6.33 degrees per second. The resulting vulnerability zone is shown in *Figure 48* for single bundles whose σ_c is assumed much greater than σ_T.

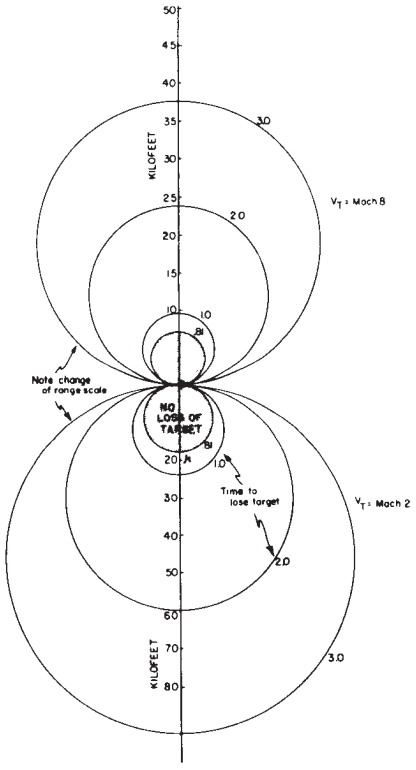

FIGURE 48 – ATU Chaff Vulnerability Zone

It is evident that, at any point outside a rather small circular contour on the target's beam, loss of angle tracking is only a matter of time. The diameter of this contour is inversely proportional to the square root of the angular acceleration tracking capability of the ATU, and is directly proportional to target velocity. The case of delayed blossom was not examined, but after inspection it is believed to cause a negligible decrease in the diameter of the invulnerable zone. The effect

of forward firing of single bundles is shown in *Figure 49* in which the dimension of the invulnerable zone at a = 90 degrees is plotted versus the angle subtended at the interceptor by the distance. Note that the shape of the invulnerability contour will deviate slightly from circular.

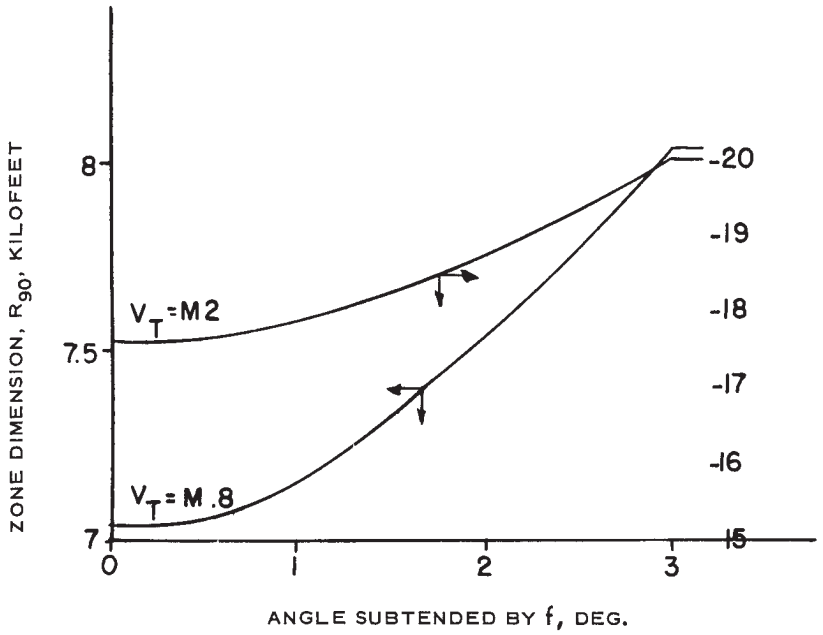

FIGURE 49 – Effect of Forward Firing on ATU, Single Bundles

$\sigma_c >> \sigma_T$

The ATU response to multiples differs from the RTU response because the ATU has no clipping or edge tracking features. It attempts to follow geometric centre of all the bundles within the antenna beamwidth. If the bundles subtend more than one beamwidth, no error signal is generated and the antenna coasts. Hence, it can be pulled off the target at any range or aspect angle, and the invulnerable zone disappears. However, this conclusion neglects the additional effect of RTU tracking, and further discussion of multiples must be deferred until the next section where both RTU and ATU are considered together.

To determine the effect of the chaff rocket on the ATU one must bear in mind the fact noted in the preceding section that the rocket opening rate must not exceed 200 fps. Hence the angular rate of the rocket itself, as seen by the ATU, is only 1/4 to 1/10 (and opposite in sense to) that of the bundles of chaff it dispenses. If one now plots the position of the centroid of all the chaff bundles sown, it will be seen to move steadily behind the target at an angular rate equal to the average of the angular rate of the rocket and the rate of the chaff, i.e., at a rate between 0.375 and 0.45 of the chaff angular rate. The ATU initially attempts to follow the centroid. If, however, the array of chaff bundles subtends more than the beamwidth (e.g. at a = 90 R < 20,000, the ATU receives no further error signal and coasts off the target. Thus the ATU tries to move behind the target while the RTU tries to move ahead of it. The net result will be discussed at the end of the next section.

Effect on RTU and ATU Combined

The RTU and ATU are mutually dependent in that the ATU "sees" only those signals within the 120-foot edge gate, and the RTU "sees" only those signals lying within a 6-degree beamwidth. It now becomes necessary to consider the length of time that the chaff or target lies within the gate or beamwidth. For single bundles, the following eight possibilities cover all but the marginal cases.

Successful Tracking if:

a) Chaff lost from ATU .2 second before target lost from RTU

b) Chaff lost from RTU before target lost from ATU

c) Both RTU and ATU reject chaff and retain target .

Break Lock if:

d) Chaff lost from ATU less than .2 second before target lost from RTU

e) Target lost from RTU before chaff lost from ATU

f) Target lost from ATU before chaff lost from RTU

g) Both RTU and ATU accept chaff and lose target

h) ATU accepts chaff, RTU loses both chaff and target.

The allowance of .2 second in "a" and "d" is designed to permit the RTU to recover from the chaff impetus, without coasting off the target. It is an approximate figure and is applicable only in the region of the RTU vulnerability contour. The ATU reverses slope sharply as soon as the chaff is lost and does not require a similar allowance.

In order to delineate the areas in which conditions "a" to "h" apply, it was necessary to determine the times involved in the process of losing chaff or target.

The results of the time study are shown qualitatively in *Figure 50* which indicates the regions in which each condition applies. Successful combined tracking is possible only in areas "a", "b" and "c"; for the subsonic target areas "f", "d" and "e" become negligibly small.

The final chaff vulnerability zone for single gravity-launched chaff bundles is shown in *Figure 51*. As noted before, forward firing or delayed blossoming has negligible effect on these zones.

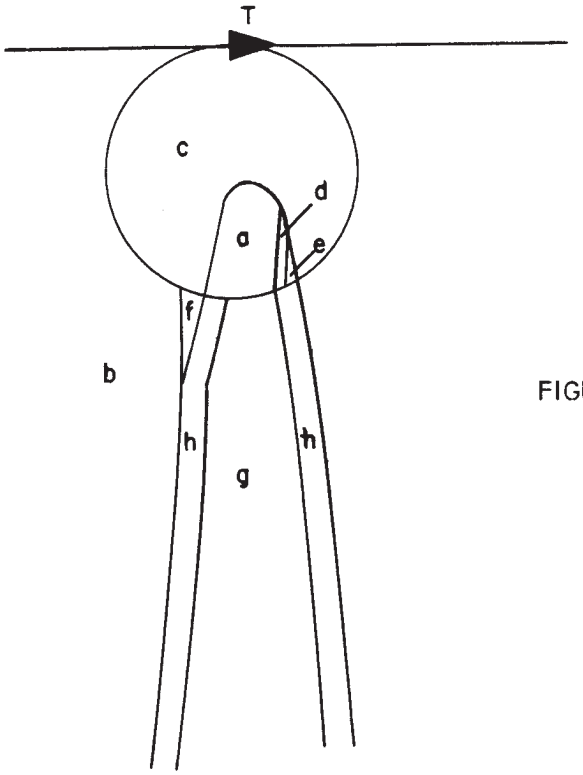

FIGURE 50 – Illustration of RTU/ATU Response Regions, Single Chaff Bundle

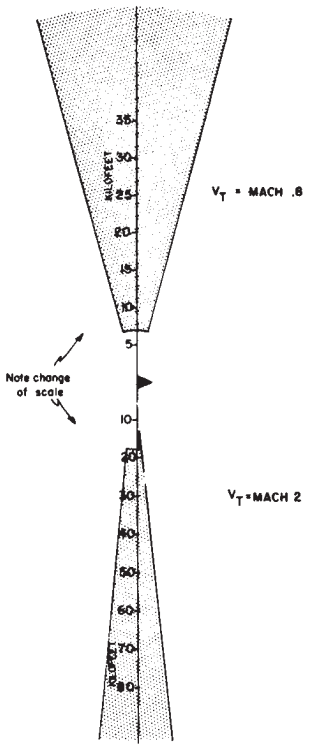

FIGURE 51 – Final RTU/ATU Vulnerability Zone Single Chaff Bundles

When the target releases a series of bundles, the RTU prevents the ATU from seeing chaff bundles which lie within its beamwidth but outside the range gate. This situation is illustrated in *Figure 52*.

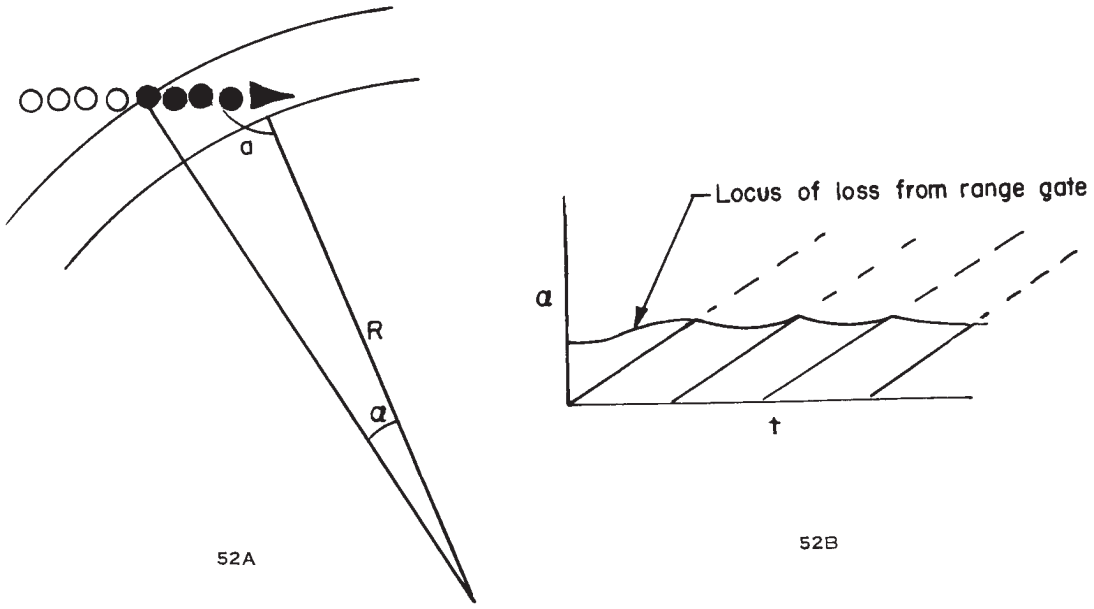

FIGURE 52 – Effect of Multiple Chaff Bundles on RTU and ATU Combined.

Hence, for all conditions in which angle α subtended by the visible chaff trail is less than one beamwidth, relatively stable range and angle tracking of a point close behind the target occurs. If α exceeds one beamwidth the ATU loses the target and breaklock occurs.

To determine the breaklock region in target co-ordinates the tracking error of the range gate must be known. For a dispensing rate of 5 bundles per second and for the region of interest near a = 90 and R > 10,000 feet, the maximum tracking bias is about 20 feet for the Mach 2 target and less for the Mach 0.8 target. A bias of 20 feet will be assumed for all cases to ensure conservative results.

For leading edge tracking the relation between R, α and a is approximated very closely by

$$\tan (a + \alpha) = \frac{-R\alpha}{\frac{R\alpha^2}{2} + \frac{G}{2} + b},$$

where G is the RTU edge gate width and b is the RTU tracking bias.

The corresponding relation for trailing edge tracking is

$$\tan a = \frac{R\alpha}{\frac{R\alpha^2}{2} + \frac{G}{2} + b}$$

The breaklock contours are obtained by setting $\alpha = 5$ degrees. The contours are shown in *Figure 53*. It is evident that the combined action of the RTU and ATU rejects a series of chaff bundles almost completely. The zone can be halved in width if leading edge tracking is used until "a" is a few degrees less than 90. Forward firing would also decrease the vulnerable zone. The AI tracking bias of 2.5 degrees will not impair the slaving or homing performance of Sparrow II (provided K-band chaff is not used); however, the MBI miss-distance will increase by an amount varying from 0 to 870 feet as "a" varies from 0 to 90 and from 180 to 90 degrees. The miss-distance increase is less than 350 feet except in a 10-degree region near the target's beam, hence the average loss in P_k is not serious.

Finally the combined reaction of the RTU and ATU to a chaff rocket will now be discussed. As noted above, the range gate follows the chaff rocket forward from the target. Unless the ATU can reject the chaff rocket from the antenna beamwidth, loss of range lock will occur. The situation is very similar to that shown in *Figure 52*, except that as the range gate moves forward following the rocket, the locus of loss of chaff from the RTU (and hence the ATU) moves with it. This is illustrated in *Figure 54*.

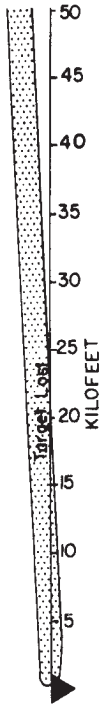

FIGURE 53 – Final RTU/ATU Vulnerability Zone. Multiple Chaff Bundles.

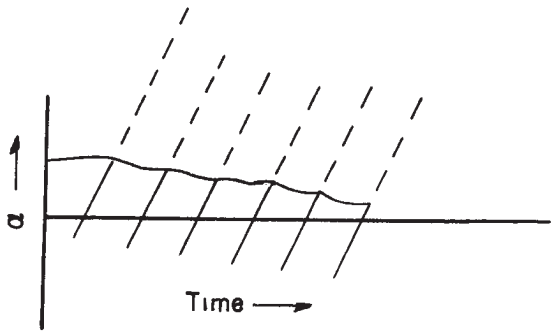

FIGURE 54 – Effect of Chaff Rocket on RTU and ATU Combined

The angle α within which each chaff bundle is visible to the ATU is dependent on range and aspect angle. α will equal or exceed one beamwidth whenever the fighter lies within a zone very similar to that shown in *Figure 53*. Within this zone, either the ATU or the RTU will lose the target; outside this zone, the RTU will lose the target. There may be a small circular zone around the target similar to that of *Figure 48* within which the ATU may protect the RTU against breaklock, but this effect is not significant. The chaff rocket remains a most effective means

of disrupting Astra tracking. Unless an attack procedure can be found which does not require lock-on, the chaff rocket, launched just before the missile, or at intervals of about 10 seconds, can abort an Arrow interception. The IR track - AI range mode may help once the use of chaff rockets is detected.

Area Sown Chaff

There are several factors which seem to militate against the use of this countermeasure:

a) The survival probability of the sowing aircraft is likely to be very low, since they must precede the formation and their course is clearly marked by the trail sown. Hence they would have to be crewless aircraft, and would be effective only in the early stages of the raid.
b) There are several clues which permit an interceptor to discriminate against them: the chaff echoes show less fading than a target blip at the same range; they are in general more diffuse; they have radically different range and/or azimuth rates from the target blips. As a final check they can be tracked long enough to obtain a range rate reading. Their main effect is a delay in locking onto an aircraft. Once the radar has locked onto an aircraft, discrete chaff bundles have less disruptive effect than if gravity-launched by the target being tracked. If large areas of chaff are encountered they can be rejected by selecting video pre-gating, which permits the RTU and ATU to coast at constant range and azimuth rates until the cloud is past.

CONCLUSIONS REGARDING THE "HARDWARE" DUEL

The four countermeasures which are most effective against Astra are listed in descending order of importance.

Countermeasure	Effect
1. Barrage jamming	No useful crossover range, AI angle tracking at ranges less than about 20 nautical miles (discrimination problem). Passive infra-red tracking at ranges less than about 20 nautical miles on supersonic target.
2. Barrage Jamming with amplitude modulation at conical scan frequency.	No useful crossover range, No passive AI tracking, Passive infra-red tracking as above.
3. Chaff Rockets launched continuously.	Lock-on prevented, but range and angle available on search mode.
4. Chaff Rocket launched just before interceptor missile launch.	Loss of lock-on at missile launch range, aborted pass.

Threats 2 and 4 are placed after 1 and 3 respectively because the increased complexity of the jamming equipment they require makes them less likely to be used. The other threats are either ineffective or force the use of the infra-red auxiliary with its attendant range and look angle limitations. If the attacking aircraft are in formation, the infra-red range limitation is not considered serious, since there will nearly always be an enemy aircraft placed in a relative position which requires little corrective manoeuvre after lock-on. The look angle limitations are relatively serious, as indicated in the section on Astra ECCM vs Chaff, particularly in the presence of evasion. However, the use of non-co-altitude approach and attack courses other than lead collision (see next Section) permit successful approach within the look angle limits of the infra-red system.

In view of threats 1 to 4, there is a strong requirement for some means of carrying out an AI approach from detection to launch, using only angle information derived either from passive angle-tracking or from the search display.

There is a secondary requirement for a passive means of determining an approximate launch range on a jamming target, so that once the interceptor has homed to a launch position, it may have sufficient intelligence to launch its missiles within their launch range tolerances. This requirement is secondary since the Sparrow II can itself be relied on to perform this function. However, a back-up would be desirable as insurance against K-band jamming.

PASSIVE HOMING AND RANGING IN AN ECM ENVIRONMENT

In this section, the study will go beyond the assessment of the Astra as initially designed to consider not only the tactics but also the simple equipment additions or modifications which could significantly improve its capability in ECM. This is done on the grounds that the initial design of any equipment is subject to improvements. One of the modifications to be described has already been incorporated in the Astra.

Successful AI operation in an ECM environment entails the fulfillment of two requirements.

a) The interceptor must be provided with a guidance signal which will permit it to counteract initial GCI placement errors and target evasion, home toward the target and enter the missile launch zone on a heading with the missile's acceptable launch heading tolerance.

b) Some range information is needed to indicate entry into the launch zone and to provide a missile firing signal.

These requirements have been greatly eased since the advent of the guided missile. In the era of unguided weapons, requiring high aiming accuracy, the only solution to the ECM problem was the restoration of full normal AI operation, usually by hardware fixes which permitted the AI to reject ECM. These fixes have been notoriously unreliable and impermanent. The guided missile's tolerance of range and heading errors opens a new field of passive, approximate solutions to the AI problem, which promise to be more permanent. It is only fair to add that the guided missile has achieved this relaxation of AI requirements only at the expense of the added vulnerability of its own guidance to ECM; but since its mission is to impact the target and it operates at a larger speed advantage, the homing problem for the missile itself is simpler in principle than that of the AI. The Sparrow II has the additional protection of operating on an uncommon frequency which is relatively expensive for the enemy to jam.

AI HOMING

The homing procedure has two objectives;

a) It must guide the interceptor so as to enter the launch zone on an acceptable launch heading from any aspect angle.

b) It should provide reasonable ability to counteract placement errors and evasion, i.e., have good placement probability.

The requirements of the missile launch zone are illustrated qualitatively in *Figures 55, 56, 57* and *58*. *Figure 55* offers a definition of geometric quantities. Only two dimensions are shown; extension to three is straightforward. Aspect angle A and range R are unknown to the interceptor; θ and, in some cases, ω, are assumed known.

For Sparrow II intercepting a Mach 2 Target the maximum θ at A = 90 degrees is about 43 degrees and the lead angle tolerance at R max about ± 12 degrees. The target speed of Mach 2 was chosen. The figures which follow are approximate and are inserted for illustration only. Numerical results will be given at the end of this section.

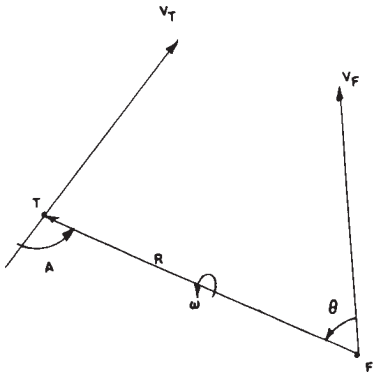

FIGURE 55 – Interception Geometry

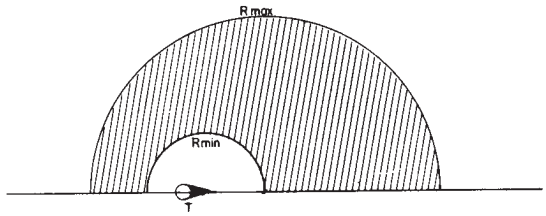

FIGURE 56

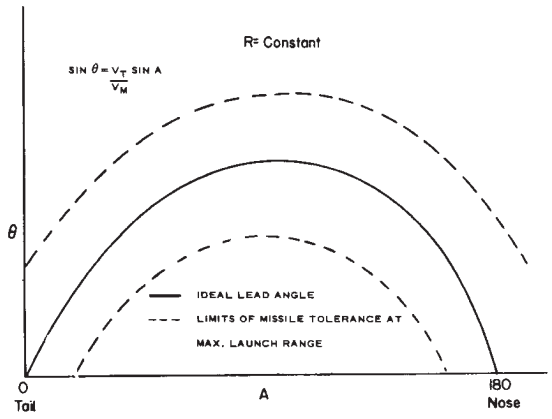

FIGURE 57

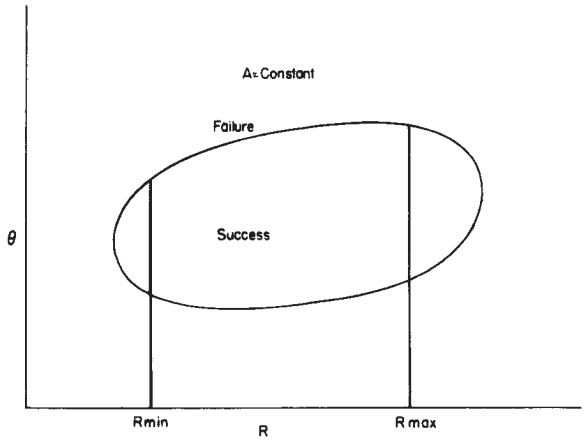

FIGURE 58

Fixed Lead

One of the homing modes commonly suggested for use in ECM is pure pursuit, i.e., lead angle θ of zero. From an examination of *Figure 57*, it is evident that zero lead satisfies the missile requirements only in a narrow region on the target's nose and tail, as shown in *Figure 59*.

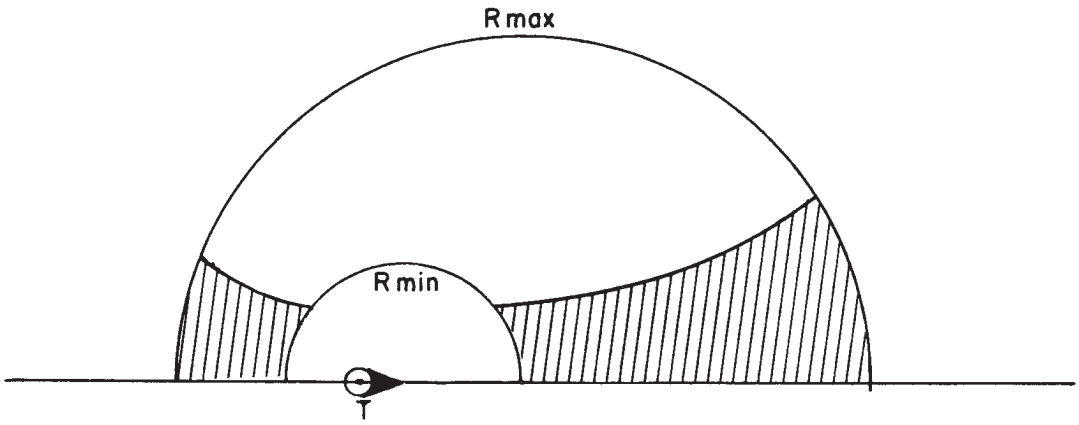

FIGURE 59

The region within which launch is possible will be termed the residual launch zone. The loss of a large angular sector around the beam causes a very serious loss in probability of successful homing, and pure pursuit is not practical for supersonic targets. As the target speed decreases, the residual launch zone increases, and pure pursuit launch is possible at all aspect angles against a Mach 0 8 target. Even for this target speed the range depth of the residual zone is small in the beam region around A = 90 degrees.

A better choice of fixed lead would be a value around 30 degrees which, by inspection of *Figure 57*, would provide a launch capability at all aspects from about 30 to 150 degrees, as indicated in *Figure 60*. Once again, the residual launch zone is not too promising; however, it improves more rapidly than pure pursuit as target speed decreases and an all round launch is possible in fixed lead against targets having speeds up to Mach 1.25. Depending on GCI ECM conditions, it may be possible to combine this mode with pure pursuit, changing from one to the other on advice from the GCI. Note that the target evasion may convert the fixed lead angle into a fixed lag angle if A changes from starboard to port during the intercept. Again, the provision of rough aspect information from GCI would be helpful.

The fixed lead modes have the advantage of not requiring passive angle tracking. They can be carried out using only the search display on the B scope, provided interceptor and target altitudes can be matched to about ± 10,000 feet. If desired, they can also be mechanized to provide the pilot with a steering dot. This has been done on the CARDE MG-2 with very little effort, using two tubes and a few relays and potentiometers. A description of this and other simple modifications will be found in CARDE Technical Memorandum 278/59 (50). The modifications were flight tested in CARDE/DSE Project Sprint IV and found satisfactory.

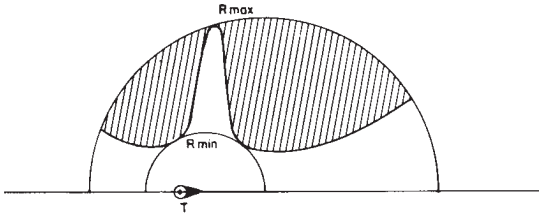

FIGURE 60

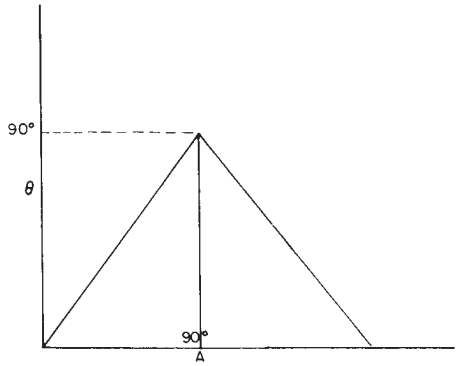

FIGURE 61 – Pure Collision Lead Angle

Fixed Angular Rate

If passive angle tracking is available, the angular rate ω permits the interceptor to execute pure collision homing by steering to null the ω signal. The lead angles which result are shown in *Figure 61* for $V_t = V_f$ = Mach 2.

On comparison with *Figure 57*, it is evident that pure collision provides a launch capability only in the target nose and tail regions. The residual launch zone is shown in *Figure 62*.

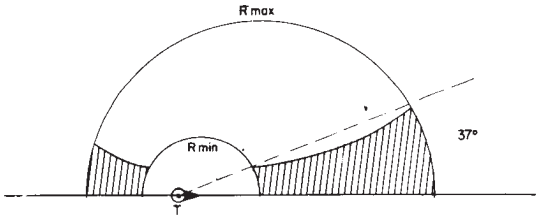

FIGURE 62 – Residual Launch Zone
Pure Collision

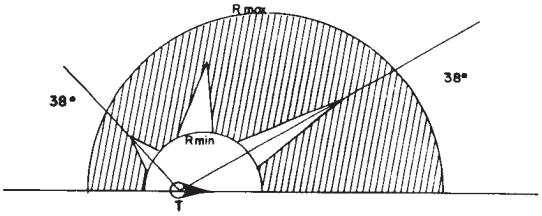

FIGURE 63 – Residual Launch Zone, Combined
Pure Collision – Fixed
Lead Pursuit

The zone does not provide acceptable effectiveness and, of course, cannot be used near the beam because of AI look angle limitations. However, a decrease of target speed to Mach 1.7 provides all-round launch capability with no AI look angle restriction.

The combination of pure collision with fixed lead makes an effective homing system. The AI would be set initially to pure collision, this providing information as to which side the fixed lead should set, independent of GCI aid. If the lead angle on pure collision is less than about 35 degrees pure collision is maintained; if it exceeds 35 degrees the AI is reset to fixed lead, with a lead angle of about 35 degrees. Both modes can be mechanized quite simply with conversion from one mode to the other accomplished either manually or automatically. The combined pure collision fixed lead mode has a residual launch zone as shown in *Figure 63* and provides good interception effectiveness at all aspects.

Pure collision implies a serious hazard to the interceptor aircraft if range information is not obtained in time. To avoid this, a fixed (non-zero) angular rate was also considered. The value of ω chosen must be small, otherwise it will not be achievable at long ranges on any heading, and will lead the interceptor toward the rear of the target. A value of 2 milliradians per second was considered, applied in a direction such as to reduce θ. The residual launch zone is almost identical with that of *Figure 62*, but a small miss-distance between the two aircraft is assured.

Fixed Range Lead Pursuit

Consider the two-dimensional steering equation for lead pursuit:

$$R\,\omega + (V_m - V_f)\sin\theta = 0$$

When passive angle tracking is available, the only unknown in the equation is R. Set the R voltage in the computer at a fixed level $\bar{R}$ by caging the range servo, where $\bar{R}$ is the mean launch range of the missile. The steering equation is now of the form $\sin\theta = K\omega$, and is free from port-starboard ambiguity. This homing mode is designated fixed range lead pursuit.* At very long ranges, it is asymptotic to pure pursuit. As range decreases, the lead angle increases until it equals the correct lead pursuit angle when $R = \bar{R}$. When $R \leqslant \bar{R}$ the lead angle demanded exceeds that of lead pursuit. Throughout the whole of the region between R min and R max, the lead angle error is less than 5 degrees, and all of the normal launch zone is available. The mode is superior to any of the others studied and is very simply mechanized. It was described to members of RCA on their first visit at CARDE, and provision for it has since been made in the first Astra.† The mode is not quite as efficient placement-wise as lead collision since it tends to lead the interceptor into the target's tail region. This is shown in the trajectories of *Figure 64*. However, the placement zone is not significantly smaller than that for lead collision. For numerical results see section entitled "Probability of Successful Homing and Ranging". Operation in the tail zone of fast targets can be improved by combining this mode with pure collision, again switching on the basis of lead angle.

PASSIVE LAUNCH RANGING

Before discussing truly passive ranging methods, the use of Sparrow II for ranging should be mentioned. If one missile could be carried extended for a period of two or three minutes, it could be angle-slaved by the passive angle tracking, and range-locked by programming its gates in and out as in the visual mode. It could be launched as soon as lock-on occurs, and the other missiles extended, slaved and launched. However, it would be preferable to launch at some fixed range corresponding to R in the fixed range lead pursuit mode, since flight trials indicate that retention of first lock-on is unreliable. This appears to be the most practical solution in the absence of K-band jamming. Passive measures to be used as back-up will now be discussed.

* (or fixed range and time-to-go if operating on the lead collision equations, Fixing T at T_f, the missile flight time, converts lead collision to normal lead pursuit).

† If the Nav AI selects AI or infra-red homing on the CCM selector then selection by the pilot of lead collision or lead pursuit on the attack mode selector will in fact provide pure collision or fixed range lead pursuit, respectively.

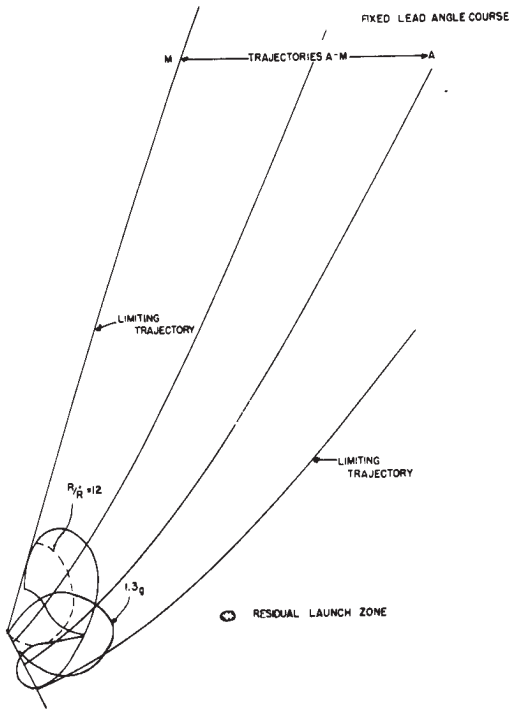

FIGURE 64 – Sketch of Some of the $L\alpha = 20°$ Command Trajectories with Residual Launch Zone, $R/\ddot{R} = 12$ sec. Contour, and 1.3 g Isogee Contour for these Trajectories.

Optical Ranging

If the interception occurs during daylight hours, which at high latitudes average less than 12 hours out of 24, visual ranging estimation may be used. The unaided eye can probably achieve a detection range of 6 miles and range estimation will be in error by about 40%. Hughes Aircraft Corporation have investigated the use of telescopes with magnifications from 5 to 8 having a fixed reticle whose size is chosen to represent the image size of a known target wing span at some pre-selected range. Range estimations were found to be accurate to ± 5%. However, the problem of training the telescope in any mode but pure pursuit is serious.

Infra-Red Ranging

Methods have been devised for passive ranging with infra-red. General Electric Co. have developed the "Stranger" System which determines the location of the point of focus of the infra-red rays in a long focal length system. The focus point is related to the range. This procedure requires extremely accurate measurement of the focus point location and is impractical at long ranges. It can be designed to provide a single launch-range indication with fair accuracy.

It is also possible to determine range by measurement of infra-red radiation at two different wavelengths. The ratio of signal strength at the two wavelengths is a function of range, since the absorption of infra-red radiation at the two wavelengths differs. The method requires some knowledge of the infra-red properties of the target.

A similar method proposed by CARDE is to insert an additional known absorption into the infra-red path and measure the additional attenuation which results. If the range absorption law is known, it can be used to determine range but this requires some knowledge of target properties.

Incident Power Measurement

It is possible to determine $\frac{R}{\dot{R}}$, which is a pseudo time-to-go, by measuring the power received from the jammer, since from the simple propagation law

$$P = \frac{K}{R^2} \quad \text{where P is power received,}$$

one can obtain $\frac{R}{\dot{R}} = -\frac{2P}{\dot{P}}$

The automatic gain control bias voltage could be used to represent P. With appropriate smoothing this method can tolerate considerable fluctuation in jammer output or jammer antenna gain pattern, and may provide useful range information even against multiple targets.

Line-of-Sight Rate

If the two aircraft are flying straight courses, time-to-go can also be expressed as follows:

$$\frac{R}{\dot{R}} = -\frac{2\omega}{\dot{\omega}}$$

where ω is the angular rate of the line-of-sight. The measurement of ω and $\dot{\omega}$ appears difficult and the calculation gives very large errors if the target manoeuvres.

Ground Echo Tracking

The best known system of ground echo tracking is that developed by Fairchild Corp. under the trade names Padar or Pacor. This system was built-up primarily for passive detection of fighters by a bomber. Using two antennas, Padar measures the time delay between reception of the direct and ground-reflected pulses from the radar of an approaching fighter. This quantity, when combined with the elevation angle of the direct signal, provides range. The system gives reasonable accuracy for pulsed signals and is now being developed for use with noise signals.

Padar requires searching the ground in angle to find the ground echo with the smallest time delay. However, it may be possible to locate and track this ground echo solely on the basis of its stronger signal strength, as compared with that received from other areas of the ground. The range equation is as follows:

$$R = \frac{2h \cos E}{\sin (D + E)}$$

where h = fighter altitude

D = depression angle of the direct signal

E = depression angle of the ground echo

This procedure depends on the ground return being partially specular in nature. It has been noted that sharp reflections of the moon can be seen from ground surfaces whose roughness greatly ex-

ceeds the Rayleigh roughness criterion. Hence, there may be some hope for angle tracking of ground echo at high altitude, and airborne trials have been proposed for Project Spartan to investigate this possibility.

Acceleration Measurements

The pursuit courses all require the gradual increasing of lateral accelerations by the interceptor as the range decreases. The possibility of using an accelerometer to launch the missile was considered. The general shape of the lateral acceleration contours for the pursuit modes is shown in *Figure 65*. It is evident that acceleration is not suitable to provide launch information except in a narrow zone, about 40 degrees wide on the beam of the target.

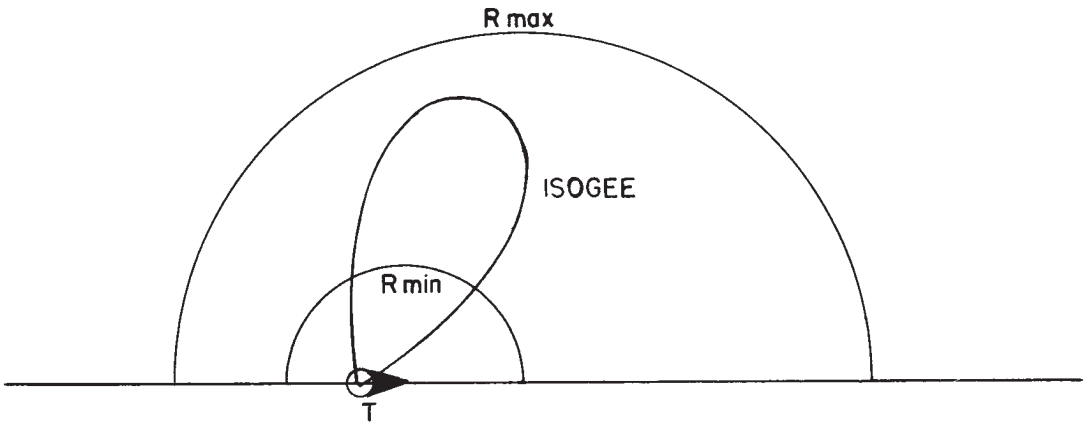

FIGURE 65 – Lateral Acceleration Contour

Launch by GCI Command

If the GCI is not jammed and the bombers are so few or so dispersed that unambiguous designation of a specific target is possible, a GCI controller can estimate launch range with acceptable accuracy. However, it is unlikely that these requisite conditions will ever be fulfilled.

Range Finding Manoeuvres

Range finding manoeuvres were first suggested (to the writer's knowledge) in Project Lamplight. The procedure proposed in that report was to turn to a collision course, with lead angle θ_c, then off collision course to some other heading so as to produce a lead angle θ_1 and a line-of-sight rate ω_1. R is then approximated by the formula:

$$R \approx \frac{V_F \ (\sin \theta_1 - \text{Sin } \theta_c)}{\omega_1}$$

The feasibility of the manoeuvres is critically dependent on the ability to measure small values of ω, of the order of 1 or 2 milliradians per second. Better filtering of the ω signal could be done if the manoeuvre were a continuous oscillation, since range would then be proportional to the amplitude ratio of the oscillations in θ and ω. Unit square-wave filtering could be applied to the ω signal to reduce the noise. Experiments were carried out with an APG40 radar tracking a pulse return from a corner horn, which was actuated to produce sinusoidal ω with a peak value of 0.6 milliradian per second. The measured ω output from the APG40 was 0.58 milliradian per second, with a standard deviation of .03 milliradian per second, indicating the efficiency of the square wave filtering. There are other practical problems, such as the effect of aircraft motion and radome aberration on the ω signal and the difficulty of phasing the square-wave filtering correctly.

A modification of the above procedure is to measure the lateral excursion of the fighter from a pure collision course and to use this as a base line for a triangulation method for determining range. A base line can also be provided by longitudinal acceleration or deceleration, but a longer time is required to achieve useful base line lengths.

CARDE has done some theoretical and experimental work on the use of a vertical manoeuvre; this work is described in CARDE Technical Letter 1239/59 (49). A vertical manoeuvre has several advantages:

a) The target is more likely to fly level than to fly straight.

b) The vertical aspect angle between the target velocity vector and line-of-sight is usually known to the fighter, whereas the horizontal aspect is not known.

c) A single diving or climbing manoeuvre can provide both range and range rate at all times after completion of the manoeuvre.

The relevant geometry is shown in *Figure 66* and equation is given below.

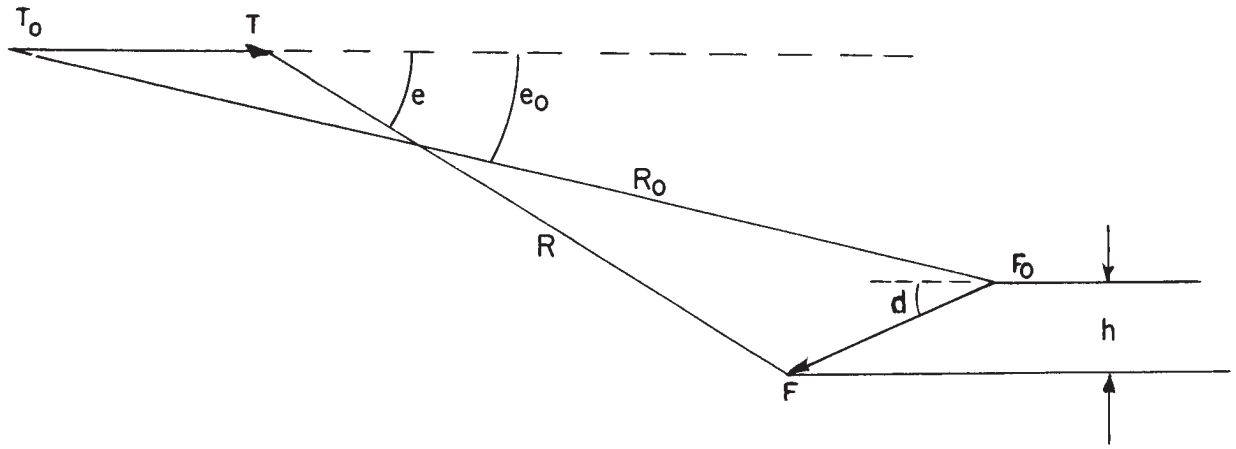

FIGURE 66 – Geometry of Vertical Manoeuvre

$$R \doteq \frac{h}{e - e_o} .$$

The accuracy of the equation decreases as e_o increases, hence the manoeuvre should be initiated from approximately co-altitude. CARDE has developed an air-borne ranging computer to solve this equation and will flight test it during Project Spartan. The output of the ranging computer could be fed to the fire control computer which would then revert to normal lead collision homing.

Range Keeping

A range keeping formula can be derived from the basic kinematic equation which will provide continuous R and $\dot{R}$ information once an initial value of R is known. It assumes no target manoeuvre but permits any fighter manoeuvre. The equation is as follows:

$$R\dot{\omega} \doteq 2\dot{R}\,\omega = - V_F \cos\theta\,\dot{H},$$

where $\dot{H}$ is the rate of change of heading of the fighter. RCA has built and tested a computer using this equation. It provides range to sufficient accuracy for launch of Sparrow and possibly of Genie, once given an accurate initial input. It is unlikely that an initial range input will be obtained from the AI since even responsive jammers will be initiated by the period of continuous painting which precedes lock-on. However, the range keeper would be useful when combined with passive ranging methods such as I.R. or GCI described above. It may also have some application in a non-ECM environment as a means of detecting target evasion.

Conclusions re Passive Ranging

There are several devices of relatively low complexity which will provide an approximate launch range by passive means. Of those studied, echo tracking, power measurement and vertical manoeuvre are the most promising. Using one of these methods, it should be possible to determine launch range to ±30%, which is adequate for launch of the Sparrow II.

PROBABILITY OF SUCCESSFUL HOMING AND RANGING

Probability of successful attack (within the limits defined in Chapter II of this report) can be calculated by an extension of the placement analysis already described. However, the probability of successful measurement of launch range must be added. Two mean launch range contours were chosen: one representing constant $\frac{R}{\dot{R}}$ of 12 seconds for use with the incident power ranging methods and with the line-of-sight rate method, and the second contour a constant range of 25,000 feet for use with the other ranging methods. The two mean contours are shown in *Figure 67*. The fixed range contour evidently provides the better fit.

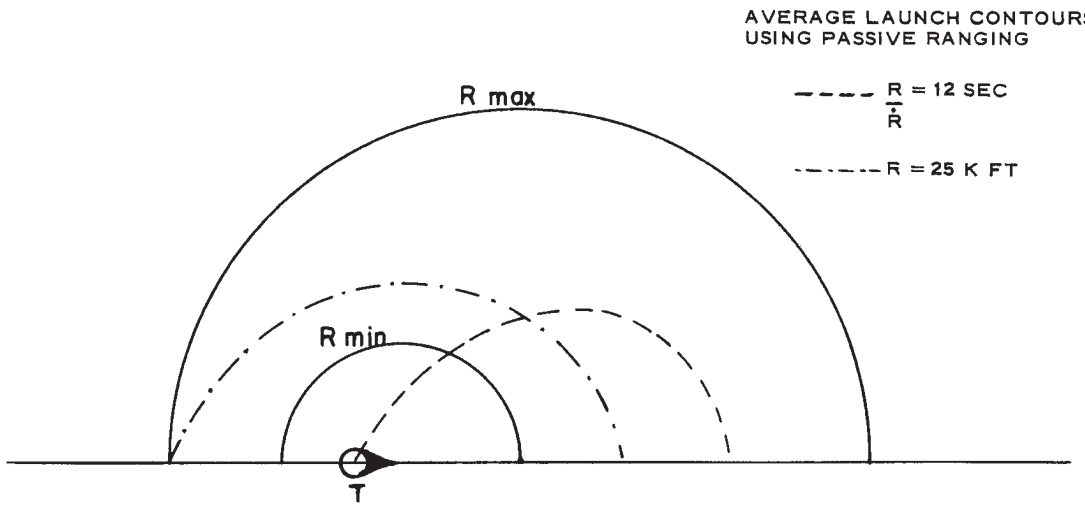

FIGURE 67

It was assumed that passive ranging errors were normally distributed about these mean contours. Two standard deviations were used, ± 20% and ± 60% of mean range or mean time-to-go, so as to bracket the expected range errors. Next, the placement zone for each homing mode was determined on the REAC, bearing in mind the limitations of the appropriate residual launch zone. Two initial course differences were used, 110 and 180 degrees, with and without target evasion. On examination of the residual launch zones, it is evident that the probability of successful measurement of launch range will vary with aspect angle A. If the zone is entered at a point where it has little range depth, ranging probability will be low. This variation with aspect was handled by dividing the placement zone into 14 equal lanes. A trajectory was run from the centre of each lane and the range depth of the residual launch zone along each trajectory was noted. These range limits formed the limits of integration of the Gaussian range error distribution. Thus for each lane the product $p_p\ p_r$ was found: where p_p is the probability that GCI would place the interceptor in that lane, and p_r the average probability of successful launch ranging for trajectories initiated within the lane. The sum, over the 14 lanes of the individual $p_p\ p_r$'s, provided the total probability $p_p\ p_r$ of successful placement and ranging. The fixed lead modes showed good probability at certain aspects, but were very ineffective at others, as might be expected from their residual launch zones. They were also ineffective against evading targets. The same was true for pure collision. The results for fixed range lead pursuit mode are shown in *Table XXI* for a Mach 1.5 target. Probabilities for the Mach 2 target were the same for 180-degree course difference and about 10% less for the 110-degree.

The relative decrease in these figures caused by evasion is almost the same as occurs in the non – ECM environment at the same target speed. Combined modes have not been analysed. It is estimated that pure collision-fixed lead would provide probabilities slightly less than those of *Table XXII*, and pure collision-fixed range lead pursuit slightly greater.

TABLE XXII

$P_p P_r$ for Fixed Lead Pursuit

V_t = M 1.5 no manoeuvre

σ_{GCI} = 3 n.m.

Ranging Method	Ranging Accuracy	$\Gamma = 110°$	$\Gamma = 180°$
$\frac{R}{\dot{R}}$ – 12 sec.	± 20%	.75	.85
$\frac{R}{\dot{R}}$ – 12 sec.	± 60%	.30	.45
$\overline{R}$ = 25K ft.	± 20%	.93	.93
$\overline{R}$ = 25K ft.	± 60%	.40	.55

NOTE ON MB–1

The launch range and lead angle tolerances of the MB-1 as presently constituted prevent the use of passive homing and ranging. Hence, its effectiveness against the four threats listed in the Section on "Conclusion on the Hardware Duel" is nil. Since barrage jamming is very likely to occur, the usefulness of MB-1 in a realistic combat environment is very low.

It is possible to redeem the missile by supplying it with a long-range influence fuze. It can then be used with the fixed range lead pursuit mode, launching at a fixed range, $\overline{R}$, and will tolerate a ± 20-per-cent launch-ranging error at high altitudes with little loss in P_k. (This is not true if any other homing mode is used). If the present missile were used in this regime, the errors in setting its time fuze would make it completely ineffective. This topic is further discussed in CARDE Technical Memoranda 278/59 and 283/59. (50, 51).

FLIGHT TRIALS

A series of about 100 interceptions were carried out by CF-100 aircraft during Project Sprint IV to assess some of the homing and ranging procedures just described. Ranges, turn radii, and decelerations during turn were all scaled to provide an exact 3/8 scale model of the Arrow kinematic environment in attacks against Mach 2 and Mach 1.2 targets. Three homing modes were studied:

a) Lead collision on AI search mode, with the navigator replacing the fire control computer.
b) Fixed lead pursuit, controlled by the navigator observing the AI search display.
c) Fixed range lead pursuit mechanized so as to display a steering dot to the pilot.

Only thirty interceptions have yet been analysed and most of the results are not yet statistically significant. However, the LCS mode a) above appears very vulnerable to evasion, and the FRLP mode c) seems to perform as predicted by the theoretical study. A description of the trials and the final results will be published when data reduction and analysis are completed.

CONCLUSION RE PASSIVE HOMING AND RANGING

The fixed range lead pursuit mode, either used alone or in combination with pure collision, provides a means of passive ECM homing using angular information only which is almost as effective in terms of placement probability as lead collision in the absence of ECM. The requisite hardware modifications are extremely simple. For successful launching of Sparrow II in this mode, launch range must be determined with an error not greater than ± 30% R.M.S. Padar vertical manoeuvre ranging, and possibly power rate measurements, all promise to provide launch range accuracy within this requirement. However, the need for passive ranging devices is considered secondary, since in the ECM environment envisaged Sparrow II can itself supply launch range information.

The effectiveness of the MB-1 missile in the expected ECM environment is nil because of the excessive demands it makes on the AI system. However, it can be utilized very effectively in the presence of ECM if its time fuze is replaced by an influence fuze.

GENERAL CONCLUSIONS ON ECM

In general, the effectiveness of Astra against ECM is very good provided proper anti-ECM procedures are used. The two most serious ECM threats against the Astra are barrage jamming and the chaff rocket. Normal chaff, fired singly or continuously, is ineffective. Repeater jammers can be countered using the quasi-passive ranging mode. Barrage jamming can be overcome by using passive homing and ranging. The chaff rocket can only be defeated by radical re-design of the Astra AI so as to utilize the doppler effect. However, the rocket is rated as a less likely threat because of its complexity, bulk and intelligence requirements.

The infra-red auxiliary is an extremely useful aid against some of the major jamming threats. It should be further developed to provide increased sensitivity and angular discrimination.

The fixed conical scan frequency of Astra should be made variable, if not on each aircraft, at least from one Astra to another.

It is possible by very simple means to modify an AI radar to simulate barrage jamming from a single aircraft and to provide steering dot information for several passive homing modes. The requisite device should be installed in all ADC aircraft to provide valuable aircrew training in anti-ECM techniques. Interception training and practice in an ECM-free environment is of dubious value. Interception exercises against realistic jamming threats are essential to the maintenance of ADC effectiveness.

CHAPTER IX – EVASION

INTRODUCTION

This chapter deals with the effect of target evasion on placement probability. The question of evasion by the target during the Al phase of the attack is usually ignored in interceptor studies. This assumption is made more because of difficulty in handling the subject analytically than from a conviction that evasion will not occur. Yet, it may not be valid to assume that conclusions regarding desired tactics, which are obtained from a study of straight flying targets, may be applied if the target is expected to evade.

Essentially, no information was available on either the methods of study or the results of target evasion. The present chapter must be regarded as a first attempt to solve a complex problem. Some of the results may appear to be contradictory, but it must be borne in mind that conclusions stated herein largely depend on the assumptions made regarding the tactics employed by the bomber.

Whether or not bombers will evade cannot be decided on past experience. The postulated introduction of high-altitude supersonic bombers and the existence of highly effective bombs, which even if delivered in small numbers can cause immense damage, create a totally new era in strategic air warfare. Since any bomb delivered to the target area will pay tremendous dividends, it is to the bombing aircraft's advantage to use any means available for penetrating our defences. Among these means are extensive use of electronic countermeasures and target manoeuvres in the event of interception.

ASSUMPTIONS

The target flight path has been assumed to be a straight line when no evasion is used, or a circular arc with constant radius depending on the lateral acceleration used during evasion. The result of evasion is measured by its effect on the value of placement probability computed for the first interceptor approach to the bomber. Considerations of a possible re-attack have not been included.

The bomber manoeuvre load factors which have been permitted are modest, the maximum being 1.25. In some cases the amount by which the bomber turns off course was restricted.

EFFECT OF EVASION ON THE PLACEMENT ZONE

A typical placement chart for an evading target appears in *Figure 68*. Two sets of barriers are drawn, one for a target turning towards the interceptor, the other for a target turning away. It is seen that the geometrical effect of evasion is a rotation of the placement zone in the direction of the bomber's turn. The amount by which the zone is rotated depends on the rate of bomber evasion; the shape of the barriers depends on when evasion is initiated.

The evasion is assumed to occur during the AI phase of the attack. Thus the ideal approach line is the same as in the placement zone for a non-manoeuvring target. If the interceptor is approaching behind the ideal line, a bomber's turn towards it aids interception, and a turn away reduces the chance of success; however, if the interceptor is placed ahead of the ideal line the reverse is true. In computing placement probabilities, only that part of the placement zone which is common to both cases has been used.

This is tantamount to assuming that the bomber will always evade in the most advantageous way. This is not unreasonable, since the bomber requires only a simple computer and a listening device which can measure the aspect at which the attacking fighter appears.

Figure 69 shows how the size and shape of the resultant placement zones vary with the instant of commencement of target manoeuvre. Typical expected AI acquisition ranges for the Astra system are indicated on this figure. If the full effect of evasion is to be realized, it should begin at some time before lock-on. However, evasion beginning at lock-on still appreciably degrades the chance of interception and, therefore, both cases have been considered.

For intelligent evasion before lock-on the bomber also requires an AI radar. The interception then becomes a duel between two essentially similar machines. This problem has not been carried further than the derivation of probabilities of interception at the first approach.

EVASION IN THE BASIC CASE

Chapters V and VII reviewed the tactical situation considered as basic, where a Mach 2 fighter attacked a Mach 2 bomber flying at a 60,000-foot altitude. This section describes the effect of target evasion in this basic case. It was assumed that the target evaded with a 1.25 load factor (.75 g lateral), beginning shortly after the bomber was continuously illuminated by the AI. *Figures 70* and *71* illustrate a comparison of results for two course differences in the case of co-altitude attacks and *Figures 72* and *73*, in the case of snap-up attacks. The general results are summarized in *Table XXIII*.

TABLE XXIII

EVADING MACH 2 TARGET AT 60,000 FEET SNAP-UP ATTACK FROM 40,000 FEET

Course Difference (degrees)	P_p for $\sigma = 1.5$ (%)	P_p for $\sigma = 3.0$ (%)	P_p for $\sigma = 9.0$ (%)
180	100 for AI .5S to S	100 for AI .85S to S	65
135	0 at S 100 at .5S	5 at S 85 at .55S	25 at S 47 at .6S
110	0 at S 65 at .5S	0 at S 65 at .5S	0 at S 35 at .6S

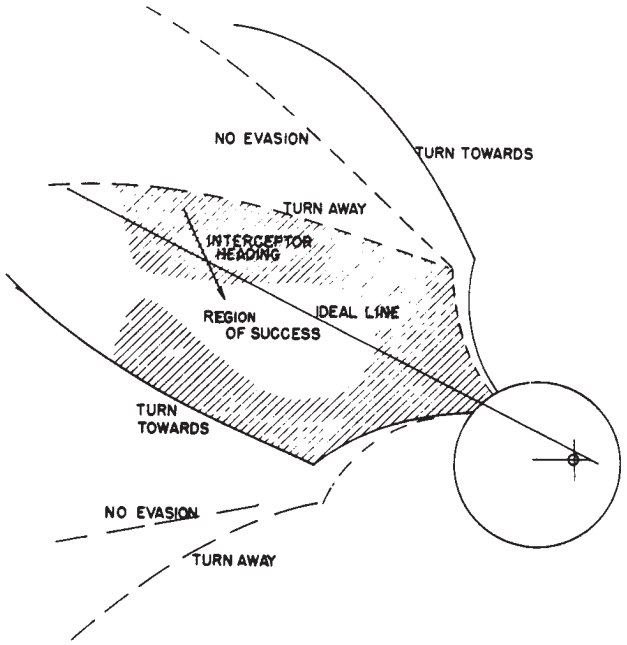

FIGURE 68 – Typical Placement Zone for Evading Target

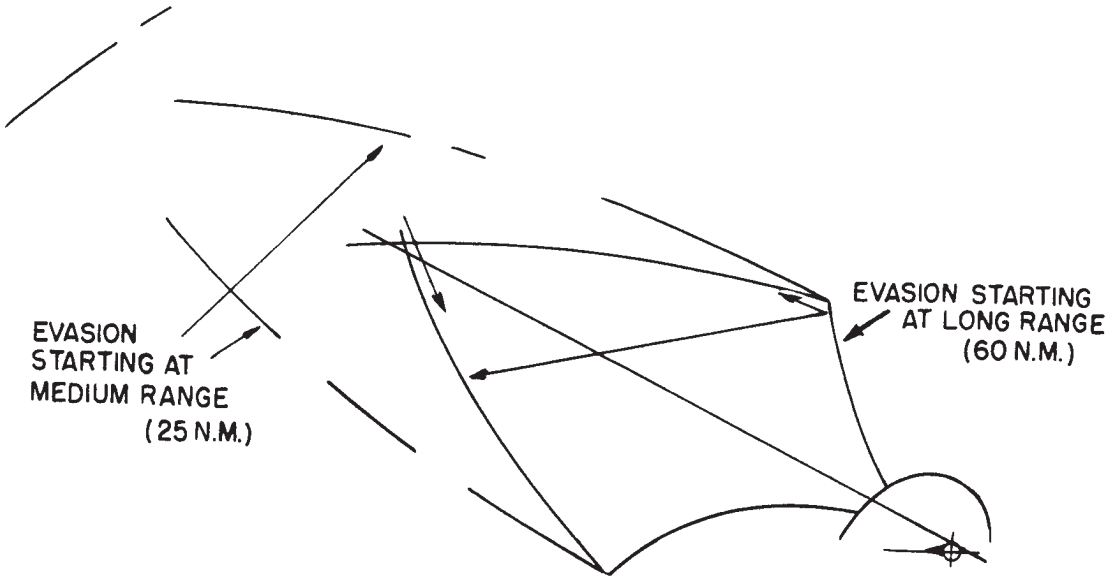

FIGURE 69 – Variation of Resultant Zone with Range of Initiation of Target Manoeuvre

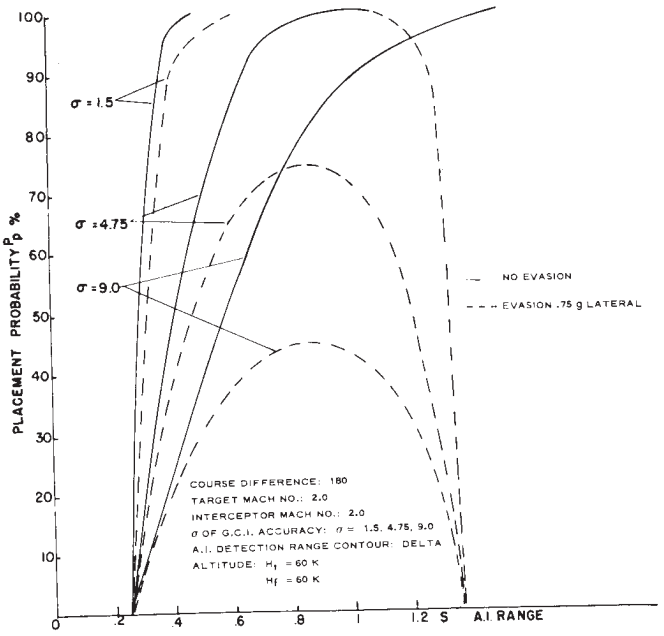

FIGURE 70

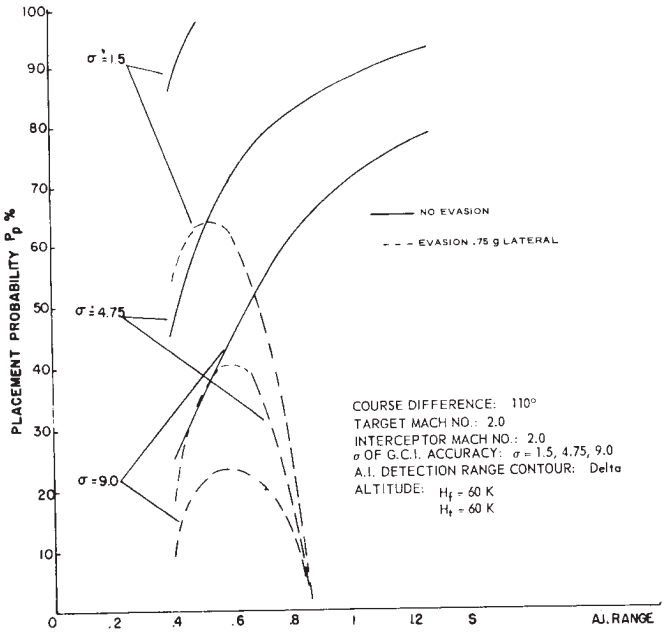

FIGURE 71

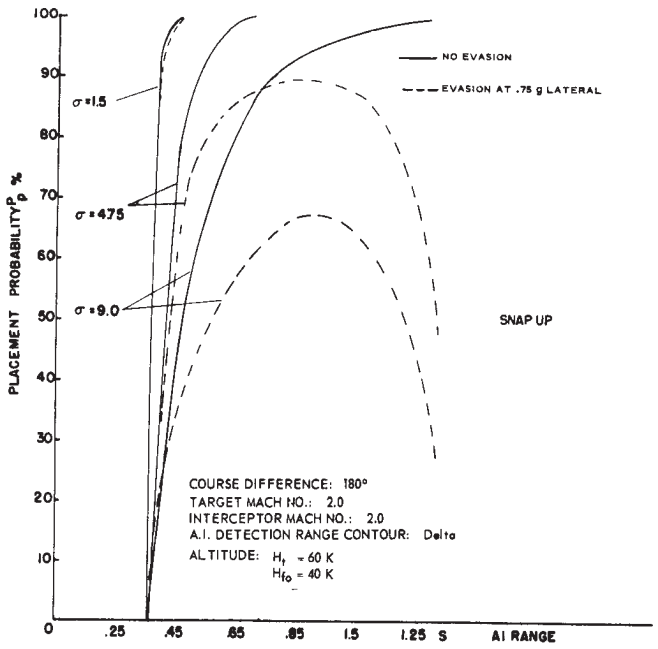

FIGURE 72

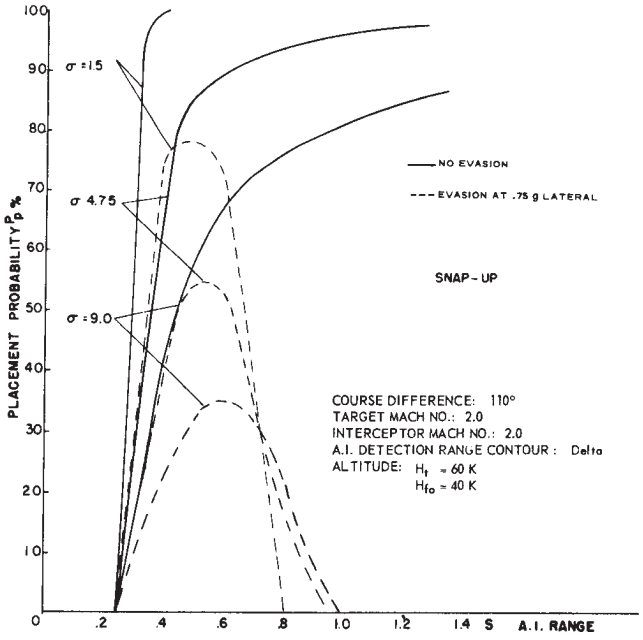

FIGURE 73

The use of a differential altitude improves placement probability for an evading target, but the extent of this improvement strongly depends on the attack course difference. The effects are outlined in *Table XXIV*.

TABLE XXIV

COMPARISON OF VARIOUS TYPES OF ATTACK FOR EVADING TARGET

Course Difference	Effect
180°	Snap-up from 10,000 feet is 10% better than co-altitude; climb, 5% Snap-up from 20,000 feet is 15% better than co-altitude; climb, 5%
135°	Results for snap-up, climb, and co-altitude are equal, unless $\Delta h = 20{,}000$ feet, when snap-up is better.

The results at 110 degrees depend on the values of S and σ that are chosen so that average results cannot be stated. For snap-up attacks, the AI range versus P_p curves are generally shifted towards lower values of S by about 10%.

EFFECT OF EVASION STARTING AT LONG RANGE

Referring again to *Figures 70* to *73*, the most striking factor in the evasion graph is probably the fact that P_p falls off at long range. This fall off is due to the assumption that evasion begins at AI lock-on and continues indefinitely. For very long AI ranges a great deal of manoeuvre on the part of the target is permitted and results in a decrease in P_p.

This effect for a special case of quite mild evasion (1.12 load factor) is illustrated in *Figure 74*. It is noted that if evasion begins at very long range (50 nautical miles or more) P_p is not much better for a small value of GCI error than for large σ.

The effect of evasion can be countered somewhat by head-on attacks. It is most desirable from the point of view of lessening the effect of evasion for the GCI to place the interceptor as near head on as possible. This fact is illustrated in *Figure 75* where placement probability is plotted against initial course difference.

HIGH-ALTITUDE TARGET EVASION

Most of the work on evasion was done for the basic case. A very mild evasion (load factor 1.1 g) was given the Mach 2 target at 70,000 feet to note the effect. A sample graph is shown in *Figure 76* which compares the evading and non-evading situations.

EFFECT OF TARGET LOAD FACTOR

Most of the cases studied, wherein the target load factor varied, were for a constant speed interceptor. It is felt that these results are not pertinent to the variable speed fighter. In the instances where the target load factor was varied for a decelerating fighter, the aerodynamic data of aircraft performance were estimates used earlier in the study and, therefore, have somewhat more pessimistic drag characteristics than those employed later on. However, to illustrate the topic in question, P_p has been plotted against lateral target g's in *Figure 77*. These graphs should be regarded as illustrative only.

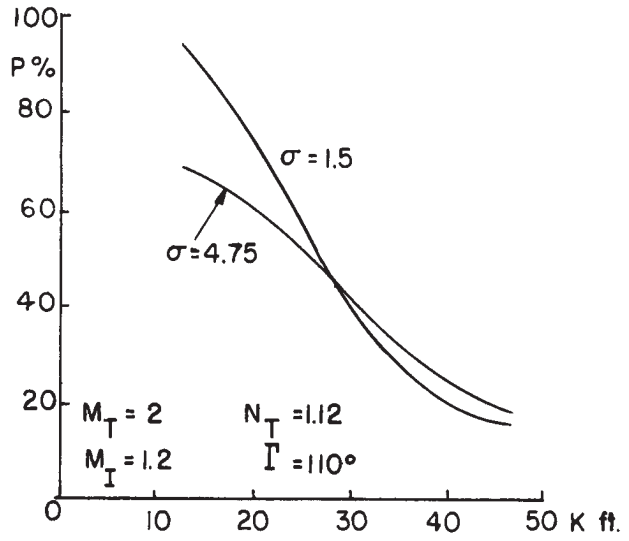

FIGURE 74 – Variation of P_p with Range of Initiation of Target Evasion

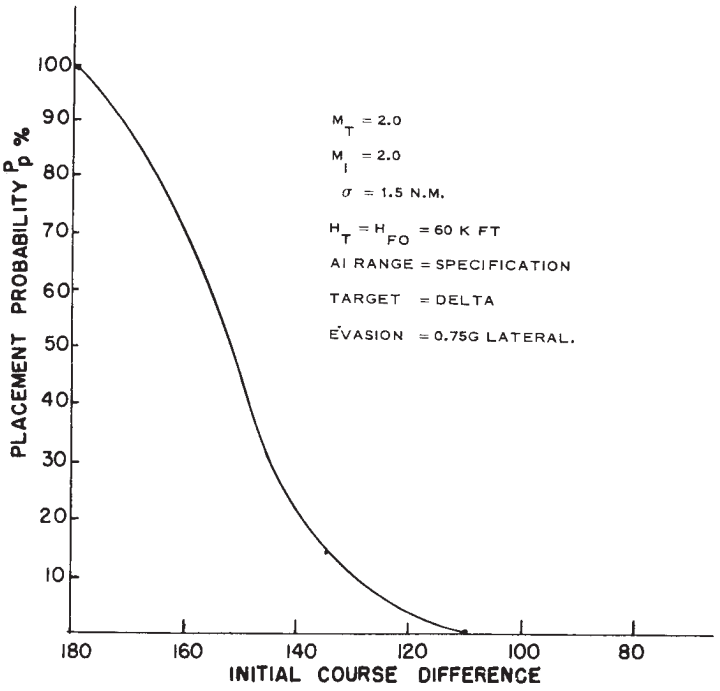

FIGURE 75 – Effect of Course Difference Under Evasion

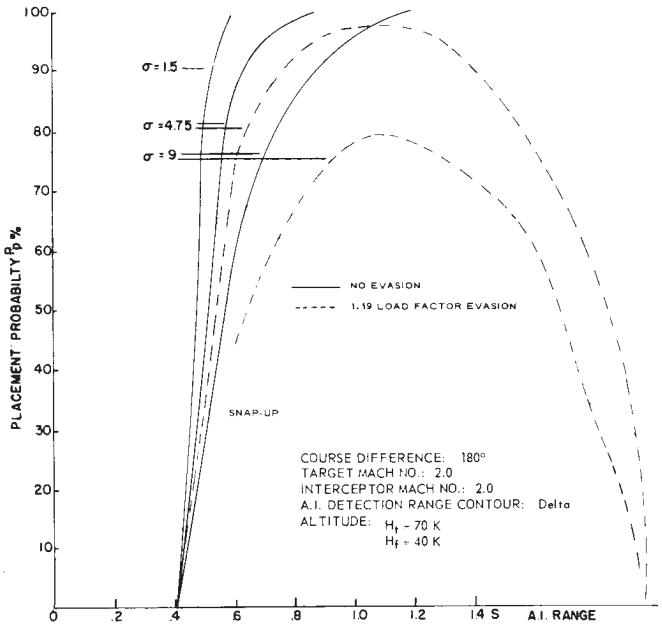

FIGURE 76

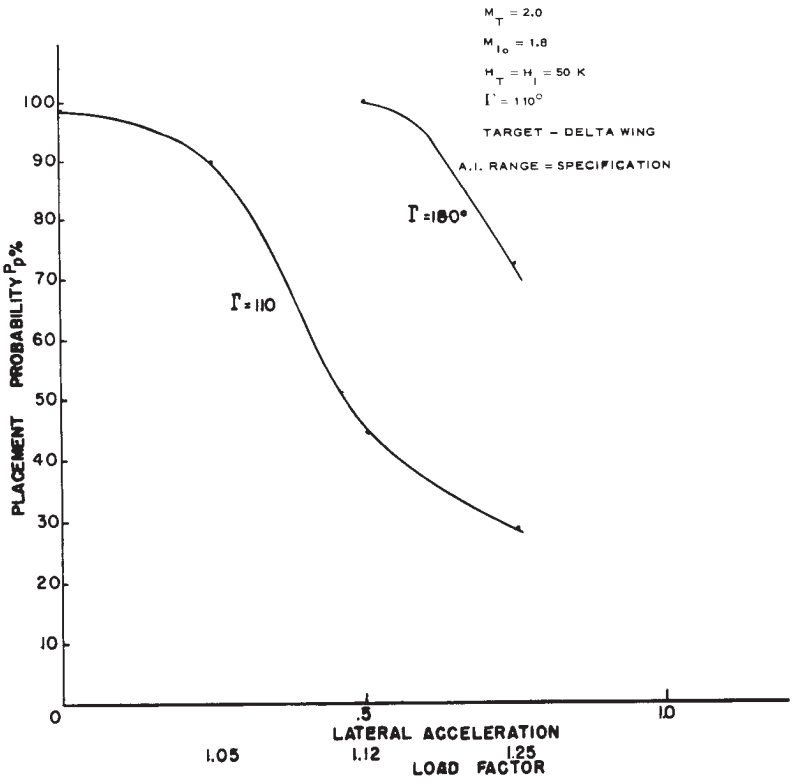

FIGURE 77

AMOUNT OF TARGET TURN

The effect of the amount of angular turn that the bomber is permitted was investigated. The bomber was allowed to turn a certain number of degrees off course, but after this turn it flew a straight line. The limits imposed in the study on the amount of turn were 30 and 60 degrees.

The results are again for the early aerodynamic data mentioned in the above paragraph. The amount of lateral acceleration on the bomber was 0.75 g, the target speed was Mach 2 and the initial interceptor speed was Mach 1.8. No straightforward conclusions can be drawn from results, and the complexity of the problem is summarized in *Table XXV*.

TABLE XXV

EFFECT OF VARIATION IN AMOUNT OF TARGET ANGULAR TURN OFF A STRAIGHT LINE COURSE

$M_T = 2.0$ $N_T = 1.25$ $M_I = 1.8$ Delta	Head-on Attacks		Beam Attacks	
	$\sigma = 1.5$	$\sigma = 9.0$	$\sigma = 1.5$	$\sigma = 9.0$
Good AI .4S	$P_p > 95\%$ 0° to 60°	$P_p = 25\%$ 0° to 60°	P_p 90% at 0° P_p – 32% at 30° and 60°	$P_p = 20\%$ 0° tp 60°

Results are so variable from case to case that the illustration of a particular graph would be misleading. The interested reader is referred to the third Progress Report (18) for specific cases. It should be reiterated that these results are based on aerodynamic characteristics different from the results stated elsewhere in this report.

CORRECTIVE MEASURES

It has been shown that even mild target evasion is quite effective in reducing placement probability. Trends and conclusions are complex, but certain general recommendations may be made.

If at all possible the interceptor should be vectored on a head-on attack. The effect of evasion is especially severe for a beam attack.

A displacement of the ideal approach line such that the aircraft homes on a point ahead of the target tends to increase P_p, since this places the line nearer the center of the placement zone. The maximum probability attained is increased by about 5 to 8% absolute. However, the greatest advantage comes from the fact that this maximum P_p is maintained over a much wider band of AI ranges. The effects are illustrated in *Figure 78* but they should be regarded as qualitative only.

These trends hold for either co-altitude or differential attacks. However, in differential altitude the desired displacement of the ideal line is much greater than for $\Delta h = 0$. This fact is qualitatively illustrated in *Figure 79*.

In many cases, evasion can reduce P_p essentially to zero and is particularly effective at long AI acquisition ranges. It could be completely countered by leaving the AI on search until 20 miles range, with the navigator making approximate heading corrections for gross positioning errors. This procedure has been proved practicable in project Sprint trials.

These corrections require the navigator to have an approximate knowledge of bomber heading and air speed. Neither of these items are included in the SAGE close control message form as it now exists.

Bomber evasion on the part of a subsonic bomber has no effect, as noted in the next chapter.

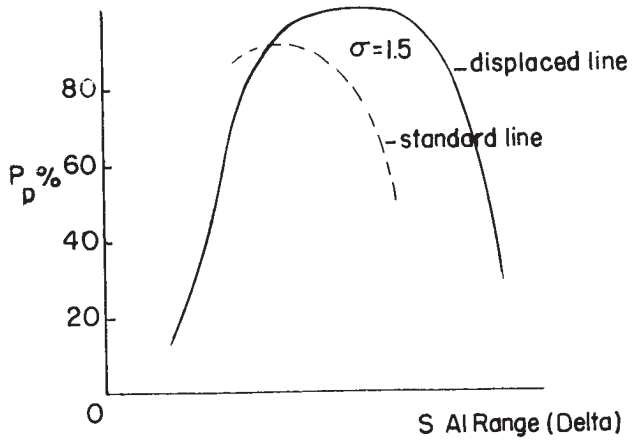

FIGURE 78 – Illustration of the Effect of Displacing Ideal Line

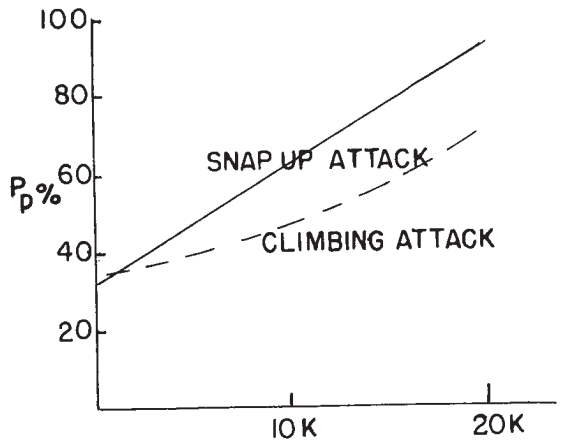

FIGURE 79 – Distance in Front of Target (K feet)

CONCLUSIONS

The following general conclusions on evasion may be stated.

1) Evasion by a high-speed bomber appreciably reduces the chance of interception (P_p).

2) Evasion reduces P_p more for beam attacks than for head-on attacks.

3) Lock-on by the interceptor should be delayed as long as possible, so as not to give warning to the bomber. Lock-on or hand-track should not start until 20 nautical miles range.

4) The better approach path for an interceptor against an evading target is one on a collision course on a point ahead of the target rather than behind.

5) Evasive turns by a Mach 2 target against a Mach 1.5 interceptor of more than 60 degrees do not in general cause further appreciable reduction in P_p.

CHAPTER X – SUMMARY OF SYSTEM CAPABILITIES

INTRODUCTION

This chapter outlines the general conclusions and findings on the system as a whole. The statements made are to be regarded as overall impressions rather than a detailed commentary. As noted in the preceding pages the main emphasis of the study was placed on the AI phase of the attack, and statements made on other aspects of the system were inferred from results obtained by the study of this phase.

A particular topic which is dealt with herein is that of subsonic targets. The study as a whole was not concerned with this threat since it did not offer a great challenge to the system.

EFFECTIVENESS AGAINST SUBSONIC BOMBERS

The major effort of the CARDE study was placed on the supersonic bomber threat: principally Mach 1.5 to Mach 2.0 but with some attention to a Mach 3.5 target. The emphasis was placed on these targets, not because they seemed to be the most likely threat, but because they were the best vehicles to illustrate the capabilities or limitations of the interceptor system.

The Arrow has a high capability of interception for subsonic targets such as Bear or Bison. Because of the interceptor speed advantage, in most cases the placement zone will be limited only by the initial look angle and the time required for interception. The available look angle of the Astra System is so large that even for the poorest GCI control accuracy which has been considered (σ = 9 nautical miles) the placement chance is essentially 100%. Only if the AI is quite seriously degraded in range performance does the placement probability become small. This fact is illustrated in *Table XXVI* wherein the AI is degraded to .33 of specification.

TABLE XXVI

Placement probability for Mach 1.5 Interceptor versus a Mach 0.85 bomber
(AI Range degraded to 0.33 of specification)

σ (n.m.)	1.5	3	4.75	6.75	9.0
Γ 70	100	93	80	65	58
150	85	65	55	51	45

With very degraded AI the limiting factor in the placement zone is the manoeuvre barrier; it may be seen that for this case the chance of success is better for rear aspect attacks.

If the interceptor is attacking at its subsonic speed, M = .92, the placement probability for this amount of degradation remains above 85% since the manoeuvre barrier is not so restrictive.

TACTICS FOR A SUBSONIC BOMBER

Simpler tactics are required against a subsonic target than against a supersonic bomber. In the standard situation where the missile has a microwave seeker and the AI radar may be used, placement probability is very high even against a rapidly manoeuvring target. The interceptor's success is ensured if the initial interceptor speed is high and if it restricts itself to low load-factor manoeuvres at long and medium ranges. It would appear that the best a subsonic bomber may hope to do is to force the fighter into a tail chase at reduced speed and so considerably increase the time required for interception. The implications of this tactic would become apparent in an operational study with reference to geography.

Some comments on tactics with regard to weapon requirements are given below.

a) As a subsonic target is a much weaker infra-red source than the supersonic target discussed above, the success of the infra-red missile in frontal attacks is even less certain. However, since the interceptor has a speed advantage, small initial course differences give high placement probability: course differences of 110 degrees or less are successful. Again snap-up attacks may be successful from head-on.
b) Infrared AI suffers very much from the low infra-red emission of a subsonic target. By reducing the bank angles which are used in the attack, the interceptor may keep lock-on without the wings obscuring the target, but attacks should be restricted to the beam and tail to ensure lock-on at sufficient range to launch the missiles.
c) Most modes of navigation are successful against a slow target provided the missile may be launched satisfactorily. Again by using fixed range lead pursuit the interceptor may ensure that the missile is correctly headed in the launch zone.
d) The unguided missile is subject to the same limitations as in the supersonic target case. In general, the slower the target, the more chance an unguided missile will have to succeed.

The figures given in *Table XXVI* are for the probability of interception at the first approach. If the interceptor continues in its turn it will eventually reach a point from which interception can be made. However, in the course of the manoeuvre it will often lose sight of the target, and will have to continue the turn using extrapolated target path, or obtain instructions from GCI.

Studies of a multiple target situation might reveal that traffic and saturation problems l limit re-attack capability. The necessity of controlling many interceptors may impose a restriction on the amount of turn permitted to each of them. The difficulty of retaining identity of a given target and interceptor over a long period may make re-establishment of GCI control for a second pass difficult to achieve.

MISSILE PERFORMANCE

It appears that missile performance against the subsonic threat is adequate. The target altitude and Mach number range are well within the capabilities of Sparrow II missiles. Some doubt may be expressed, however, as to the effectiveness of fragmenting warheads with the present V.T.

fuzing. The work done in the present study is not sufficient to lead to detailed answers. However, a more intensive study of this subject was carried out under project Ash Can and the interested reader is referred to relevant reports on this project (Ref. 52 - 67).

GENERAL CONCLUSIONS

With a system as complex as an interceptor and its associated equipment it is very hazardous to make blanket statements on performance, especially on the results of a study on a limited portion of the system. However, they are sometimes desirable. *Table XXVII* attempts to sum up briefly the trends that appear to emerge from this study. The last two rows of the table concern aspects of the system which were not studied in detail and represent estimates rather than calculated conclusions.

TABLE XXVII

	Expected Subsonic Threat	Proposed Supersonic Threat	More Advanced Threat
Airframe	Adequate	Adequate	Some Potential
AI	Adequate	Adequate	Growth Potential
Weapon	Adequate	Marginal	Inadequate
Warheads	Marginal	Inadequate	Inadequate
Present GCI	Marginal	Inadequate	Inadequate

The study indicated that the Arrow system had the following interception potential:

a) Targets up to 58,000 feet altitude can be intercepted in co-altitude attacks.
b) Targets up to 70,000 feet altitude can be intercepted in climbing or snap-up attacks.
c) Probability of positioning is 80% for targets of Mach numbers up to 2.5 with correct approach course difference.
d) For the subsonic bomber, target evasion load factor of 2.5 can be countered.
e) For the supersonic bomber, target evasion load factor up to 1.25 can be countered using proper tactics.

Chapter VIII gives more detailed conclusions on the ECM situation.

It was stated in the beginning of this report that a supersonic interceptor presents some new concepts which do not permit direct extrapolation of results from subsonic studies. One of these aspects is that during many manoeuvres on the part of the fighter the Mach number may decrease quite rapidly when the aircraft is subjected to high, or even moderate lateral acceleration. This deceleration can be quite detrimental to achieving interception. It may be concluded that the value of power limited g capability is not a satisfactory criterion of aircraft performance when interceptions at Mach numbers of about 1.5 and at altitudes of the order of 50,000 feet are considered. However, it is difficult to suggest an alternative single figure which can be used as a standard of comparison..